NASA Reference Publication 1057

Handbook of Lunar Materials

FEBRUARY 1980

NASA

NASA Reference Publication 1057

Handbook of Lunar Materials

Edited by
Richard J. Williams
Lyndon B. Johnson Space Center
Houston, Texas

James J. Jadwick
Lockheed Electronics Co., Inc.
Houston, Texas

National Aeronautics
and Space Administration

**Scientific and Technical
Information Office**

1980

Contents

Tables

Figures

Introduction

Recent scenarios for future space programs have stressed the need to utilize space in ways beneficial to mankind. One class of these scenarios includes the use of nonterrestrial materials as industrial feedstocks. If nonterrestrial materials are to be so used, it is of considerable importance to characterize their physical and chemical properties. This document is an attempt to compile in a concise format such data on the lunar materials.

Lunar samples returned during the Apollo missions have been studied intensively for the last 8 years. This research has resulted in a large number of published studies that include the abstracts and proceedings of nine lunar science conferences, dozens of papers scattered through the scientific literature, many special publications from conferences and workshops, plus a large number of internal reports and publications of various universities and research institutes. It is a substantial undertaking to locate and read even a small portion of this literature—an undertaking which is complicated by the fact that many of the early contributions have proven to be inaccurate or incomplete.

We have chosen to construct a current compilation of data pertaining to lunar materials. Several sections of the document present the positions of various experts who have contributed to the document, and the most reliable modern data available on the various subjects are summarized. In addition, we have compiled some data on terrestrial materials and chemicals which, by analogy, apply to lunar materials; and we have attempted, insofar as possible, to define the unusual technical terms that are used, particularly if the terms have a somewhat different meaning when applied to lunar materials.

We have not extensively referenced this work, preferring to cite only recent summary material, and we apologize to our colleagues for sometimes removing their data from context without formal citation.

This document has been prepared by members of the Geology and Geochemistry Branches of the Lunar and Planetary Sciences Division, NASA Lyndon B. Johnson Space Center, Houston, Texas. The overall editing and assembling was by James Jadwick, Lockheed Electronics Co, Inc., and Dr. Richard J. Williams, Lyndon B. Johnson Space Center.

In compliance with the NASA's publication policy, the units of measure are given, as far as possible, in the Systeme International d'Unites (SI). There are, however, some exceptions in that the editors have retained secondary units in those cases in which the primary source data are given in such units, because simple conversion of units often does not accurately express the original data.

In some cases, the SI units are written first and the original units are written parenthetically thereafter.

We express our appreciation to the following people who have provided summaries of data and technical guidance during the preparation of this document. Lyndon B. Johnson Space Center: U. S. Clanton, F. Horz, G. E. Lofgren, J. W. Minear, D. S. McKay, D. D. Bogard, E. K. Gibson, R. V. Morris, and J. W. Warner. Lockheed Electronics Co., Inc.: J. E. Wainwright.

1. General Information

General properties of the Moon, Earth's only natural satellite, have been known for years. Results of the Apollo Program have, however, enormously amplified our knowledge of the Moon as a planet. Table 1-I summarizes important lunar physical properties.

TABLE 1-I.—Bulk Lunar Properties

Mean density, g/cm^3	3.344 ± 0.004
Mean radius, km	1738.09
Moment of inertia	0.392 ± 0.003
Mean Earth-Moon distance, km	384 402
Surface gravity, cm/sec^2	162
Central pressure, N/m^2 (bars)	42×10^8 (42×10^3)
Seismic energy release, J/hr (ergs/hr)	$<10^8$ ($<10^{15}$)
Surface heat flux, μW/cm^2	2

Perturbations exist in the gravity field on a scale of a few hundred kilometers. Large positive increases of several hundred cm/sec^2 (milligals) are associated with the circular maria and are interpreted to be due to basalt filling meteorite craters. The permanent magnetic dipole moment is negligible, being less than 4.4×10^9 tesla/cm^3 or approximately 10^{-12} that of Earth. However, remanent magnetic fields, ranging from 3×10^{-9} to 327×10^{-9} tesla (3 to 327 gammas), have been measured on the lunar surface. These fields, existing over the entire lunar surface, are quite variable spatially in both magnitude and direction on a scale of less than a kilometer.

Several thousand moonquakes occur every year. Their energy is generally less than Richter magnitude 2; the largest being approximately magnitude 4. A large number of the moonquakes occur below the lunar lithosphere (the cold relatively brittle thermal boundary layer) at depths of 600 to 1000 kilometers. A crust of gabbroic anorthosite ranges in thickness from 60 kilometers on the near side to approximately 100 kilometers on the far side.

LUNAR SURFACE

Figure 1-1 is a photograph of the full Moon (Lick Observatory photograph L-4). Inspection of the photograph indicates that the Moon is divided into two major regions. The low albedo (dark) regions are maria and the high albedo (light) regions are highlands. Further inspection of the photograph shows that the (dark) maria are topographically low and fill circular and irregular basins or depressions. It is now known that they consist of mafic basalts of several different chemical types. Differences in albedo (amount of visible light

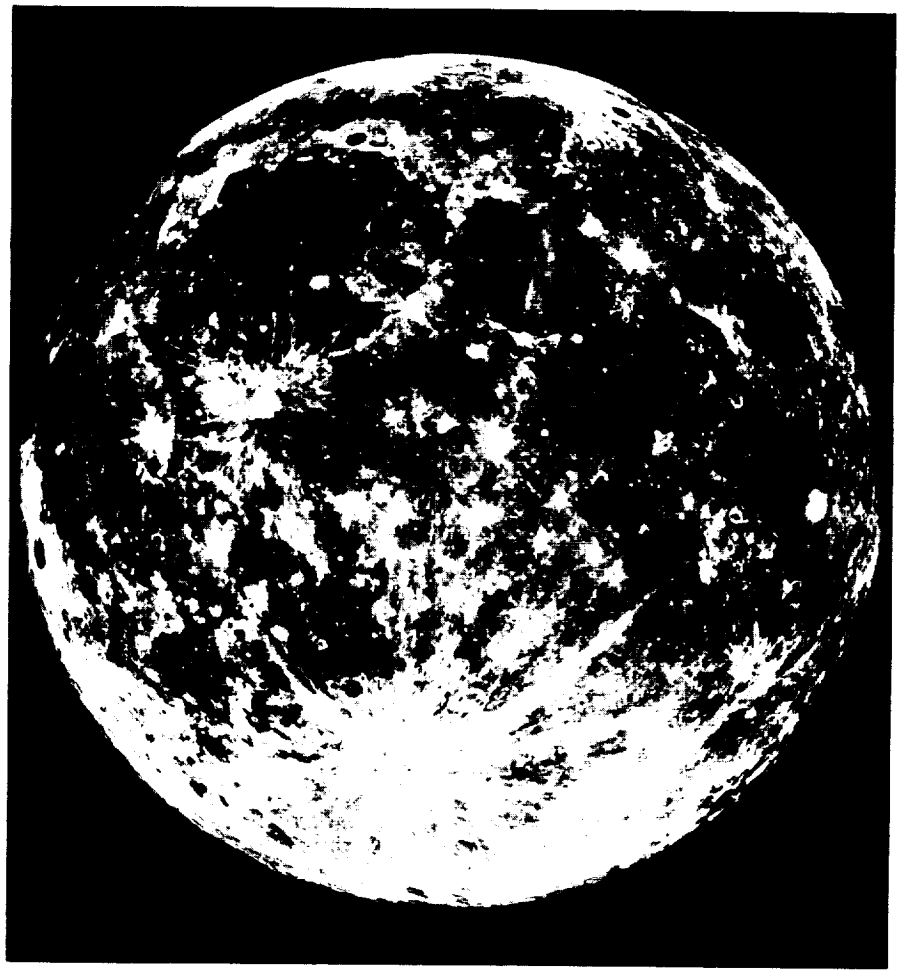

FIGURE 1-1.—Lick Observatory photograph L4 of the full Moon. The albedo differences between mare, highlands, and fresh ejecta are enhanced in this photograph.

reflected from the surface) within the mare result primarily from these differences in chemistry. The (light) highlands stand topographically about a kilometer above the maria and are heavily marked with circular features. These features are meteorite impact craters, which range in size from the limit of visibility to large, circular basins hundreds of kilometers across. The highlands consist of a mixture of mostly feldspar-rich (anorthositic) plutonic material and minor amounts of an aluminum and trace-element-rich basaltic material known as KREEP.

Figure 1-2 is a composite of two half-Moon photographs also taken at the Lick Observatory. The two halves are joined along a north-south line through

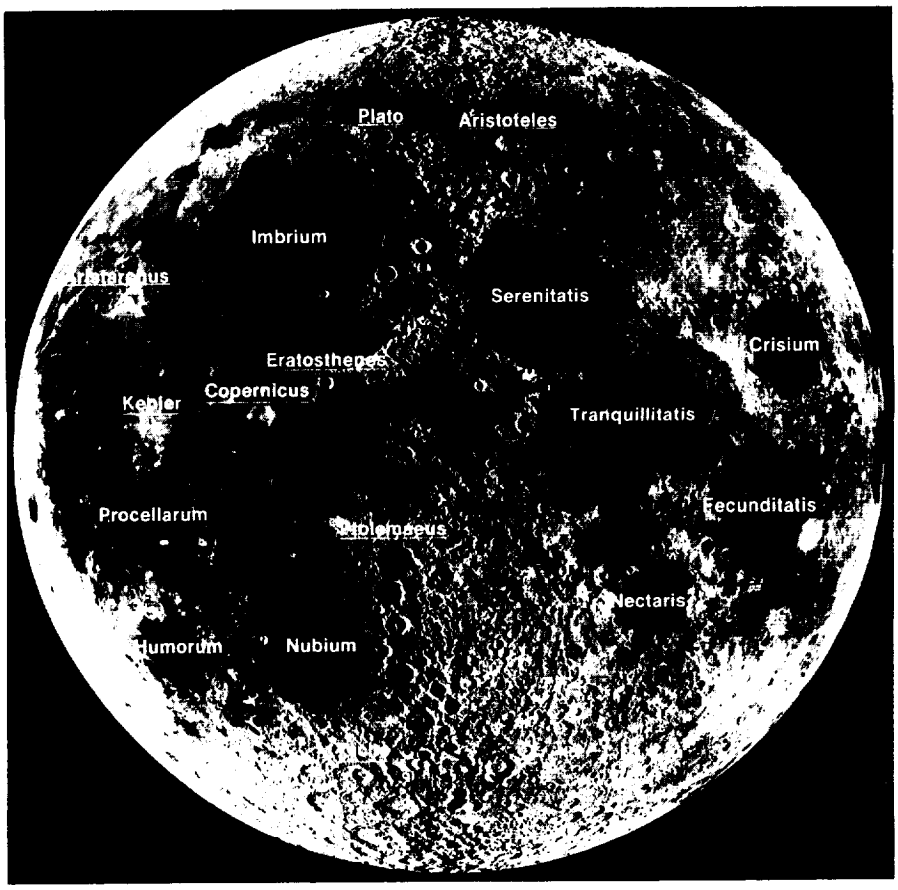

FIGURE 1-2.—Lick Observatory photograph L9, a composite of two half-Moon photographs. The high density of craters in the highlands shows up well in a pole-to-pole band in the center of the Moon's near side. (Underlined labels refer to craters directly beneath the label; other labels refer to mare basins.)

the middle of the photograph. In the region where the two halves are joined, the Sun angle is low and the topography stands out very clearly. In contrast, in figure 1-1 where the Sun angle is high, topography is subdued and albedo differences stand out. The smooth maria and cratered highlands are strikingly different in appearance in figure 1-2.

Chemical differences between the maria and the highlands were demonstrated by the orbiting X-ray fluorescence experiment. Data from one orbit each of Apollo 15 and 16 are shown in figure 1-3. The maria have consistently lower aluminum/silicon (Al/Si) ratios than the highlands. In addition, the various maria do not have the same Al/Si ratio. The major variations of the Al/Si ratio are consistent with the mafic basalts returned from the mare (lower Al/Si) and the anorthositic rocks of the highlands (higher Al/Si).

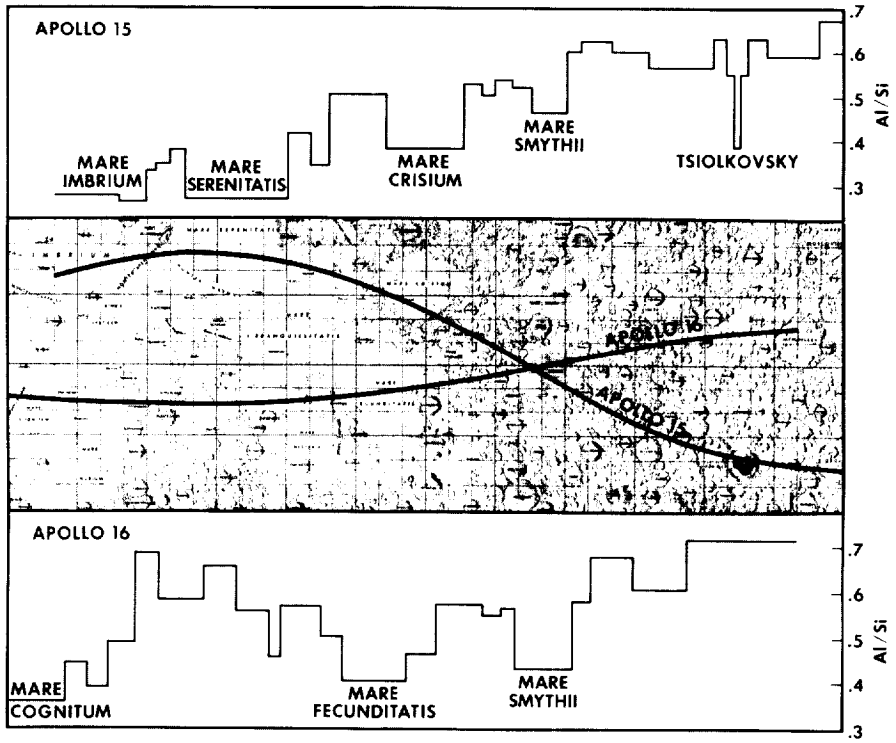

FIGURE 1-3.—Data from the X-ray fluorescent experiment that orbited the Moon during Apollo 15 and 16. The map shows one typical orbit from each mission. The top and bottom graphs show changes in the ratio of Al to Si. Low values are consistent with the feldspar-poor mare regions; high values are consistent with the feldspar-rich highlands.

CRATER MORPHOLOGY

Craters are formed by meteorite impact. Approximately 150 meteorite craters are known on Earth; the Meteor Crater in Arizona, Gosses Bluff in Australia, and Ries Crater in Germany are examples. Both erosional and depositional processes are associated with meteorite impact. The erosional feature is the excavated crater itself. Depositional features include the basin fill, continuous ejecta blanket, and rays. The basin fill is either excavated material, which has fallen back into the crater, or lavas, erupted into the crater. The continuous ejecta blanket is a series of deposits surrounding a crater out to a distance of several crater diameters. It contains both tangential and radial topographic features which, by comparison with large artificial explosions on Earth, probably were deposited from a base surge dust-gas cloud. The base surge phenomenon is analogous to that of turbidity flows in water. Examples of continuous ejecta deposits may be seen in figures 1-1 and 1-2 surrounding the craters Copernicus and Plato, located in the center of the mare region on the western side of the Moon. Rays are light colored deposits that extend out from a crater for hundreds of crater diameters. Rays were formed from material that was transported in ballistic trajectories. Excellent rays can be seen about the crater Tycho in the Southern Highlands as shown in figure 1-1.

Crater morphology is directly related to crater diameter. Small lunar craters, less than a millimeter across and commonly known as zap pits, are found on lunar rocks returned from the Moon during the Apollo Program. These craters consist of a central pit that is glass lined and a surrounding spall (splinter) zone that is approximately two pit-diameters across. There is no Earth equivalent of these microcraters because the micrometeorites that make them are destroyed in the Earth's atmosphere.

It is not experimentally possible, at this time, to produce a glass lined zap pit with a small projectile, even though velocities up to 7 km/sec have been achieved. Therefore, one can assume that the impacting particles which produced the lunar zap pits had velocities of tens of kilometers per second.

Lunar craters with diameters from several centimeters to approximately 15 to 20 kilometers are bowl shaped, with the bottom of the crater lower than the surrounding ground level. The crater rim is raised above the surrounding level; it consists of fine-grain material and large blocks. Outward from the rim for several crater diameters is the continuous ejecta blanket. Loops of small secondary craters extend farther out from the main crater. Narrow, linear rays stretch for many crater diameters in all directions, making craters look like sunbursts.

Medium-size lunar craters, 20 to 100 kilometers in diameter, display the

same extra-crater features as the small craters, but there are major differences in the crater itself. They are not bowl shaped but have a flat floor. Slumping and terraces are common on the crater walls and there is a central peak—a small cluster of hills in the center of the crater floor.

Like the medium-size craters, large lunar craters, more than 100 kilometers across, have extra-crater deposits, flat floors, slumped and terraced walls, and central peaks. But the basin has many rings and instead of one crater wall, there are several bands of mountains around the basin.

The primary effect of these impacts has been the creation of deposits of fine-grain rubble, covering the lunar surface (regolith). The heat and pressure generated by these impacts has lithified (by sintering or melting) loose material, producing lunar breccias. Regolith and breccias are discussed in part 3 of this handbook.

LUNAR GEOLOGICAL TIME SCALE

Stratigraphy (i.e., the study of the layers of rock) on the Moon is unlike terrestrial stratigraphy because the Moon lacks a series of fossil-bearing sedimentary rocks that permit investigators to correlate terrestrial rocks. Lunar stratigraphy is based on the photogeologic mapping of material ejected from craters, the interpretation of crater age, and the abundance of craters on specific surfaces. The principle of superposition holds, i.e., the overlying ejected material and its associated crater is younger than the underlying ejected material and its crater. Relative crater age is judged by the sharpness of the crater and the structure of its ejecta: sharp, fresh-looking craters are younger than rounded, subdued-looking craters. The abundance of craters on a surface is another relative measure of age: a surface with a high density of craters must be older than a surface with a low density of craters. This is illustrated in figure 1-4. Crater abundances range from mare basins which have few craters to the highlands that are saturated with craters. A surface is saturated when there are so many craters present that any new craters will destroy old craters of the same size.

Figure 1-5 is a chart of lunar stratigraphy. It is simplified in that there is probably more time overlap between the mare basalts, the plains-forming units, and the multi-ringed basins than is indicated. The absolute ages reported in figure 1-5 are determined from analyses of samples acquired during the Apollo Program.

The oldest rocks are of the Pre-Imbrian system. These rocks form the high albedo, highly cratered highlands, a region saturated with craters as large as 50 kilometers across. Approximately 75 percent of the near side of the Moon is underlain with Pre-Imbrian material. The craters are very subdued and have no rays, secondary craters, or ejecta deposits; the rims are low, rounded, and

cut by later craters; and the floors are shallow. Most of the Pre-Imbrian craters are so subdued and so overlain by younger craters that they are often not obvious as craters.

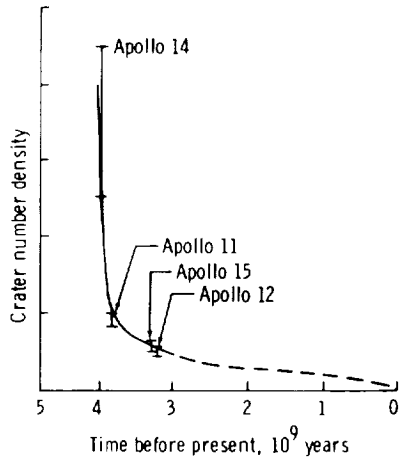

FIGURE 1-4.—Number density of craters per unit area as a function of the age of a surface. Data points (bars) are derived by crater counts surrounding each landing site, and matching those values with the radiometric age of rocks returned from each site. Dashed line is an extrapolation to zero based on the cratering model.

LUNAR STRATIGRAPHY

Era	Rock deposits	Crater morphology	Time, $\times 10^9$
Copernican	Crater ejecta	Fresh	
Eratosthenian	Crater ejecta	Partly subdued	≈3
Imbrian	Mare basalts	Subdued	
	Plains-forming units		
	Multi-ringed basins		3.9 to 4.0
Pre-Imbrian	Highly cratered highlands	Very subdued	
	Crustal formation		4.4 to 4.6

FIGURE 1-5.—Generalized chart of lunar stratigraphy. The time of the Copernican-Eratosthenian boundary is unknown, and the time of the Eratosthenian-Imbrian boundary may be as young as 2×10^9 years.

Pre-Imbrian time ended with the formation of the multi-ringed basins. Orientale is the youngest multi-ringed basin and Imbrium is the next youngest. Based on radiometric dating of rocks formed by the Imbrian impact, these events occurred approximately 3.9 to 4.0 $\times$ 10^9 years ago. Large areas of the Moon are covered with ejecta from these events (e.g., Fra Mauro formation sampled at the Apollo 14 site). Such deposits are characterized by a gross structure that is radial to basins (fig. 1-6).

There are two widespread types of deposits of Imbrian age. The older is a "plains-forming" unit (e.g., Cayley formation sampled at the Apollo 16 site). "Plains" material is intermediate in albedo and in crater density, being darker

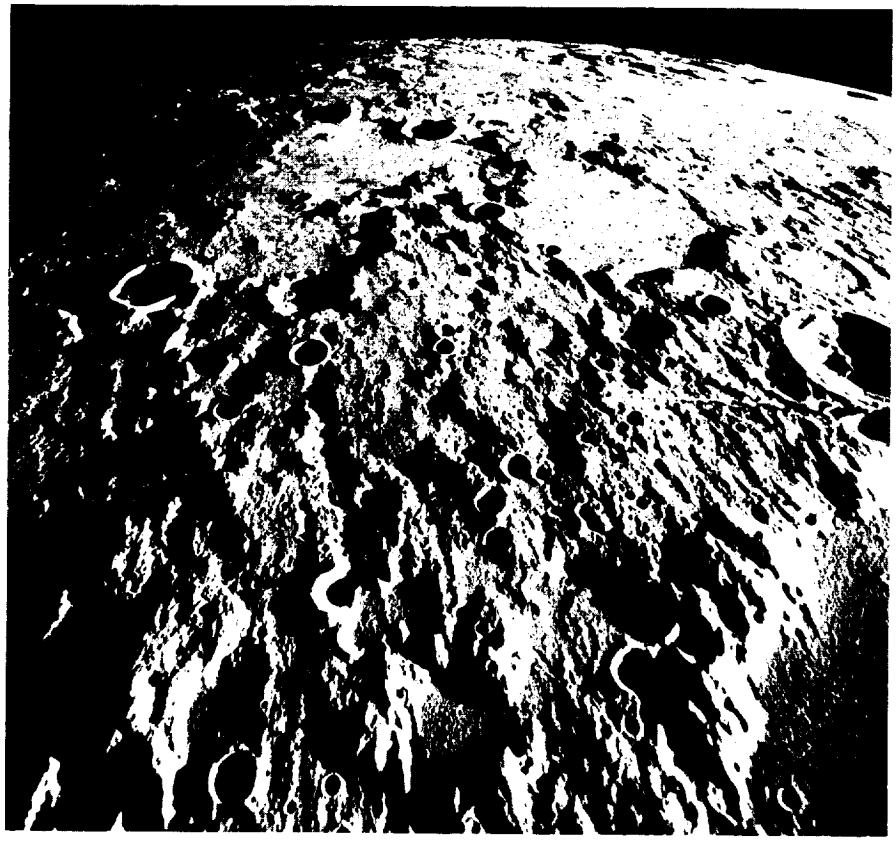

FIGURE 1-6.—Apollo 16 oblique metric photograph (A16-M-0847) looking north along the ridges that are radial to the Imbrian basin. These ridges, located just northwest of the crater Ptolemaeus, define Imbrium sculpture.

and less cratered than the Pre-Imbrian highlands and lighter and more cratered than the basalts that fill the mare basins (fig. 1-7). "Plains" units make up approximately 10 percent of the Moon's near side. They are more or less

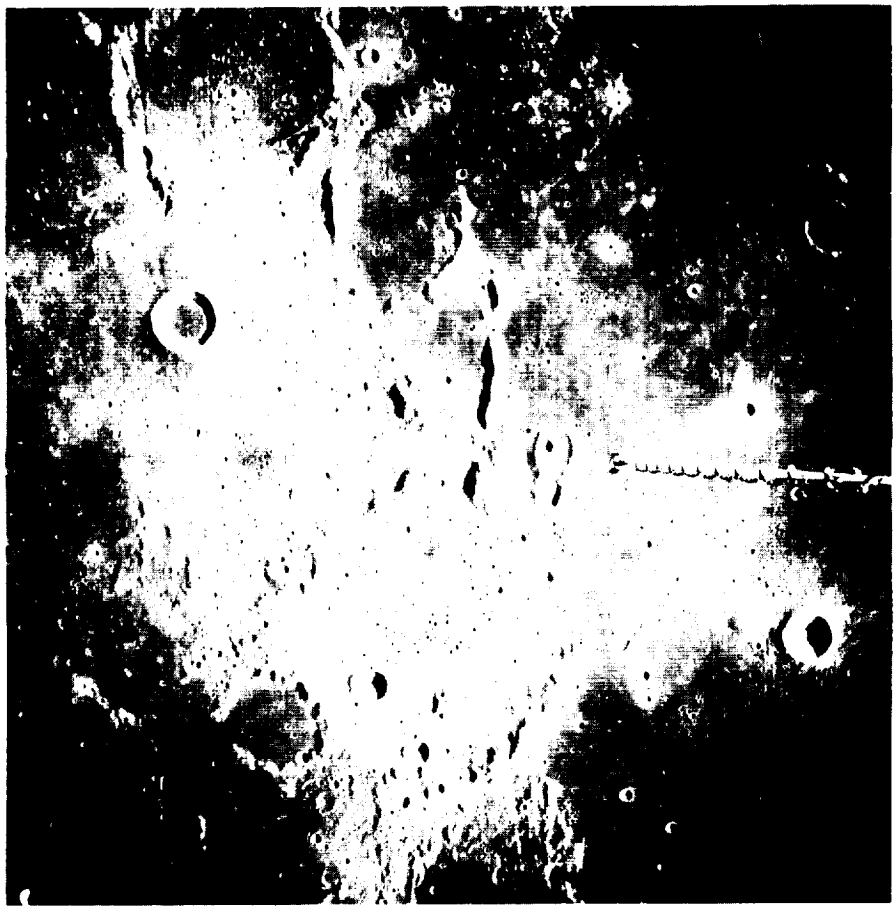

FIGURE 1-7.—Apollo 16 vertical metric photograph (A16-M-2820) illustrating plains material filling lowlands in the lunar highlands adjacent to a mare unit. The plains material is characterized by intermediate to high albedo and a high density of craters. By contrast the mare material has a low albedo and a low crater density. In this photograph, a lobe of highlands projects southward into Mare Nubium which appears in the right half and the lower left corner of the photograph. The linear object with a cable coiled about it is a boom on the spacecraft that carried the gamma-ray experiment. The large crater in the center of the photograph is Guericke.

level deposits of reworked ejecta material that fill craters in the highlands and are found along the inner margins of some of the multi-ringed basins. Based on radiometric dating of rocks on a "plains" unit, the Early Imbrian period ranged from 3.85 to 4.0 $\times$ 10^9 years ago.

The low albedo, lightly cratered, mare filling deposited in the later part of the Imbrian system, is a series of basalt flows that make up approximately 15 percent of the Moon's near side. Mare basalts fill most of the near-side multi-ringed basins, flood the large low-lying areas, and flood the floor of some 100 kilometer-size craters on the Moon's far side (fig. 1-8). Radiometric dating of

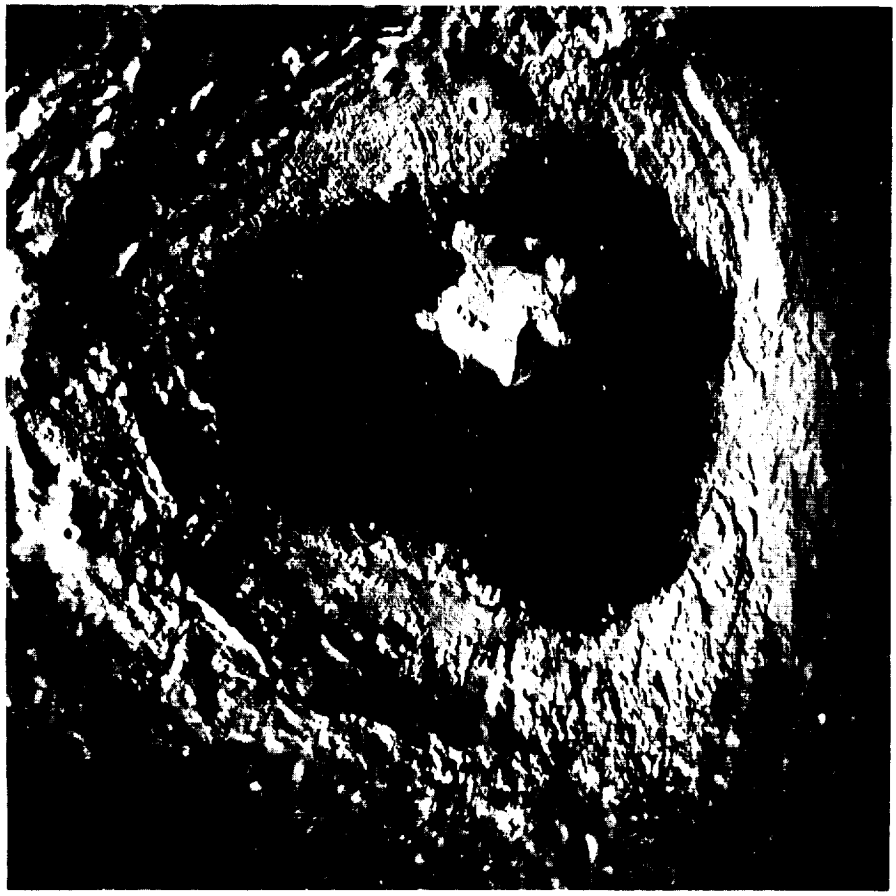

FIGURE 1-8.—Apollo 15 vertical metric photograph (A15-M-1327) of the crater Tsiolkovsky illustrating mare fill in a large far-side crater. Tsiolkovsky is approximately 175 kilometers across. The mare fill is characterized by low albedo and low crater density. Other features that are illustrated by the crater Tsiolkovsky include a central peak complex and slump terraces along the inner crater walls.

mare basalts suggests that the Late Imbrian period ranged from 3.9 to 3.2 × 10^9 years. Unsampled mare units with very low crater densities may be as young as 2 × 10^9 years.

Craters of the Imbrian period are subdued but, unlike Pre-Imbrian craters, are clearly recognizable. Archimedes and Gassendi are typical Imbrian craters. Ejecta deposits and secondary craters are subdued; crater rims are low, broken, and rounded; and crater floors are shallow or filled with later material. No rays have been recognized.

The Eratosthenian period marks the beginning of greatly reduced rates of cratering and the virtual cessation of volcanism. The period has left partly subdued craters with accompanying ejecta, and has left minor features that are interpreted as volcanic. The craters (such as Eratosthenes and Aristoteles) display well developed, but partly subdued, ejecta deposits and secondary craters. No rays have been recognized. Crater rims are ragged, and crater floors are not filled with later material.

The time when the Eratosthenian period ended and the Copernican period started is not known. The Copernican age craters (such as Copernicus, Tycho, and Kepler) are fresh and well-defined ejecta, secondary craters, and rays. The crater rims are sharp and the crater floors are deep and are not filled with deposits.

APOLLO LANDING SITES

Figure 1-9 locates the six Apollo and three Luna landing sites on a map of the near side of the Moon. Apollo 11 and 12 and Luna 16 and 24 are mare sites; Apollo 14 and 16 and Luna 20 are highland sites; and Apollo 15 and 17 are combined mare and highland sites. Figures 1-10 to 1-14 are sketch maps of Apollo sites 12 to 17 that show the locations of samples and stations. There is no map for Apollo 11; all samples were collected within 10 meters of the lunar module (LM).

OTHER INFORMATION SOURCES

1. Head, James W., III: Lunar Volcanism in Space and Time. Rev. Geophys. Space Phys., vol. 14, 1976, pp. 265-300.

2. Howard, K. A.; and Wilhelms, D. E.: Lunar Basin Formation and Highland Stratigraphy. Rev. Geophys. Space Phys., vol. 12, 1974, pp. 309-327.

3. Toksoz, M. Nafi: Geophysical Data and the Interior of the Moon. Ann. Rev. Earth Planet. Sci., vol. 2, 1974, pp. 151-177.

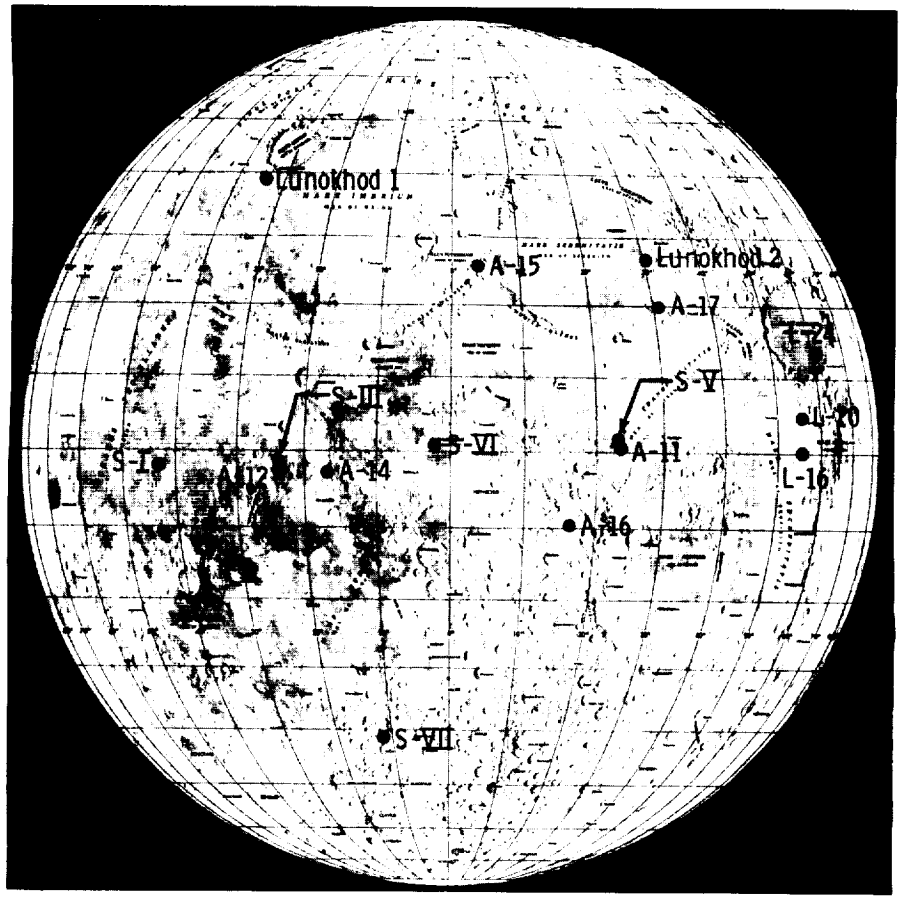

FIGURE 1-9.—Map of the near side of the Moon indicating the locations of landing sites for all missions of exploration (S-I to S-VII are U.S. Surveyor spacecraft, A-11 to A-17 are U.S. Apollo spacecraft, L-16 to L-24 are U.S.S.R. Luna spacecraft, and Lunokhod 1 and 2 are U.S.S.R. spacecraft).

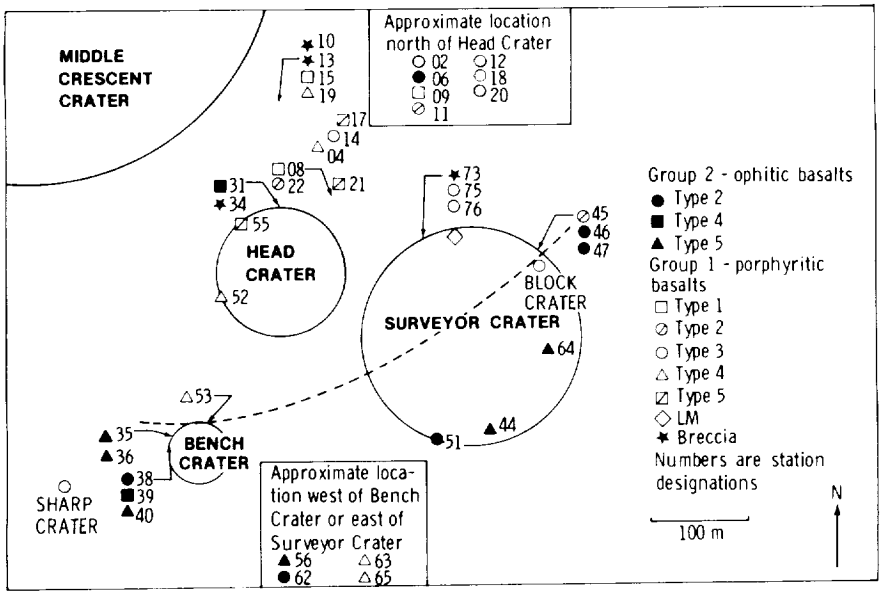

FIGURE 1-10.—Map of the Apollo 12 landing site.

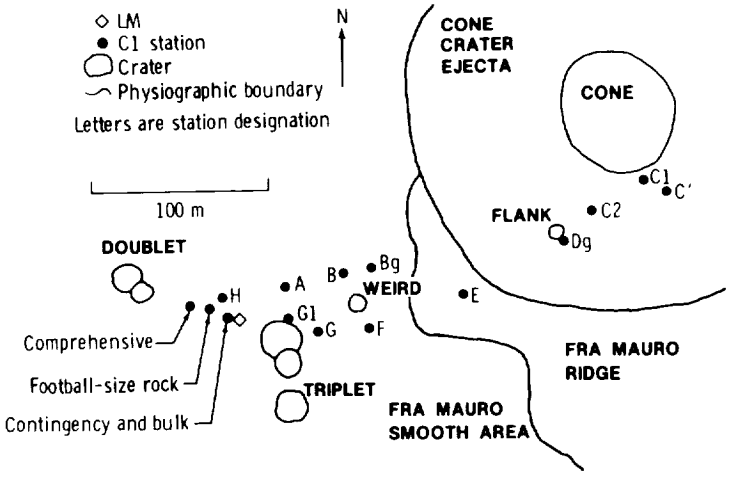

FIGURE 1-11.—Map of the Apollo 14 landing site.

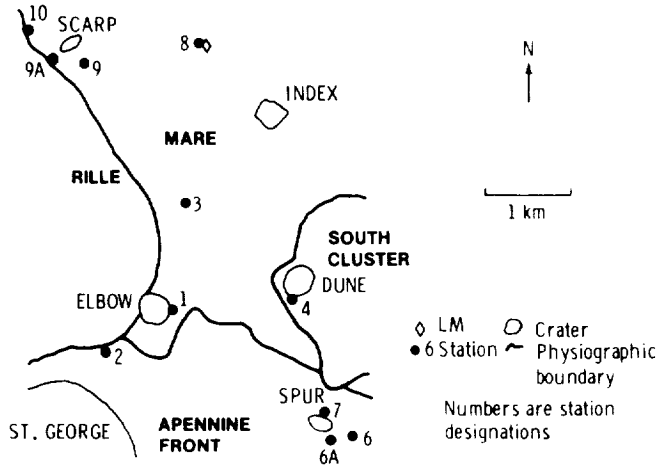

FIGURE 1-12.—Map of the Apollo 15 landing site.

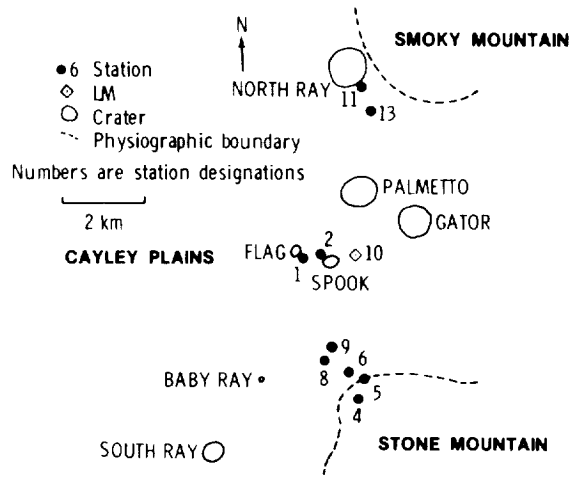

FIGURE 1-13.—Map of the Apollo 16 landing site.

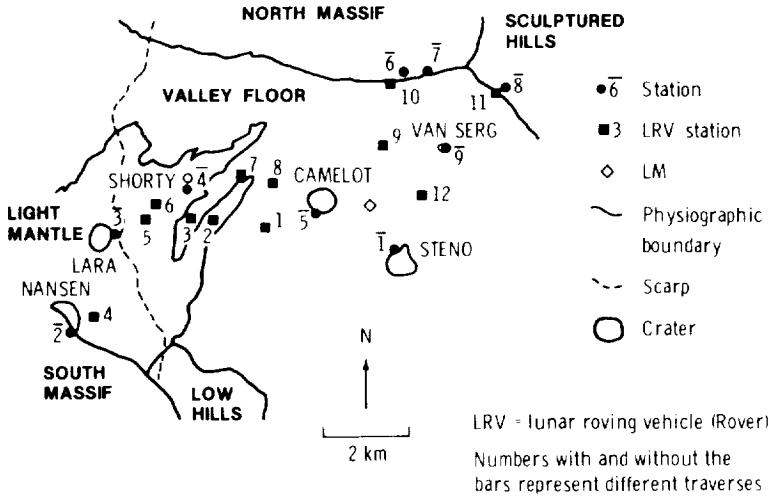

FIGURE 1-14.—Map of the Apollo 17 landing site.

2. Lunar Minerals

The mineralogy of lunar materials is dominated by five minerals: pyroxenes, olivines, plagioclase feldspars, ilmenite, and spinel. A host of other minerals have been reported from analyses of lunar samples; they are listed in table 2-I. The mineral chemistries are presented in more detail in the subsections that follow; however, the following overview will be helpful.

Pyroxene—The basic chemistry of the pyroxenes can be represented by a mixing of the end member minerals: enstatite ($MgSiO_3$), wollastonite ($CaSiO_3$), and ferrosilite ($FeSiO_3$).[1] These are usually abbreviated as En, Wo, and Fs, respectively. There are three structural forms: orthopyroxene, pigeonite (or low-calcium clinopyroxene), and augite (or high-calcium clinopyroxene); they are chemically differentiated by their $CaSiO_3$ content—orthopyroxene lowest and augite highest. All forms have a wide range of enstatite and ferrosilite contents. The minerals accept large amounts of Al (up to 12 percent Al_2O_3), Ti (up to 5 percent TiO_2), Mn (up to 0.5 percent MnO), Cr (up to 1.25 percent Cr_2O_3), and Na (up to 0.2 percent Na_2O) into solid solution. An average chemistry cannot be defined easily.

Olivine—The basic chemistry of the olivines is represented by a solid solution of forsterite (Mg_2SiO_4) and fayalite (Fe_2SiO_4), represented as Fo and Fa. The mineral accepts limited amounts of Ca, Cr, Ti, and Al into solution. There are several ranges of compositions—most are between Fo_{75} and Fo_{50}.

Feldspar—Lunar plagioclase feldspars are solid solutions of anorthite ($CaAl_2Si_2O_8$) and albite ($NaAlSi_3O_8$), An and Ab, respectively. They can contain up to 2 mole percent of orthoclase ($KAlSi_3O_8$).

Ilmenite—Lunar ilmenites are mixtures of ilmenite ($FeTiO_3$) with small amounts of geikielite ($MgTiO_3$). They have a varied minor element chemistry.

Spinel—Spinel minerals are complex mixtures of ulvöspinel (Fe_2TiO_4), chromite ($FeCr_2O_4$), hercynite ($FeAl_2O_4$), picrochromite ($MgCr_2O_4$), spinel ($MgAl_2O_4$), and magnesium-titanate (Mg_2TiO_4). Their chemistries are complex and varied with substitutions of many minor and trace elements reported.

In subsequent portions of this handbook, many of the physical and chemical properties of minerals and some other materials are summarized. These data represent a simplified and condensed form of information that can be found in the "Handbook of Physical Constants," S. P. Clark, Jr., editor,

[1] Compositions of this and other minerals are often reported as mole percent of end member minerals, written as $Wo_2En_{80}Fs_{18}$, for example.

TABLE 2-I.—Lunar Minerals

Major minerals, while variable in abundance, are known to occur in concentrations up to 100 percent. Minor minerals generally occur at less than 2 percent, although some, particularly ilmenite, achieve abundances of 10 percent. Trace minerals never exceed a few tenths of a percent and some are reported only as isolated single grains. Those marked with question marks are controversial with respect to indigenous lunar origin.

Major

Olivine $(Mg, Fe)_2SiO_4$
Pyroxene $(Ca,Mg,Fe)SiO_3$
Plagioclase feldspars
$(Ca,Na)\ Al_2Si_2O_8$

Minor

Spinels $(Fe,Mg,Al,Cr,Ti)O_4$
Armalcolite (Fe_2TiO_5)
Silica (quartz, tridymite, cristobalite) SiO_2
Iron Fe (variable amounts of Ni and Co)
Troilite FeS
Ilmenite $FeTiO_3$

Trace

Phosphates

Apatite[a] $Ca_5(PO_4)_3(F,Cl)_3$
Whitlockite[a] $Ca_9(Mg,Fe)\ (PO_4)_7(F,Cl)$

Zr mineral

Zircon[a] $ZrSiO_4$
Baddeleyite ZrO_4

Silicates

Pyroxferroite $(Fe,Mg,Ca)SiO_3$
Amphibole $(Ca,Mg,Fe)(Si,Al)_8O_{22}F$
Garnet(?)
Tranquilletyite[a] $Fe_8Zr_2Ti_3Si_3O_4$

Sulfides

Mackinawite $(Fe,Ni)_9S_8$
Pentlandite $(Fe,Ni)_9S_8$
Cubanite $CuFe_2S_3$
Chalcopyrite $CuFeS_2$
Sphalerite (Zn,Fe)S

Oxides

Rutile TiO_2
Corrundum(?) Al_2O_3
Hematite(?) Fe_2O_3
Magnetite Fe_3O_4
Goethite(?) FeO(OH)

Metals

Copper(?) Cu
Brass(?)
Tin(?) Sn

Zr-rich mineral

Zirkilite or zirconolite[a] $CuZrTi_2O_7$

Meteoritic minerals

Schreibernite $(Fe,Ni)_3P$
Cohenite (Fe,Ni,Co),C
Niningerite (Mg,Fe,Mn)S
Lawrencite(?) $(Fe,Ni)Cl_2$

[a]These minerals are known to exhibit complex substitutions, particularly of elements like Y, Nb, Hf, U, and the rare earth elements that are concentrated in these minerals.

published by the Geological Society of America (1966), and in "Thermodynamic Properties of Minerals and Related Substances at 298.15 K and One Bar (10^5 Pascals) Pressure and at Higher Temperatures," U.S. Geological Survey, by R. A. Robie, B. S. Hemingway, and J. R. Fisher. These data are always referenced to the stable form of the materials or elements at the cited temperature and at 10^5 N/m^2.

Some data are presented on melting and transformation points—that is, on the phase chemistry of minerals. There is, unfortunately, no single source from which all the relevant information on phase chemistry can be extracted. The best source for basic information is "Phase Diagrams for Ceramists," 1964 and 1969 Supplement, by E. M. Levin, C. R. Robbins, and H. F. McMurdie, published by the American Ceramics Society, Inc.

Finally, the mineralogical data presented here are highly abstracted. More complete data are available in "Rock Forming Minerals," five volumes by W. A. Deer, R. A. Howie, and J. Zussman, published by John Wiley and Sons, Inc.

OTHER INFORMATION SOURCES

More detailed discussions of lunar mineralogy may be found in the following sources:

1. Papike, J. J.; Hodges, F. N.; Bence, A. E.; Cameron, M.; and Rhodes, J. M.: Mare Basalts: Crystal Chemistry, Mineralogy and Petrology. Rev. Geophys. Space Phys., vol. 14, 1976, pp. 475-540.

2. Smith, J. V.: Lunar Mineralogy: A Heavenly Detective Story. Presidential Address, Part I, Amer. Mineralogist, vol. 59, 1974, pp. 231-243; Part II, Amer. Mineralogist, vol. 61, 1976, pp. 1059-1116.

PYROXENE

Pyroxenes are mixtures of the minerals enstatite ($MgSiO_3$), wollastonite ($CaSiO_3$), and ferrosilite ($FeSiO_3$), abbreviated En, Wo, and Fs respectively. There are three structural forms: orthopyroxene, pigeonite (low-calcium clinopyroxene), and augite (high-calcium clinopyroxene). All forms have a wide range of enstatite and ferrosilite contents and accept large amounts of Al (up to 12 percent Al_2O_3), Ti (up to 5 percent TiO_2), Mn (up to 0.5 percent MnO), Cr (up to 1.25 percent Cr_2O_3), and Na (up to 0.2 percent Na_2O) into solid solution. Average chemistry is not easily defined. The occurrence of pyroxene on the lunar surface is shown in table 2-II, and two analyses of typical pyroxenes are given in table 2-III.

Pyroxenes are potential ores for silicon, calcium, magnesium, oxygen, and possibly aluminum and iron. Based upon the occurrence shown in table 2-II, mare basalts may be considered ores for lunar pyroxenes.

TABLE 2-II.—Abundance of Lunar Pyroxene

Lunar material	*Percent pyroxene, vol.%*	*Comments*
Mare basalts	40 to 65	A few samples contain less pyroxene (as low as 30 percent in some cases and down to 5 percent in one vitrophyre).
Anorthositic rocks	0 to 40	Pyroxene in these rocks is mostly Ca-poor.
Fragmental breccias	5 to 30	The quoted value is for mineral grains more than 25 micrometers across.
Soils	5 to 20	The pyroxene composition and amount resembles that of the local rocks. Pyroxene is high-Ca in mare regions and low-Ca in highland regions.

TABLE 2-III.—Analyses of Typical Lunar Pyroxenes

Compound	*Mare,* [a] *wt.%*	*Highland,* [b] *wt.%*
SiO_2	47.84	53.53
TiO_2	3.46	.90
Cr_2O_3	.80	.50
Al_2O_3	4.90	.99
FeO	8.97	15.42
MnO	.25	.19
MgO	14.88	26.36
CaO	18.56	2.43
Na_2O	.07	.06
Total	99.73	100.39

[a]Pyroxene 74255; from reference 2-1.
[b]Pyroxene 72395; from reference 2-2.

The following data summarize the physical properties of enstatite, wollastonite, and ferrosilite. Many of these data are taken from studies of analogous terrestrial or synthetic materials.

Physical Properties of Pyroxenes

1. Density and Molar Volume:

Density of a pyroxene group, g/cm^3 ..... 2.8 to 3.7
(at room temp. and 1 atmosphere)
Mean density for eight samples of pyroxenite, g/cm^3 ..... 3.231
(Range: 3.10 to 3.318)

Enstatite, $MgSiO_3$

Density, g/cm^3 ..... crystal: 3.175
(at room temp. and 1 atmosphere) glass: 2.743

Enstatite, $MgSiO_3$ (artificial, monoclinic)

Density, g/cm^3 ..... crystal: 3.183
(at room temp. and 1 atmosphere) glass: 2.735

Wollastonite, $CaSiO_3$

Density, g/cm^3 ..... crystal: 2.906
(at room temp. and 1 atmosphere) glass: 2.895

Clinoenstatite, $MgSiO_3$ (monoclinic)

Molar volume, cm^3 ..... 31.47 ± 0.07
Formula weight, g 100.39
Cell volume, cm^3 ..... 417.9×10^{-24}

Enstatite, $MgSiO_3$ (orthorhombic)

Molar volume, cm^3 ..... 31.40 ± 0.07
Formula weight, g 100.41
Cell volume, cm^3 ..... 834.0×10^{-24}

Wollastonite, $CaSiO_3$ (triclinic)

Molar volume, cm^3 ..... 39.94 ± 0.08
Formula weight, g 116.7
Cell volume, cm^3 ..... 397.8×10^{-24}

Parawollastonite, $CaSiO_3$ (monoclinic)

Molar volume, cm^3 ..... 39.67 ± 0.08
Formula weight, g 116.17
Cell volume, cm^3 ..... 790.3×10^{-24}

Pseudowollastonite, $CaSiO_3$ (triclinic)

Molar volume, cm^3 ..... 40.08 ± 0.08
Formula weight, g 116.17
Cell volume, cm^3 ..... 1597.0×10^{-24}

2. X-Ray Crystallographic Data:

Enstatite ($MgSiO_3$)

Crystal system ..... orthorhombic
Space group ..... *Pcab*
Z (gram formula weights per unit cell) 16
Unit cell base vector magnitudes: (at 299 K (26° C))
$a_o = 8.829 \pm 0.01$ Å (1 Å = 10^{-10} meter)
$b_o = 18.22 \pm 0.01$ Å
$c_o = 5.192 \pm 0.01$ Å
$\alpha_o = \beta_o = \gamma_o = 90°$
Note: α_o = angle subtended by **b** and **c**
β_o = angle subtended by **a** and **c**
γ_o = angle subtended by **a** and **b**

Clinoenstatite ($MgSiO_3$)

Crystal system ..... monoclinic
Space group ..... $P2_1/C$
Structure type ..... diopside
Z (gram formula weights per unit cell) 8
Unit cell base vector magnitudes: (at room temp.)
$a_o = 9.618 \pm 0.005$ Å (1 Å = 10^{-10} meter)
$b_o = 8.825 \pm 0.005$ Å
$c_o = 5.186 \pm 0.005$ Å
α_o or α_r (angle subtended by **b** and **c**) = 90°
β_o (angle subtended by **a** and **c**) = 108°21′ ± 5′
γ_o (angle subtended by **a** and **b**) = 90°

Wollastonite ($CaSiO_3$)

Crystal system ..... triclinic
Space group ..... $P\bar{1}$
Structure type ..... wollastonite
Z (gram formula weights per unit cell) 6

Unit cell base vector magnitudes: (at room temp.)
$a_o = 7.94 \pm 0.01$ Å (1 Å $= 10^{-10}$ meter)
$b_o = 7.32 \pm 0.01$ Å
$c_o = 7.07 \pm 0.01$ Å
α_o or α_r (angle subtended by **b** and **c**) $= 90°02' \pm 15'$
β_o (angle subtended by **a** and **c**) $= 95°21' \pm 15'$
γ_o (angle subtended by **a** and **b**) $= 103°26' \pm 15'$

Parawollastonite ($CaSiO_3$)

Crystal system ..... monoclinic
Space group ..... $P2_1$
Z (gram formula weights per unit cell) 12
Unit cell base vector magnitudes: (at room temp.)
$a_o = 15.417 \pm 0.004$ Å (1 Å $= 10^{-10}$ meter)
$b_o = 7.321 \pm 0.002$ Å
$c_o = 7.066 \pm 0.002$ Å
α_o or α_r (angle subtended by **b** and **c**) $= 90°$
β_o (angle subtended by **a** and **c**) $= 95°24' \pm 3'$
γ_o (angle subtended by **a** and **b**) $= 90°$

Pseudowollastonite ($CaSiO_3$)

Crystal system ..... triclinic
Space group ..... $P\bar{1}$
Z (gram formula weights per unit cell) 24
Unit cell base vector magnitudes: (at room temp.)
$a_o = 6.90 \pm 0.02$ Å (1 Å $= 10^{-10}$ meter)
$b_o = 11.78 \pm 0.02$ Å
$c_o = 19.65 \pm 0.02$ Å
α_o or α_r (angle subtended by **b** and **c**) $= 90°$
β_o (angle subtended by **a** and **c**) $= 90°48' \pm 15'$
γ_o (angle subtended by **a** and **b**) $= 119°18'$

3. Thermal Expansion:

Mineral	*Symmetry and orientation*	*Expansion,[a] in percent, from 20° C to —*						
		100° C	*200° C*	*400° C*	*600° C*	*800° C*	*1000° C*	*1200° C*
Enstatite	Ortho, vol[b]	0.18	0.45	1.05	1.74	2.28	—	—
Clinoenstatite	Mono, vol	.19	.42	.96	1.61	2.28	2.95	3.68
Pseudowollastonite	Tri, vol	.24	.52	1.12	1.76	2.52	3.28	4.03
	Wollastonite-ferrosilite solid solutions[c]							
$Wo_{69}Fs_{31}$	Tri, vol	0.12	0.30	0.69	1.08	—	—	—
$Wo_{45}Fs_{55}$	Tri, vol	.12	.30	.72	1.20	—	—	—

[a]Data reported in Celsius ($T_K = T_C + 273.15$).
[b]vol = volumetric expansion.
[c]Composition in mole percent.

4. Compressibility and Elastic Constants:

$$\frac{V_o - V}{V_o} = aP - bP^2$$

where: V = volume
V_o = initial volume
P = pressure in megabars (Mb)
a = proportional limit
b = elastic limit

Form	a, Mb^{-1}	b, Mb^{-2}	*Remarks (a)*
Enstatite ($En_{88}Fs_{12}$)	1.01	—	Mean value for 2 to 12 kb, $\rho = 3.254$

[a]ρ = density.

Values of Elastic Constants for Terrestrial Samples of Pyroxenite

Sample (a)	*Density, g/cm³*	*Young's modulus,[b] Mb*	*Modulus of rigidity,[b] Mb*	*Poisson's ratio*	*Notes (c)*
Bronzitite (Stillwater Complex, Montana)					
#1	3.27	1.513	0.654	(0.156)[d]	D
$P = 500$			.681		D
$P = 4000$			.692		
#2		1.526	.648	(.177)[d]	D
$P = 500$			.666		D
$P = 4000$			.680		
$P = 1$	3.287		.660		D
$P = 10\ 000$			.714		
Bronzitite (Bushveld Complex, Transvaal)					
	3.28	1.557	0.628	(0.239)[d]	D
$P = 500$			.665		D
$P = 4000$			.680		
Bronzitite (Star Lake, St. Lawrence Co., New York)					
Fresh (moderately altered)	3.43	1.24	0.50		D
	3.31	1.13	.41		

[a]The notation "$P = 500$," for example, indicates measurement made under hydrostatic pressure of 500 bars. Where no notation is given, pressure is one atmosphere.
[b]Original data reported in megabars (1 Mb = 10^{11} N/m^2).
[c]The symbol "D" indicates dynamic measurement.
[d]Values in parentheses were obtained indirectly with the aid of formulas for isotropic elasticity.

5. Seismic Velocities:

Compressional Wave Velocities, V_p, as a Function of Pressure

Rock	*Density,*	V_p, *in km/sec, for pressures[a] of —*						
		10	*500*	*1000*	*2000*	*4000*	*6000*	*10 000*
Pyroxenite (Sonoma Co., California)	3.247	6.8	—	7.73	7.79	7.88	7.93	9.01
Wollastonite	2.873	—	—	7.21	7.42	7.56	7.64	7.71

[a]Original data reported in bars (1 bar = 10^5 N/m^2).

6. Strength and Ductility:

Stress-Strain Relationship

Temp., K	*Confining pressure, bars*[a]	*Differential stress in bars for strain percent of —*				*Ultimate strength, bars*	*Total strain, percent*	*Fault angle, deg*
		1	*2*	*5*	*10*			
				Pyroxenite (California)				
297	5070	12 230	16 500	16 660	—	17 350	9.8	—
573	5070	6 370	9 630	11 650	12 500	12 350	10.3	—
773	5070	4 400	7 400	8 400	9 100	9 300	25.9	—
[b]773	5070	3 400	4 200	4 000	3 400	4 250	23.6	—
1073	5070	3 300	5 000	6 700	6 700	6 700	12.1	—
				Pyroxenite (North Carolina)				
423	1010	1 600	4 150	—	—	5 310	3.1	28
773	5050	2 940	5 660	6 150	6 400	6 400	14.4	37

[a]Original data reported in bars (1 bar = 10^5 N/m^2).
[b]Extension test.

Shearing Strength Under High Confining Pressure

Normal pressure of — in kilobars	*Shear strength, kilobars*
Pyroxene [a]	
10	1.4
20	4.4
30	8
40	11
50	15
Pyroxenite [b]	
10	2.7
20	6.3
30	9
40	12
50	14

[a]Rotates with snapping, radial fibers.
[b]Rotates with snapping.

7. Viscosity:

Viscosity of Wollastonite Glass (at 1 atmosphere)[a]

Temperature, °C	*Viscosity, poises*
1550	2.73
1600	2.40
1650	2.38

[a]Data reported in customary units of measurement (1 atm = 1.013×10^5 N/m^2; $T_K = T_C + 273.15$; 1 poise = 10^{-1} N sec m^{-2}).

8. Melting and Transformation Points:

Enstatite, clinoenstatite ($MgSiO_3$)

Incongruent melting point to forsterite and liquid (60.9% SiO_2), K (°C) ..... 1830 ± 2 (1557 ± 2)
Dimorphous transition, K (°C) 1413 (1140)
(transition point to rhombohedral-monoclinic)
Eutectic with cristobalite, K (°C) ..... 1816 ± 2 (1543 ± 2)
(64.9% SiO_2)

Wollastonite ($CaSiO_3$)

Melting point, K (°C) ..... 1813 ± 2 (1540 ± 2)
Dimorphous transition, K (°C) ..... 1423 ± 10 (1150 ± 10)
Eutectic with tridymite, K (°C) ..... 1709 ± 5 (1436 ± 5)
(63% SiO_2)

Clinoferrosilite ($FeSiO_3$)

Ideal Fe limit of monoclinic pyroxenes, crystals in obsidian from Kenya and elsewhere; may exist in system only at low temperature.

9. Thermodynamic Properties:

Enstatite, $MgSiO_2$(clinoenstatite)

Crystals ..... 298.15 K to melting point 1830 K
Formula weight, g 100.39
Molar volume, cm^3 (J/bar) ..... 31.47 ± 0.07 (3.1470)

Wollastonite ($CaSiO_3$)

Crystals ..... 298.15 to 1400 K
(Note: Pseudowollastonite is the stable phase above 1398 K.)
Formula weight, g 116.16
Molar volume, cm^3 (J/bar) ..... 39.93 ± 0.08
(3.9930)

$C_p^o = 1.1125 \times 10^2 + 1.4373 \times 10^{-2} T + 16.936 T^{-0.5} - 2.7779 \times 10^6 T^{-2}$
(for 298 to 1400 K)
$S_T^o = 82.01 \pm 0.84$ J mol^{-1} K^{-1} (at 298.15 K)
$H_{298}^o - H_o^o =$ (not available)
Enthalpy of melting = (not available)

Formation From the Elements

Temperature, K	*Enthalpy, kJ/mol*	*Gibbs free energy, kJ/mol*
298.15	−1635.220 (±1.435)	−1549.903 (±1.455)
500	−1634.080	−1492.315
700	−1634.979	−1435.980
900	−1630.931	−1380.021
1100	−1630.186	−1324.375
1300	−1635.498	−1267.573
1400	−1633.657	−1239.362

Formation From the Oxides

Temperature, K	*Enthalpy, kJ/mol*	*Gibbs free energy, kJ/mol*
298.15	−89.431 (±0.540)	−90.128 (±0.860)
500	−89.435	−90.590
700	−89.866	−91.000
900	−91.101	−91.173
1100	−90.969	−91.201
1300	−90.719	−91.252
1400	−90.561	−91.318

9. Thermodynamic Properties (continued):

$C_p^o = 2.0556 \times 10^2 - 1.2796 \times 10^{-2} T - 2.2977 \times 10^3 T^{-0.5} + 1.1926 \times 10^6 T^{-2}$
(for 298 to 1600 K)
$S_T^o = 67.86 \pm 0.42$ J mol^{-1} K^{-1} (at 298.15 K)
$H_{298}^o - H_o^o = 12.113$ kJ
where: C_p^o = molar heat capacity, H_{298}^o = enthalpy, H_o^o = enthalpy at absolute zero, S_T^o = entropy, and T = temperature in kelvin.
Enthalpy of melting = 61.505 kJ

Formation From the Elements

Temperature, K	*Enthalpy, kJ/mol*	*Gibbs free energy, kJ/mol*
298.15	−1547.750 (±1.215)	−1460.883 (±1.225)
500	−1457.927	−1401.912
700	−1546.686	−1343.693
900	−1544.911	−1285.909
1100	−1551.881	−1226.831
1300	−1549.616	−1167.924
1500	−1673.000	−1096.489
1600	−1670.609	−1058.122

Formation From the Oxides

Temperature, K	*Enthalpy, kJ/mol*	*Gibbs free energy, kJ/mol*
298.15	−35.560 (±0.630)	−35.339 (±0.650)
500	−36.085	−35.180
700	−36.972	−34.669
900	−38.300	−33.846
1100	−38.098	−32.874
1300	−37.819	−31.956
1500	−37.632	−31.062
1600	−37.608	−30.616

9. Thermodynamic Properties (continued):

Pseudowollastonite ($CaSiO_3$)

Crystals ..... 298.15 K to melting point 1817 K
Formula weight, g 116.16
Molar volume, cm^3 (J/bar) ..... 40.08 ± 0.08 (4.0080)

$C_p^o = 1.0710 \times 10^2 + 1.7481 \times 10^{-2} T - 2.2965 \times 10^6 T^{-2}$ (for 298 to 1700 K)
$S_T^o = 87.45 \pm 0.84$ J mol^{-1} K^{-1} (at 298.15 K)
$H_{298}^o - H_o^o =$ (not available)
Enthalpy of melting = 27.405 kJ

Formation From the Elements

Temperature, K	*Enthalpy, kJ/mol*	*Gibbs free energy, kJ/mol*
298.15	−1628.650 (±2.594)	−1544.955 (±2.636)
500	−1627.619	−1488.464
700	−1625.838	−1433.115
900	−1625.091	−1378.051
1100	−1624.563	−1323.240
1300	−1629.991	−1267.253
1500	−1626.211	−1211.715
1700	−1672.430	−1156.285

Formation From the Oxides

Temperature, K	*Enthalpy, kJ/mol*	*Gibbs free energy, kJ/mol*
298.15	−82.861	−85.180
500	−82.974	−86.739
700	−83.725	−88.135
900	−85.261	−89.203
1100	−85.346	−90.066
1300	−85.212	−90.932
1500	−84.889	−91.834
1700	−84.395	−92.793

Ferrosilite ($FeSiO_3$)

No generally acceptable data are available for ferrosilite because the compound is unstable. However, the free energy of the reaction

$$Fe + SiO_2 + 1/2\,O_2 = FeSiO_3$$

has been determined indirectly

$$\Delta G_f = 244\,460 + 45.90T - 0.1515(P - 1)$$

where G_f = free energy in joules
T = temperature in kelvin
P = pressure in bars (1 bar = 10^5 N/m^2)

10. Electrical Properties:

Resistivity of pyroxenite near 0° C

$$\frac{\text{Resistivity at } -12°\text{ C}}{\text{Resistivity at } 20°\text{ C}} = 32 \qquad (\text{Porosity} = 0)$$

11. Thermal Conductivity:

Pyroxenite

Sample from —	*Conductivity, 10^{-1} cal(cm sec °C)$^{-1}$*	*Density, g/cm^3*
Cleveland Peninsula, S. E. Alaska (mean of three samples)	9.70	3.31
Percy Islands, S. E. Alaska (mean of three samples)	8.68	3.25
Bushveld, Transvaal	11.8	3.29

NOTE: Units of measurement are those of the original data;
1 cal (cm sec °C)$^{-1}$ = 419 J(m sec K)$^{-1}$ and $T_K = T_C + 273.15$.

12. Magnetic Properties:

Not available for lunar materials.

OLIVINE

Olivine is one of the dominant lunar minerals. It is a solid solution of forsterite (Mg_2SiO_4) and fayalite (Fe_2SiO_4), with most compositions between Fo_{75} and Fo_{50} (75 to 50 mole percent forsterite). The occurrence of olivine on the Moon is shown in table 2-IV, and two analyses of typical lunar olivines are given in table 2-V.

Olivine is a potential source of magnesium, iron, silicon, and oxygen. Based on the occurrence shown in table 2-IV, mare basalts may be considered ores for this mineral.

TABLE 2-IV.—Abundance of Lunar Olivine

Lunar material	*Percent olivine, vol.%*	*Comments*
Mare basalts	0 to 35	The olivine content is a function of the detailed chemistry of each mare lava flow.
Anorthositic rocks	0 to 40	Most anorthositic rocks contain only a few percent olivine. Rocks with up to 40 percent olivine are rare. One very rare rock contains 99 percent olivine.
Fragmental breccias	0 to 5	Olivine content is a function of the local rocks. It is higher in regions where local rocks contain olivine.
Crystalline breccias	1 to 5	Olivine in these rocks are usually clasts greater than 50 micrometers across.
Soil	0 to 4	The olivine content is a function of the local rocks.

TABLE 2-V.—Analyses of Typical Lunar Olivine

Compound	*Mare,*[a] *wt.%*	*Highland,*[b] *wt.%*
SiO_2	37.36	37.66
TiO_2	.11	.09
Cr_2O_3	.20	.15
Al_2O_3	<.01	.02
FeO	27.00	26.24
MnO	.22	.32
MgO	35.80	35.76
CaO	.27	.16
	<.01	<.01
Total	100.97	100.40

[a]Olivine 74255; from reference 2-1.
[b]Olivine 72395; from reference 2-2.

The following data summarize the physical properties of forsterite and fayalite. Many of these data are taken from studies of analogous terrestrial or synthetic materials.

Physical Properties of Olivine

1. Density and Molar Volume:

Forsterite (Mg_2SiO_4)

Density, g/cm^3 ..... 3.19 to 3.21
(at room temp. and 10^5 N/m^2 (1 bar))
Molar volume, cm^3 ..... 43.79 ± 0.03
Formula weight, g 140.694
Cell volume, cm^3 ..... 290.8×10^{-24}

Fayalite (Fe_2SiO_4)

Density, g/cm^3 ..... 4.39
(at room temp. and 10^5 N/m^2 (1 bar))
Molar volume, cm^3 ..... 46.39 ± 0.08
Formula weight, g 203.79
Cell volume, cm^3 ..... 308.1×10^{-24}

2. X-Ray Crystallographic Data:

Forsterite (Mg_2SiO_4)

Crystal system ..... orthorhombic
Space group ..... *Pbnm*
Structure type ..... olivine
Z (gram formula weights per unit cell) 4
Unit cell base vector magnitudes: (at 298 K (25° C))
$a_o = 4.758 \pm 0.002$ Å (1 Å = 10^{-10} meter)
$b_o = 10.214 \pm 0.003$ Å
$c_o = 5.984 \pm 0.002$ Å
$\alpha_o = \beta_o = \gamma_o = 90°$
Note: α_o = angle subtended by **b** and **c**.
β_o = angle subtended by **a** and **c**.
γ_o = angle subtended by **a** and **b**.

Fayalite (Fe_2SiO_4)

Crystal system ..... orthorhombic
Space group ..... *Pbnm*
Structure type ..... olivine
Z (gram formula weights per unit cell) 4
Unit cell base vector magnitudes: (at room temp.)
$a_o = 4.817 \pm 0.005$ Å (1 Å = 10^{-10} meter)
$b_o = 10.477 \pm 0.005$ Å
$c_o = 6.105 \pm 0.010$ Å
$\alpha_o = \beta_o = \gamma_o = 90°$

3. Thermal Expansion:

Composition	*Symmetry and orientation*	*Expansion,*[a] *in percent, from 20° C to —*						
		100° C	*200° C*	*400° C*	*600° C*	*800° C*	*1000° C*	*1200° C*
$Fa_{41}Fo_{59}$	Ortho, vol[b]	0.21	0.51	1.11	1.80	2.55	3.24	—
$Fa_{15}Fo_{85}$	Ortho, vol	.21	.51	1.14	1.83	2.55	3.24	—
$Fa_{10.1}Fo_{89.9}$	Ortho, ||a	0.04	0.10	0.26	0.43	0.58	0.76	—
	Ortho, ||b	.08	.18	.43	.74	1.04	1.36	—
	Ortho, ||c	.07	.18	.42	.68	.92	1.20	—
	Ortho, vol	.19	.46	1.11	1.85	2.54	3.32	—
Fo_{100}	Ortho, ||a	0.06	0.15	0.34	0.56	0.80	1.04	1.32
	Ortho, ||b	.07	.19	.47	.78	1.10	1.43	1.78
	Ortho, ||c	.07	.18	.42	.69	1.00	1.34	1.71
	Ortho, vol	.20	.52	1.24	2.05	2.92	3.86	4.88

[a]Original data reported in Celsius ($T_K = T_C + 273.15$).
[b]vol = volumetric expansion.

4. Compressibility and Elastic Constants:

$$\frac{V_o - V}{V_o} = aP - bP^2$$

where: V = volume
V_o = initial volume
P = pressure in megabars (Mb)
a = proportional limit
b = elastic limit

Form	a, Mb^{-1}	b, Mb^{-2}	*Remarks* (*a*)
Forsterite:			
Olivine (dunite)	0.79	—	mean value for 2 to 12 kb, $\rho = 3.288$
Peridot (Red Sea)	.82	1	$\rho = 3.364$
Peridot (Burma)	[b].77	—	$\rho = 3.324$
Fayalite	0.91	—	mean value for 2 to 12 kb, $\rho = 4.068$

[a] ρ = density
[b] Value derived from elastic constants.

The following table lists values of $(V_o - V)/V_o$ at pressures above 12 kilobars for olivine ($\rho = 3.364$).

Pressure, kg/cm^2	$\frac{V_o - V}{V_o}$
10 000	0.0079
20 000	.0156
30 000	.0231
40 000	.0304

Elastic constants may be obtained from the following relationships for the Voigt and Reuss schemes.

	Voigt	*Reuss*
Bulk modulus	$K = (A + 2B)/3$	$K = 1/(3a + 6b)$
Modulus of rigidity	$G = (A - B + 3C)/5$	$G = 5/(4a - 4b + 3c)$
with	$3A = C_{11} + C_{22} + C_{33}$	$3a = S_{11} + S_{22} + S_{33}$
	$3B = C_{23} + C_{13} + C_{12}$	$3b = S_{23} + S_{13} + S_{12}$
	$3C = C_{44} + C_{55} + C_{66}$	$3c = S_{44} + S_{55} + S_{66}$

where C_{pq} and S_{pq} refer to the individual crystal.

Values of C_{pq} and S_{pq} for olivine ($Fo_{92}Fa_8$, $\rho = 3.324$) are as follows:

$C_{11} = 3.24$	$C_{66} = 0.793$	$S_{11} = 0.343$	$S_{66} = 1.261$
$C_{22} = 1.98$	$C_{12} = 0.59$	$S_{22} = 0.588$	$S_{12} = -0.067$
$C_{33} = 2.49$	$C_{13} = 0.79$	$S_{33} = 0.481$	$S_{13} = -0.089$
$C_{44} = 0.667$	$C_{23} = 0.78$	$S_{44} = 1.499$	$S_{23} = -0.163$
$C_{55} = 0.810$		$S_{55} = 1.24$	

4. Compressibility and Elastic Constants (continued):

Values of Elastic Constants for Terrestrial Samples of Olivine

Sample (a)	*Density, g/cm³*	*Young's modulus,[b] Mb*	*Modulus of rigidity,[b] Mb*	*Poisson's ratio*	*Notes (c)*
		Olivine (Vinalhaven, Maine)			
#1	2.96	1.020		0.271	11
		1.015		.271	56
		1.070	0.421		D
#7 $P=500$			.430		
$P=4000$			.439		
		Dunite (New Zealand)			
#1		1.52	0.60	[d](0.27)	D
#2		1.62	.58	[d](.40)	
$P=4\,000$	3.270		.647		D
$P=10\,000$			.674		
		Olivine (Balsam Gap, North Carolina)			
#1	3.275	0.946	0.56		D
$P=500$			.64		
$P=4000$			.67		
#2		1.484	.476		
$P=500$			.654		
$P=4000$			.694		
#3			.624		
$P=500$			.681		
$P=4000$			.706		
#4			.570		
$P=500$			.612		
$P=4000$			.658		
#1L		.89			D
#2L		1.61			D
		Olivine (Twin Sisters Mt., Washington)			
#1	3.312	1.95	0.74		D
#2		1.4	.66		
#3			.72		
$P=4\,000$	3.326		.757		D
$P=10\,000$			.776		

4. Compressibility and Elastic Constants (continued)

Values of Elastic Constants for Terrestrial Samples of Olivine—Continued

Sample (a)	*Density, g/cm³*	*Young's modulus,[b] Mb*	*Modulus of rigidity,[b] Mb*	*Poisson's ratio*	*Notes (c)*
		Dunite (Mooihoek Mine, Transvaal)			
#1	3.760		0.509		D
P=10 000			.572		

[a]The notation "*P*=500," for example, indicates measurement made under hydrostatic pressure of 500 bars. Where no notation is given, pressure is one atmosphere.
[b]Original data reported in megabars (1 Mb = 10^{11} N/m^2).
[c]The symbol "D" indicates dynamic measurement; a number (e.g., 11) indicates stress (in bars) for static measurements.
[d]Values in parentheses were obtained indirectly with the aid of formulas for isotropic elasticity.

Parameters[a] for Dunite (at 4 × 10^8 N/m^2 (4 Kilobars))

Type	*Density, g/cm³*	V_p, *km/sec*	V_S, *km/sec*	*Poisson's ratio*	*Young's modulus, Mb*	*Modulus of rigidity, Mb*	B, Mb^{-1}	β, Mb^{-1}
Balsam Gap, North Carolina	3.267	8.13	4.57	0.27	1.73	0.68	0.80	0.83
Twin Sisters Mt., Washington	3.312	8.32	4.86	.24	1.94	.78	.80	—

[a]Symbols are as follows:
V_p = particle velocity
V_S = shock front velocity
β = compressibility (experimentally observed)
B = compressibility (calculated)

$$B = -\frac{1}{V}\left(\frac{\delta V}{\delta P}\right)_T = \frac{1}{\rho}\left(\frac{\delta \rho}{\delta P}\right)_T$$

where V = volume
δV = decrease in volume
P = pressure
δP = increase in pressure
T = temperature
ρ = density

5. Seismic Velocities:

Dunite: Laboratory Determination of Compressional Wave Velocity, V_p, and Shear Wave Velocity, V_s

Sample from—	V_p, *km/sec*	V_s, *km/sec*	*Remarks*[a]
Jackson City, North Carolina	7.40	3.79	200 bars
Twin Sisters, Washington	8.60	4.37	70 bars

[a]Number indicates pressure; original measurements reported in bars (1 bar = 10^5 N/m^2).

Dunite: Compressional Wave Velocities, V_p, as a Function of Pressure

Sample from—	*Density, g/cm*^{3}	V_p, *in km/sec, for pressures*[a] *of—*						
		10	*500*	*1000*	*2000*	*4000*	*6000*	*10 000*
Webster, North Carolina	3.244	7.0	—	7.54	7.59	7.65	7.69	7.78
Mt. Dan, New Zealand	3.258	7.5	7.69	7.75	7.80	7.86	7.92	8.00
Balsam Gap, North Carolina	3.267	7.0	7.82	7.89	8.01	8.13	8.19	8.28
Addie, North Carolina	3.304	7.70	—	7.99	8.05	8.14	8.20	8.28
Twin Sisters, Washington	3.312	7.7	8.11	8.19	8.27	8.32	8.35	8.42

[a]Original data reported in bars (1 bar = 10^5 N/m^2).

Dunite: Shear Wave Velocities, V_s, as a Function of Pressure

Sample from—	*Density, g/cm*^{3}	V_s, *in km/sec, for pressures*[a] *of—*						
		1	*500*	*1000*	*2000*	*4000*	*6000*	*10 000*
Webster, North Carolina	3.264	4.01	4.25	4.28	4.30	4.33	4.36	4.40
Mt. Dan, New Zealand	3.270	4.17	4.34	4.37	4.41	4.45	4.48	4.54
Twin Sisters, Washington	3.326	4.60	4.67	4.69	4.72	4.77	4.79	4.83

[a]Original data reported in bars (1 bar = 10^5 N/m^2).

6. Strength and Ductility:

Stress-Strain Relationship—Peridotite (Dan Mountain, New Zealand)[a]

Temp., K	*Confining pressure, bars*[a]	*Differential stress in bars for strain percent of—*				*Ulitmate strength, bars*	*Total strain, percent*	*Fault angle, deg*
		1	*2*	*5*	*10*			
297	5070	19 000	22 000	20 200	—	22 500	8.1	27, 33
573	5070	12 000	14 070	14 600	15 400	15 450	10.4	34
773	5070	5 400	8 700	10 350	10 750	10 800	10.9	32, 37
1073	5070	4 200	6 000	8 000	8 400	8 500	13.4	31, 36
[b]1073	5070	1 230	1 870	—	—	1 870	3.1	15, 28

[a]Data are for short-time triaxial compression tests. Orientation of the load is normal to bedding, foliation, fissility, or cleavage. Original data reported in bars (1 bar = 10^5 N/m^2).
[b]Extension test.

7. Viscosity:

Not available for lunar material.

8. Melting and Transformation Points:

Forsterite (Mg_2SiO_4)

Melting point, K (°C) ..... 2163 ± 20 (1890 ± 20)
Eutectic with MgO, K (°C) ..... 2123 ± 20 (1850 ± 20)
(36% SiO_2)

Fayalite (Fe_2SiO_4)

Melting point K (°C) ..... 1478 ± 2 (1205 ± 2)
Eutectic with wustite (Fe_{1+x}), K (°C) ..... 1450 ± 5 (1177 ± 5)
(24% SiO_2)
Eutectic with tridymite, K (°C) ..... 1451 ± 2 (1178 ± 2)
(38% SiO_2)

9. Thermodynamic Properties:

Forsterite (Mg_2SiO_4)

Crystals ..... 298.15 K to melting point 2163 K
Formula weight, g 140.694
Molar volume, cm^3 (J/bar) 43.79 (4.3790)

$C_p^o = 2.2798 \times 10^2 + 3.4139 \pm 10^{-3}T - 1.7446 \pm 10^3 T^{-0.5}$
$-8.9397 \pm 10^5 T^{-2}$
(for 298 to 1800 K)
$S_T^o = 95.19 \pm 0.84$ J mol^{-1} K^{-1} (at 298.15 K)
$H^o_{298} - H^o_o = 17.276$ kJ
Enthalpy of melting = (not available)

where C_p^o = molar heat capacity, H^o_{298} enthalpy, H^o_o = enthalpy at absolute zero, S_T^o = entropy, and T = temperature in kelvin.

Formation From the Elements

Temperature, K	*Enthalpy, kJ/mol*	*Gibbs free energy, kJ/mol*
298.15	−2170.370 (±1.325)	−2051.325 (±1.345)
500	−2170.223	−1970.578
700	−2168.114	−1891.067
900	−2165.522	−1812.218
1100	−2180.644	−1730.534
1300	−2177.196	−1648.995
1500	−2424.752	−1542.240
1700	−2466.061	−1424.709
1800	−2461.018	−1363.610

Formation From the Oxides

Temperature, K	*Enthalpy, kJ/mol*	*Gibbs free energy, kJ/mol*
298.15	−56.690 (±.610)	−56.645 (±.660)
500	−57.079	−56.509
700	−57.637	−56.194
900	−58.560	−55.663
1100	−57.810	−55.094
1300	−56.709	−54.706
1500	−55.337	−54.482
1700	−53.704	−54.452
1800	−52.783	−54.546

Fayalite (Fe_2SiO_4)

Crystals ..... 298.15 K to melting point 1490 K
Liquid ..... 1490 to 2000 K
Formula weight, g 203.778
Molar volume, cm^3 (J/bar) 46.39 (4.6390)
$C_p^o = 1.7276 \times 10^2 - 3.4055 \times 10^{-3}T + 2.2411 \times 10^{-5}T^2 - 3.6299 \times 10^6 T^{-2}$
(for 298 to 1490 K)
S_T^o = 148.32 ± 1.67 J mol^{-1} K^{-1} (at 298.15 K)
$H_{298}^o - H_o^o$ = (not available)
Enthalpy of melting = 92.173 kJ

9. Thermodynamic Properties (continued):

Formation From the Elements

Temperature, K	*Enthalpy, kJ/mol*	*Gibbs free energy, kJ/mol*
298.15	− 1479.360 (±2.410)	− 1379.375 (±2.470)
500	− 1476.520	− 1312.315
700	− 1473.253	− 1247.269
900	− 1471.590	− 1182.918
1100	− 1474.434	− 1118.527
1300	− 1471.098	− 1054.104
1500	− 1371.630	− 990.572
1700	− 1411.469	− 940.134
1800	− 1405.691	− 912.531

Formation From the Oxides

Temperature, K	*Enthalpy, kJ/mol*	*Gibbs free energy, kJ/mol*
298.15	−24.574	−20.775
500	−25.718	−17.809
700	−26.850	−14.469
900	−28.604	−10.697
1100	−28.496	−6.716
1300	−27.415	−2.820
1500	66.651	.697
1700	29.468	3.124
1800	32.238	5.188

10. Electrical Properties:

Dielectric constant of terrestrial fayalite at radio frequencies

Number of samples	*Dielectric constant, range*
3	7.45 to 8.59

Dielectric constant as a function of frequency for dry dunite (Jackson County, North Carolina)

Frequency	*Dielectric constant*
100 Hz	10
1 kHz	8.47
10 kHz	7.83
100 kHz	7.60
1 MHz	7.37
10 MHz	7.18

11. Thermal Conductivity:

Dunite, Hortonolite from Bushveld, Transvaal

Conductivity, 10^{-3} cal(cm sec °C)$^{-1}$	*Density, g/cm^3*
8.7	3.76

Effect of temperature on conductivity: Dunite, North Carolina (mean of three samples)

Temperature, °C	*Conductivity, 10^{-3} cal(cm sec °C)$^{-1}$*	*Density, g/cm^3*
0	12.4	3.26
50	10.5	—
100	9.4	—
200	8.1	—

Note: Units of measurement are those of the original data; 1 cal(cm sec °C)$^{-1}$ = 419 J(m sec K)$^{-1}$ and $T_K = T_C + 273.15$.

12. Magnetic Properties:

Not available for lunar materials.

PLAGIOCLASE FELDSPAR

Plagioclase feldspar is one of the dominant groups of lunar minerals and occurs in all natural materials found on the lunar surface. The occurrence of plagioclase in lunar materials is given in table 2-VI, and two analyses of lunar plagioclase are given in table 2-VII.

Most lunar feldspars have anorthite contents greater than An_{80}. The mineral anorthite ($CaAl_2Si_2O_8$) is a potential source of aluminum, silicate, silicon, and oxygen—all of which are required for fabrication of structures in space. Based on the known occurrence of plagioclase (table 2-VI), regions of light-matrix breccia may be considered potential ores for lunar plagioclase.

TABLE 2-VI.—Abundance of Plagioclase in Lunar Materials

Lunar material	*Percent plagioclase, vol.%*	*Comments*
Mare basalts	15 to 35	The plagioclase abundance is approximately the same in both high-Ti and low-Ti mare basalts.
Anorthositic rocks	40 to 98	Most anorthositic rocks contain more than 75 percent plagioclase; anorthositic rocks with less than 70 percent plagioclase are rare. Anorthositic rocks are uncommon on the lunar surface and no deposit of anorthositic rocks is known at this time.
Crystalline breccias	50 to 75	These rocks are limited to the lunar highlands.
Vitric breccias	15 to 50	These rocks are very fine grained.
Light-matrix breccias	70 to 90	These rocks are most abundant at North Ray Crater (Apollo 16 site).
Soil	10 to 60	Soils resemble the local bedrock. Thus, soils in mare regions contain little plagioclase whereas soils in highland regions contain more plagioclase.

TABLE 2-VII.—Analyses of Typical Lunar Plagioclase

Compound	*Mare,*[a] *wt.%*	*Highland,*[b] *wt.%*
SiO_2	46.06	46.67
TiO_2	.15	.02
Al_2O_3	33.71	33.51
FeO	.68	.25
MnO	.01	—
MgO	.31	.09
CaO	18.07	17.78
BaO	—	<.01
Na_2O	.67	1.51
K_2O	.04	.13
Total	99.70	99.97

[a]Plagioclase 12021; from reference 2-3.
[b]Plagioclase 72395; from reference 2-2.

The following data summarize the physical properties of anorthite. Many of these data are taken from studies of analogous terrestrial or synthetic materials.

Physical Properties of Anorthite

1. Density and Molar Volume:

Mean density of 12 samples of anorthosite, g/cm^3	2.734
Range of density, g/cm^3	2.640 to 2.920
Density of pure anorthite, g/cm^3 (at room temp. and 1 atmosphere)	2.76
Molar volume, cm^3 (Density: 2.762 ± 0.004 g/cm^3	100.73 ± 0.15
Formula weight, g	278.21

2. X-Ray Crystallographic Data:

Anorthite ($CaAl_2Si_2O_8$)

Crystal system ..... triclinic
Space group ..... $P\bar{1}$
Structure type ..... feldspar
Z (gram formula weights per unit cell) 8
Unit cell base vector magnitudes: (at 298 ± 5 K (25° ± 5° C))
$a_o = 8.1768 \pm 0.002$ Å (1 Å = 10^{-10} meter)
$b_o = 12.8768 \pm 0.003$ Å
$c_o = 14.1690 \pm 0.002$ Å
α_o or $\alpha_r = 93° 10.0' \pm 2'$
(angle subtended by **b** and **c**)
$\beta_o = 115° 50.8' \pm 2'$
(angle subtended by **a** and **c**)
$\gamma_o = 91° 13.3' \pm 2'$
(angle subtended by **a** and **b**)

3. Thermal Expansion:

Plagioclase (Ab_5An_{95})

Orientation	*Expansion,[a] in percent, from 20° C to —*					
	100° C	*200° C*	*400° C*	*600° C*	*800° C*	*1000° C*
	0.05	0.14	0.24	0.34	0.46	0.60
	.02	.04	.07	.12	.19	.29
⊥ (001)	.06	.15	.26	.33	.45	.57
vol[b]	.12	.32	.57	.78	1.10	1.45

[a]Data reported in Celsius ($T_K = T_C + 273.15$).
[b]vol = volumetric expansion.

4. Compressibility and Elastic Constants:

Anorthosite (Rocks)

Location (a)	*Density, g/cm³*	*Young's modulus,[b] Mb*	*Modulus of rigidity,[b] Mb*	*Poisson's ratio*	*Notes (c)*
Quebec		0.825	[d](0.328)	0.262	70 to 600
P=4000	2.708		.332	[d](.32)	D
Stillwater, Mont.					
P=1	2.770		.353		D
P=4000			.371	[d](.31)	
P=4000	2.750		.389		
P=10 000			.399		

[a]The notation "P=4000," for example, indicates measurement made under hydrostatic pressure of 4000 bars. Where no notation is given, pressure is one atmosphere.

[b]Original data reported in megabars (1 Mb = 10^{11} N/m^2).

[c]The symbol "D" indicates dynamic measurement; numbers indicate stress range (in bars) for static measurements.

[d]Values in parentheses were obtained indirectly with the aid of formulas for isotropic elasticity.

Elastic Parameters[a] for Anorthosite at 4 × 10^8 N/m^2 (4 Kilobars)

Type	*Density, g/cm³*	V_p, *km/sec*	V_S, *km/sec*	*Poisson's ratio*	*Young's modulus, Mb*	*Modulus of rigidity, Mb*	B, Mb^{-1}	β, Mb^{-1}
New Glasgow, Quebec	2.708	6.82	3.50	0.32	0.88	0.33	1.22	1.4
Stillwater Complex, Montana	2.770	7.04	3.68	.31	.98	.38	1.15	

[a]Symbols are as follows:

V_p = particle velocity
V_s = shock front velocity
β = compressibility (experimentally observed)
B = compressibility (calculated)

$$B = \frac{1}{V}\left(\frac{\delta V}{\delta P}\right)_T = \frac{1}{\rho}\left(\frac{\delta \rho}{\delta P}\right)_T$$

where V = volume
δV = decrease in volume
P = pressure
δP = increase in pressure
T = temperature
ρ = density

5. Seismic Velocities:

Anorthosite: Compressional Wave Velocities, V_p, as a Function of Pressure

Sample from —	*Density, g/cm³*	V_p, *in km/sec, for pressures[a] of —*						
		10	*500*	*1000*	*2000*	*4000*	*6000*	*10 000*
Tahawus, New York	2.768	6.73	—	6.86	6.90	6.94	6.97	7.02
Stillwater Complex, Montana	2.770	6.5	—	6.97	7.01	7.05	7.07	7.10
Bushveld Complex, South Africa	2.807	5.7	6.92	6.98	7.05	7.13	7.16	7.21

[a]Original data reported in bars (1 bar = 10^5 N/m^2).

Anorthosite: Shear Wave Velocities, V_s, as a Function of Pressure

Sample from —	*Density, g/cm³*	V_s, *in km/sec, for pressures[a] of —*						
		1	*500*	*1000*	*2000*	*4000*	*6000*	*10 000*
Stillwater Complex, Montana	2.750	3.56	3.65	3.69	3.72	3.76	3.77	3.81

[a]Original data reported in bars (1 bar = 10^5 N/m^2).

6. Strength and Ductility:

Stress-Strain Relationship—Anorthite (Marcy, New York)

Temp., K	*Confining pressure, bars[a]*	*Differential stress in bars for strain percent of—*				*Ultimate strength, bars*	*Total strain, percent*	*Fault angle, deg*
		1	*2*	*5*	*10*			
423	1010	2040	2360	—	—	5940	2.6	29
773	5050	2920	4640	7290	9040	9400	32.2	28

[a]Original data reported in bars (1 bar = 10^5 N/m^2).

6. Strength and Ductility (continued):

Shearing Strength Under High Confining Pressure — Anorthite

Normal pressure of — in kilobars	*Shear strength, kilobars*
10	2.2
20	7.6
30	11
40	14
50	14

7. Viscosity:

Viscosity of Anorthite (at 1 atmosphere)[a]

Temperature, °C	*Viscosity, poises*
1450	111
1500	60
1600	25
1555	107

[a]Data reported in customary units of measurement. (1 atm. = 1.013×10^5 N/m^2; $T_K = T_C + 273.15$; 1 poise = 10^{-1} N sec m^{-2}).

8. Melting and Transformation Points:

Anorthite ($CaAl_2Si_2O_8$)

Melting point, K (°C) ..... 1823 ± 2 (1550 ± 2)
Eutectic with tridymite, K (°C) 1632 (1359)
(10.5% CaO, 70% SiO_2)
Eutectic with $\alpha CaSiO_3$, K (°C) 1572 (1299)
(34.1% CaO, 47.3% SiO_2)
Eutectic with αAl_2O_3, K (°C) 1820 (1547)
(19.3% CaO, 41.4% SiO_2)
Eutectic with gehlenite, K (°C) 1658 (1385)
(30.2% CaO, 33% SiO_2)
Ternary eutectic with mullite and tridymite, K (°C) 1658 (1385)
(9.3% CaO, 70.4% SiO_2)

Ternary eutectic with $\alpha CaSiO_3$ and tridymite, K (°C) 1443 (1170)
(23.3% CaO, 62.2% SiO_2)
Ternary eutectic with $\alpha CaSiO_3$ and gehlenite, K (°C) 1538 (1265)
(38% CaO, 42% SiO_2)
Ternary eutectic with gehlenite and αAl_2O_3, K (°C) 1653 (1380)
(29.2% CaO, 31.8% SiO_2)
Reaction point with αAl_2O_3 and mullite, K (°C) 1785 (1512)
(15.6% CaO, 47.9% SiO_2)

9. Thermodynamic Properties:

Anorthite ($CaAl_2Si_2O_8$)

Crystals ..... 298.15 K to melting point 1825 K
Formula weight, g 278.21
Molar volume, cm^3 (J/bar) 100.79 (10.0790)

$C_p^o = 5.1683 \times 10^2 - 9.2492 \times 10^{-2} T + 4.1883 \times 10^{-5} T^2 - 4.5885 \times 10^3 T^{-0.5} - 1.4085 \times 10^6 T^{-2}$
(for 298 to 1800 K)
$S^o_T = 199.30 \pm 0.30$ J mol^{-1} K^{-1} (at 298.15 K)
$H^o_{298} - H^o_o = 33.333$ kJ
Enthalpy of melting = 81.000 kJ
where C_p^o = molar heat capacity, H^o_{298} = enthalpy, H^o_o = enthalpy at absolute zero, S^o_T = entropy, and T = temperature in kelvin.

Formation From the Elements

Temperature, K	*Enthalpy, kJ/mol*	*Gibbs free energy, kJ/mol*
298.15	−4243.040 (±3.125)	−4017.266 (±3.145)
500	−4242.328	−3864.213
700	−4237.933	−3713.703
900	−4233.976	−3564.325
1100	−4251.066	−3412.139
1300	−4251.218	−3258.811
1500	−4240.704	−3106.896
1700	−4328.857	−2955.681
1800	−4474.316	−2871.725

9. Thermodynamic Properties (continued):

Formation From the Oxides

Temperature, K	*Enthalpy, kJ/mol*	*Gibbs free energy, kJ/mol*
298.15	−110.851 (±3.430)	−118.975 (±3.450)
500	−111.159	−124.439
700	−112.463	−129.557
900	−115.021	−134.110
1100	−114.398	−138.412
1300	−112.873	−142.876
1500	−110.189	−147.689
1700	−105.958	−152.928
1800	−103.118	−155.769

10. Electrical Properties:

Composition, mole percent	*Source of sample*	*Dielectric constant:*	
		Radio frequencies	*Optical frequencies*
Ab_4An_{96}	Otaru, Japan	7.24	2.51
Ab_2An_{98}	Tsushima, Japan	7.14	2.51
Ab_7An_{93}	Hokkaido, Japan	7.05	2.49
Ab_4An_{96}	Miyakeshima, Japan	7.15	2.49
	Average	7.15	2.50

Dielectric constant of dry anorthosite (Crystal Bay, Minnesota) as a function of frequency.

Frequency	*Dielectric constant*
100 Hz	167
1 kHz	73
10 kHz	25
100 kHz	10.9
1 MHz	9.93
10 MHz	9.03

11. Thermal Conductivity:

Anorthosite

Sample from —	*Conductivity,* 10^{-3} *cal(cm sec °C)*$^{-1}$	*Density,* g/cm^3
Bushveld, Transvaal	5.0	2.83

Effect of temperature on conductivity:

Temperature, °C	*Conductivity,* $10^{-3} \times$ *cal(cm sec °C)*$^{-1}$	*Density,* g/cm^3
	Transvaal (Bytownite)	
0	4.43	2.74
100	4.54	
200	4.69	
	Quebec (Labradorite)	
0	4.13	2.70
100	4.20	
200	4.34	
300	4.50	
	Montana (Bytownite)	
0	4.02	2.74
100	4.10	
200	4.27	

NOTE: Units of measurement are those of the original data; 1 cal(cm sec °C)$^{-1}$ = 419 J(m sec K)$^{-1}$ and $T_K = T_C + 273.15$.

12. Magnetic Properties:

Not available for lunar materials.

ILMENITE

Ilmenite is one of the minor lunar minerals, and its abundance is generally less than 2 percent. However, there are areas on the Moon where ilmenite abundance surpasses 10 percent. The occurrence of ilmenite on the Moon is shown in table 2-VIII, and two analyses of typical lunar ilmenite are given in table 2-IX.

The mineral ilmenite ($FeTiO_3$) is a potential source for iron, titanium, and oxygen. Based upon the occurrence of ilmenite (table 2-VIII), high-titanium mare basalts may be considered as potential ores for this mineral.

TABLE 2-VIII.— Abundance of Ilmenite in Lunar Materials

Lunar material	*Percent ilmenite, vol.%*	*Comments*
Mare basalts	0 to 25	Ilmenite abundance is a strong function of basalt type. High-Ti basalts tend to contain more than 15 percent ilmenite while low-Ti basalts tend to contain less than 10 percent. Vitrophyres of both high- and low-Ti contents contain less than 1 percent.
Anorthositic rocks	trace	Almost no ilmenite occurs in these rocks.
Fragmental breccias	2 to 12	These values are for ilmenite grains larger than 25 micrometers across. The ilmenite content of a breccia resembles the local terrain. In high-Ti mare regions the value is approximately 10 percent, in low-Ti mare regions it is approximately 4 percent and in the highlands it is approximately 1 percent.
Crystalline breccias	1 to 2	These rocks are limited to highland regions. The ilmenite is generally approximately one micrometer across.
Soil	0.5 to 5	The ilmenite content is a function of local rocks. It is high in regions where local rocks are high in ilmenite content and vice versa.

TABLE 2-IX.— Analyses of Typical Lunar Ilmenite

Compound	*Mare,*[a] *wt.%*	*Highland,*[b] *wt.%*
SiO_2	0.01	0.21
TiO_2	53.58	54.16
Cr_2O_3	1.08	.44
Al_2O_3	.07	<.01
FeO	44.88	37.38
MnO	.40	.46
MgO	2.04	6.56
ZrO	.08	.01
V_2O_2	.01	<.01
Nb_2O_5	<.01	.13
Total	102.16	99.37

[a]Ilmenite 74255; from reference 2-1.
[b]Ilmenite 72395; from reference 2-2.

The following data summarize the physical properties of ilmenite. Many of these data are taken from studies of analogous terrestrial or synthetic materials.

Physical Properties of Ilmenite

1. Density and Molar Volume:

Density, g/cm^3 (at room temp. and 10^5 N/m^2 (1 bar))	4.44 to 4.9
Molar volume, cm^3	31.71 ± 0.05
Formula weight, g	151.75
Cell volume, cm^3	315.9×10^{-24}

2. X-Ray Crystallographic Data:

Ilmenite ($FeTiO_3$)

Crystal system	hex-R
Space group	$R\bar{3}$
Structure type	ilmenite
Z (gram formula weights per unit cell)	6 (hex) 2 (rhomb)

Unit cell base vector magnitudes: (at room temp.)
$a_o = 5.093 \pm 0.005$ Å (hex); $a_o = 5.534$ Å (rhomb)
$c_o = 14.055 \pm 0.010$ Å (hex)
α_o or α_r (angle subtended by **b** and **c**) = 54°51′
(Note: 1 Å = 10^{-10} meter.)

3. Thermal Expansion:

Not available for lunar material.

4. Compressibility and Elastic Constants:

$a = 0.56\ \text{Mb}^{-1}$ where: $\frac{V_o - V}{V_o} = aP - bP^2$

and
V = volume
V_o = initial volume
P = pressure in megabars (Mb)
a = proportional limit
b = elastic limit

5. Seismic Velocities:

Not available for lunar material.

6. Strength and Ductility:

Not available for lunar material.

7. Viscosity:

Not available for lunar material.

8. Melting and Transformation Points:

Ilmenite ($FeTiO_3$)

Melting point, K (°C)	1640 (1367)
Eutectic with Fe_2TiO_2, K(°C) (47% TiO_2)	1593 (1320)
Dimorphous transition, K(°C)	488 (215)

9. Thermodynamic Properties:

Ilmenite ($FeTiO_3$)

Crystals ..... 298.15 K to melting point 1640 K
Liquid ..... 1640 K to 1800 K
Formula weight, g 151.745
Molar volume, cm^3 (J/bar) ..... 31.71 ± 0.05 (3.1690)

$C_p^o = -2.9895 + 6.5049 \times 10^{-2} T + 2.4266 \times 10^3 T^{-0.5} - 5.1057 \times 10^6 T^{-2}$
(for 298 to 1640 K)
$S_T^o = 105.86 \pm 1.25$ J mol^{-1} K^{-1} (at 298.15 K)
$H_{298}^o - H_o^o =$ (not available)
Enthalpy of melting = 90.667 kJ
where C_p^o = molar heat capacity, H_{298}^o = enthalpy, H_o^o = ethalpy at absolute zero, S_T^o = entropy, T = temperature in kelvin.

Formation From the Elements

Temperature, K	*Enthalpy, kJ/mol*	*Gibbs free energy, kJ/mol*
298.15	−1236.622 (±1.590)	−1159.170 (±1.632)
500	−1234.099	−1107.341
700	−1231.587	−1057.125
900	−1230.104	−1007.463
1100	−1230.896	−957.935
1300	−1232.068	−908.028
1500	−1226.333	−858.572
1700	−1132.527	−812.407
1800	−1125.878	−793.789

9. Thermodynamic Properties (continued):

Formation From the Oxides

Temperature, K	*Enthalpy, kJ/mol*	*Gibbs free energy, kJ/mol*
298.15	−19.829 (±2.300)	−18.568 (±2.340)
500	−20.074	−17.599
700	−20.239	−16.585
900	−20.399	−15.512
1100	−20.161	−14.441
1300	−19.209	−13.463
1500	−17.303	−12.713
1700	51.595	−12.014
1800	56.450	−15.980

10. Electrical Properties:

Number of samples	*Reported resistivities, ohm meter*	
	Low	*High*
5	10^{-3}	4.0

11. Thermal Conductivity:

Ratio of principal conductivities (no absolute values determined)

$A/C = 1.23$ (for ilmenite trigonal system)

where A and C are two of the principal conductivities (A, B, C) along the three orthogonal axes.

12. Magnetic Properties:

Susceptibility,[a] cm^{-3}	*Field strength,*[b] oersted
0.031	—
.044	0.6

[a]In the centimeter-gram-second system of units.
[b]Original data reported in oersteds (1 oersted = 79.577 A/m).

REFERENCES

2-1. Dymek, R. F.; Albee, A. L., and Chodos, A. A.: Comparative Mineralogy and Petrology of Apollo 17 Mare Basalts: Samples 70215, 71055, 74255, and 75055. Proceedings of the Sixth Lunar Science Conference, Vol. 1, 1975, pp. 49-77.

2-2. Dymek, R. F.; Albee, A. L.; and Chodos, A. A.: Petrology and Origin of Boulders #2 and #3, Apollo 17 Station 2. Proceedings of the Seventh Lunar Science Conference, Vol. 2, 1976, pp. 2335-2378.

2-3. Weill, D. F.; Grieve, R. A.; McCallum, I. S.; and Bottinga, Y.: Mineralogy-Petrology of Lunar Samples. Microprobe Studies of Samples 12021 and 12022; Viscosity of Melts of Selected Lunar Compositions. Proceedings of the Second Lunar Science Conference, Vol. 1, 1971, pp. 413-430.

3. Lunar Materials

Lunar materials may be classified as follows: (1) regolith, a fine-grain deposit loosely referred to as "lunar soil"; (2) igneous rocks that were derived from the Moon's interior by well-known igneous processes; and (3) breccias which represent lunar deposits that were lithified by the effects of meteorite impact. Data on these types of lunar material are given in this section.

REGOLITH

The relatively young basalt surfaces inside the large mare basins are dominated by craters less than 1 kilometer in diameter and are particularly influenced by the cumulative bombardment of meteoroids. This bombardment resulted in the fine-grain deposit known as "regolith" and more loosely referred to as "lunar soil." The lunar highland, though not dominated by these small craters, also has a regolith resulting from meteoroid bombardment.

Because of the numerous impacts in the regolith, it is highly comminuted and very rich in glass. Descriptions of the regolith are given here in terms of grain size, chemistry, and mineralogical constituents.

Physical properties of the lunar regolith are known with a high degree of confidence. Unfortunately, however, direct sampling was limited to a maximum depth of approximately 3 meters. In addition, data from geophysical experiments (such as the active seismic, traverse gravimeter, and surface electrical experiments) have not permitted unambiguous interpretation of soil thickness or depth to rock. Deep drill holes and a more definitive geophysical program will be required to characterize the subsurface physical properties.

Quantitative measurements of the regolith thickness are given in table 3-I; they are very few and are essentially confined to the Apollo landing sites.

TABLE 3-I.—Mean Regolith Thickness

Location	*Photogeology,*[a] *m*	*Seismometer,*[b] *m*
Flamsteed Ring	3.3	—
NE of Wichmann Crater	3.3	—
Apollo 12 site	4.6	3 to 4
Apollo 15 site	≈7	5
Apollo 11 site	4.6	3 to 6
SE Mare Tranquillitatis	7.5	—
Apollo 17 site	≈8	≈8
Apollo 16 site	≈8 to 10	12 to 15
Highland Plains	16	—
Apollo 14 site	—	10 to 20

[a]From Oberbeck and Quaide (ref. 3-1).
[b]From Watkins and Kovach (ref. 3-2).

Physical Properties

In situ measurements of lunar surface properties have been made at the five Surveyor landing sites, at the Apollo 15 and 16 landing sites, and at the Luna 16, 20, and 24 landing sites. In addition, certain physical properties can be deduced from observational data provided by Apollo crewmembers during extravehicular activity (EVA), from postflight crew debriefings, and from detailed studies of photographs and television coverage during the Apollo missions. The self-recording penetrometer used during the Apollo 15 and 16 missions provided the most complete, albeit limited, measurements of the penetration properties of the lunar surface. Laboratory studies of returned samples and simulated lunar materials provided the basis for other parameters.

It is important to point out that the observational base for in situ physical measurements is severely limited both horizontally and vertically. If one considers as "measurements" the tracks of the lunar roving vehicle (LRV), the modular equipment transporter (MET), the Soviet Lunokhod and the footprints of the astronauts, then the horizontal base can be extended for several kilometers. However, the deepest direct depth samples of the Moon

are limited to the depth penetrated by the lunar drill during the Apollo 15, 16, and 17 missions. The total depth of penetration in each instance was approximately 3 meters.

1. Lunar Soil Densities:

Summary—Data sources used as part of the soil mechanics experiment (S-200) are summarized in table 3-II to provide a synthesis of data for relative density and bulk density.

TABLE 3-II.—Summary of Results From Lunar Soil Density Studies[a]

Source	*Depth range, cm*	*Bulk density or absolute density, g/cm³*	*Relative density,*[b] *percent*	*Standard deviation for relative density*
Core tube samples:				
Apollo 15	0 to 15	1.50 ± 0.05	[c]64	
Apollo 16	0 to 30	1.58 ± 0.05	[c]74	
	30 to 60	1.74 ± 0.05	[c]92	
Apollo 17	0 to 60	1.66 ± 0.05	[c]83	
Lunar drill samples (all drill cores)	0 to 30	1.69 ± 0.08		
	30 to 60	1.77 ± 0.08		
Astronaut footprint analyses (all missions)	0 to 15		65 to 66	≈10
LRV and MET tracks	0 to 15		62 to 71	
Boulder tracks	0 to 300 or 400		65	≈20
Penetration resistance	0 to 60		83 to 84	≥10?

[a]From Houston, W. N.; et al. (ref. 3-3), which contains more detailed references.

[b]Relative density is

$$D_r = \frac{\rho_{max}}{\rho_{min}} \frac{\rho - \rho_{min}}{\rho_{max} - \rho_{min}} \times 100\%$$

where ρ_{max} = maximum density, which corresponds to minimum void ratio and minimum porosity, and ρ_{min} = minimum density, which corresponds to maximum void ratio and maximum porosity.

[c]Calculated, based on average $G_s = 3.1$, $e_{max} = 1.7$ and $e_{min} = 0.7$ (where e = void ratio).

Average Bulk Density—The best estimates for the average bulk density of soil on the lunar surface are as follows (ref. 3-3):

Depth range, cm	*Bulk density, g/cm³*
0 to 15	1.50 ± 0.05
0 to 30	1.58 ± 0.05
30 to 60	1.74 ± 0.05
0 to 60	1.66 ± 0.05

Average Relative Density—The best estimates for the average relative density of soil on the lunar surface are as follows (ref. 3-3):

Depth range, cm	*Relative density, percent*
0 to 15	65 ± 3
0 to 30	74 ± 3
30 to 60	92 ± 3
0 to 60	83 ± 3

Analysis of Tracks—Surface soil properties based on an analysis of LRV tracks and the tracks made by the Soviet unmanned vehicle Lunokhod 1 (ref. 3-4) are as follows:

Soil consistency	G,[a] *N/cm³*	*Porosity, percent*	*Void ratio,* e	D_r,[b] *percent*	ϕ_{TR},[c] *deg*	ϕ_{PL},[d] *deg*
Soft	0.15	47	0.89	30	38	36
Firm	0.76 to 1.35	39 to 43	0.64 to 0.75	48 to 63	39.5 to 42	37 to 38.5

[a] G = penetration resistance gradient.
[b] D_r = relative density = $(e_{max} - e)/(e_{max} - e_{min})$, based on standard American Society for Testing Materials methods.
[c] Φ_{TR} = angle of internal friction, based on triaxial compression tests.
[d] Φ_{PL} = angle of internal friction, based on in-place plate shear tests.

Shear Strength Parameters—The lunar soil has typical shear strength parameters of (ref. 3-5)

Cohesion = 1 kN/m²
Friction angle = 35°

Modulus of Subgrade Reaction—The modulus of subgrade reaction for the lunar surface is typically 1000 $kN/m^2/m$, based on astronaut bootprint measurements. However, a footing applying a pressure of 10 kN/m^2 would normally settle approximately 1 centimeter but could settle as much as 10 centimeters or as little as 0.1 centimeter (ref. 3-5).

Fluid Conductivity—Based on the grain size analysis of returned samples, the fluid conductivity of the lunar soil would be too low ($<1 \times 10^{-5}$ cm/sec) to permit its use as a drain field for liquid waste (ref. 3-5).

2. Color:

Lunar soil was described by the Surveyor observation team as being gray in color. The Apollo astronauts, while on the lunar surface, described the soil as consisting of shades of gray except when viewed along zero phase (down Sun), when the soil appeared light tan or gray. They also noticed that the upper few centimeters of regolith consisted of a thin, light-gray cohesive unit overlying a zone of dark-gray to cocoa-gray soil.

Most soils range from dark gray (10YR3/1) to white (10YR8) with the most common color being gray (N5) (colors are based on those of the *Munsell Color Company, Inc.* (1954)). Exceptions to this include the pale-green soils collected at Spur Crater, Apollo 15 site, and the orange-brown soils from Shorty Crater, Apollo 17 site; these soils contain a substantial amount of green and orange glass, respectively.

3. Grain Size Characteristics:

The mean grain size of lunar soils ranges from 40 to 802 micrometers with most falling between 45 and 100 micrometers (fig. 3-1). Lunar soils are poorly to very poorly sorted, with sorting values (standard deviations) ranging from 1.99 to 3.73 Φ, and many exhibit a bimodal grain size distribution. There is an inverse correlation between the mean grain size and sorting values (standard deviation), with the coarsest samples being the most poorly sorted. Weight percents in each grain size fraction are shown in table 3-III for the Apollo 11 soil 10084,853. This is a typical mare soil. Notice that approximately one-fourth of the soil is finer than 20 micrometers.

Most lunar soils have grain size characteristics consistent with those of the debris from meteorite impacts. Exceptions include the black and orange "soils" collected at the Apollo 17 site, which are finer grain (M_z = 37.9 and 40 micrometers) and better sorted (σ_I = 1.69 and 1.57 Φ). These samples have been interpreted as pyroclastic ejecta and not as soils. (Note: M_z is the mean size and σ_I is the inclusive standard deviation.)

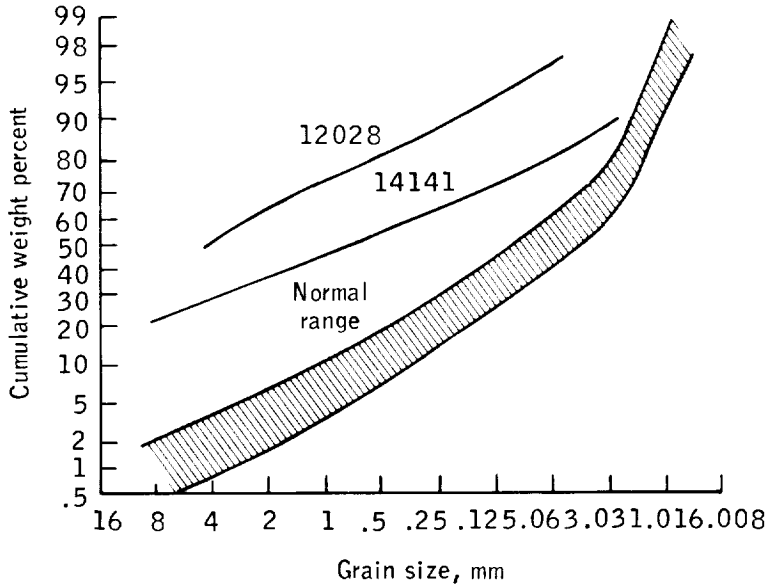

FIGURE 3-1.— Cumulative grain size distribution for lunar soils. Most soils lie within the envelope (shaded area). Two particularly coarse soils (samples 12028 and 14141) are also shown.

TABLE 3-III.—Grain Size Fractions for Apollo 11 Soil 10084,853 (Old Soil)

Grain size	*Weight percent*	*Cumulative weight percent*
4 to 10 mm	1.67	1.67
2 to 4 mm	2.39	4.06
1 to 2 mm	3.20	7.26
0.5 to 1 mm	4.01	11.27
250 μm to 0.5 mm	7.72	18.99
150 to 250 μm	8.23	27.22
90 to 150 μm	11.51	38.72
75 to 90 μm	4.01	42.73
45 to 75 μm	12.40	55.14
20 to 45 μm	18.02	73.15
$<$20 μm	26.85	100.00

4. Particle Types and Relative Abundance:

Lunar soils consist mostly of (1) lithic and mineral debris derived by impact comminution of the underlying bedrock and (2) glass particles formed by impact melting. Microscope identification of these particles shows that they can be grouped into several major categories.

Agglutinates—Agglutinates were recognized immediately during the examination of Apollo 11 samples as an important soil component and as one of the keys to a genetic history of lunar soil. An agglutinate consists of comminuted lithic, mineral, and glass fragments bonded by glass droplets (fig. 3-2). The glass droplets generally are black to dark brown. Agglutinates contain fine-grain metallic iron formed by reduction of iron dissolved in the glass. The glass is vesicular, containing vesicles ranging from less than 1 micrometer to several centimeters in diameter. The morphology of agglutinate grains ranges from simple irregular grains to more complex elongate, branching forms. Mineral and lithic clasts are randomly distributed throughout the agglutinate grains and on their surfaces.

FIGURE 3-2.— Scanning electron microscope photograph (S-73-24575) of an agglutinate particle from an Apollo 17 soil sample. This agglutinate is approximately 1 millimeter long.

Basalt Fragments—Fragments of basalt are common at all mare sites. Basalt generally consists of plagioclase and pyroxene and may also have olivine, ilmenite, and small amounts of other minerals. Basalts may be subdivided on the basis of composition (olivine bearing, etc.) or texture (equigranular, variolitic, etc.).

Breccia—Breccias are fragmental rocks created by impacts. They may be subdivided on the basis of composition (anorthositic, etc.) or textures (low grade or glassy, high grade or crystalline, melt matrix, etc.).

Mineral Fragments—Constituent mineral fragments are liberated when lithic fragments are broken up by impacts. The most common mineral fragments in lunar soils are plagioclase feldspar and pyroxene. Olivine, ilmenite, and dozens of minor minerals may also be present.

Glass—In addition to agglutinates, which are the major form of glass, other glass particles are present in the soil. Glass droplets, teardrops, and other regular shapes are generally present in small amounts (usually less than 1 percent). Blocky glass and vesicular glass are also found. Glass may be classified on the basis of shape, color, or chemical composition.

Relative Amounts of Each Particle Type—Tables 3-IV and 3-V show the relative amounts of the particle types in two typical soils, one from the mare region and one from the highland region of the Apollo 17 site. Data are shown for each of 10 size fractions. In general, lithic fragments are most common in the coarsest size fractions, and mineral and glass fragments are most abundant in the finest size fractions. The grain size distribution for each size fraction is also shown. Data in the tables were extracted from reference 3-6.

5. Maturity of Lunar Soils:

Most lunar soils have evolved in response to the meteoroid flux. This response includes both constructional (e.g., agglutination and brecciation) and destructional (e.g., comminution) processes. The concept of the maturity of a lunar soil has evolved to represent the relative length of time a soil has been exposed to the meteoroid flux at the lunar surface. A number of indices are used to quantitatively represent the maturity or length of surface exposure. These include the gases derived from the solar wind (e.g., ^{36}Ar, ^{4}He, and N), agglutinates, mean grain size, and the ferromagnetic resonance (FMR) maturity index, I_s/FeO. The parameter I_s is the relative concentration of fine-grain metal ($\leq 300 \times 10^{-10}$ meter in diameter) and FeO is total iron concentration of the soil. The fine-grain metal is produced in agglutinatic glass by micrometeoroid impact of the lunar surface.

The index which appears to be the most free of complicating effects not related to surface exposure is I_s/FeO. Effects that complicate the application of

the other maturity indices include composition and nonlinearity with time (saturation). An additional advantage of using I_s/FeO is that it has the largest data base.

Table 3-VI is a compilation of the values of I_s/FeO together with values for other maturity indices and exposure-related properties (ref. 3-7).

TABLE 3-IV.—Petrography of a Series of Size Fractions From 71061,1[a] (a Typical Apollo 17 Mare Soil)

Components[b]	Petrographic description, vol.%, for—							Visual estimate (%) in Lunar Receiving Laboratory for—			
	< 20 μm	20 to 45 μm	45 to 75 μm	75 to 90 μm	90 to 150 μm	150 to 250 μm	250 to 500 μm	0.5 to 1 mm	1 to 2 mm	2 to 4 mm	4 to 10 mm
Agglutinates	17.0	17.3	13.0	17.3	9.3	11.8	10.0	10.0			
Basalt, equigranular			9.0	15.0	19.6	30.9	51.5	65.0	100.0	100.0	100.0
Basalt, variolitic			.6	1.6		3.4					
Breccia:											
Low grade, brown			1.0	4.0	3.6	5.1	6.9				
Low grade, colorless			.3	1.3	.6	—	—	5.0			
Medium, high grade			1.0	1.3	1.6	2.8	1.5				
Anorthosite			—	—	.3	—	—				
Cataclastic anorthosite			1.0	—	—	—	—				
Norite			—	—	—	—	—				
Gabbro			—	—	—	—	.5	5.0			
Subtotal			12.9	23.2	25.7	42.2	60.4	75.0	100.0	100.0	100.0
Plagioclase			16.3	7.0	17.3	9.0	8.5				
Clinopyroxene			21.3	26.3	21.0	17.4	10.8				
Orthopyroxene			—	—	—	—	—				
Olivine			—	—	—	—	—				
Ilmenite			6.0	3.3	4.6	3.3	2.3				
Subtotal			43.6	36.6	42.9	29.7	21.6				
Glass:											
Orange			7.6	5.0	6.3	4.5	.8				
"Black"			18.7	10.6	9.6	5.1	6.1	5.0			
Colorless			1.0	1.0	1.3	—	1.5				
Brown			.3	5.2	4.6	3.3	—				
Gray "ropy"			.7	.6	—	1.7	—	10.0			
Other			2.0	—	—	1.0	—				
Subtotal			30.3	22.4	21.8	15.6	8.4	15.0			
Total number of grains counted	300	161	300	300	300	178	130	20	100	?	?
Wt.% of total sample for each size fraction	17.98	12.21	8.39	3.0	8.66	7.04	7.08	3.44	6.15	6.74	10.16

[a]Sample 71061,1 was taken from station 1 on the mare surface. Agglutinate versus nonagglutinate grains were identified using a scanning electron microscope in the size ranges of < 20 μm and 20 to 45 μm. The >10 mm fraction of the sample made up 9.42 percent of the sample.

[b]The < 20 μm fraction is 83 percent nonagglutinate, the 20 to 45 μm fraction is 82.7 percent nonagglutinate.

TABLE 3-V.—Petrography of a Series of Size Fractions From 72441, 7[a] (a Typical South Massif Soil)

Components[b]	*Petrographic description, vol.%, for—*							*Visual estimate (%) in Lunar Receiving Laboratory for—*			
	< 20 μm	*20 to 45 μm*	*45 to 75 μm*	*75 to 90 μm*	*90 to 150 μm*	*150 to 250 μm*	*250 to 500 μm*	*1 to 2 mm*	*2 to 4 mm*	*4 to 10 mm*	*> 10 mm*
Agglutinates	21.0	50.0	39.3	45.5	41.7	54.6	30.5	20.0	25.0	25.0	
Basalt, equigranular			.6	1.5	1.3	1.3	—				None present
Basalt, variolitic			.3	—	1.3	—	1.0				
Breccia:											
Low grade, brown			9.3	6.6	9.3	10.7	9.4				
Low grade, colorless			2.7	2.3	6.3	.7	6.3	80.0	74.0	75.0	
Medium high grade			22.7	29.0	19.3	20.0	30.5				
Anorthosite			—	—	1.0	—	—		1.0		
Cataclastic anorthosite			.7	1.2	1.3	.7	2.1				
Norite			—	—	.7	.7	1.0				
Gabbro			—	—	—	—	—				
Subtotal			36.3	40.6	40.5	34.1	50.3	80.0	75.0	75.0	
Plagioclase			10.7	1.2	6.7	3.3	7.3				
Clinopyroxene			6.0	3.9	3.0	2.7	2.1				
Orthopyroxene			1.0	—	3.3	—	—				
Olivine			—	1.2	.7	—	2.1				
Ilmenite			—	—	.3	—	—				
Subtotal			17.7	6.3	14.0	6.0	11.5				
Glass:											
Orange			.3	1.2	.3	—	—				
"Black"			1.3	1.5	.3	—	1.0				
Colorless			1.0	1.5	1.3	—	—				
Brown			3.3	3.0	1.0	5.3	4.2				
Gray "ropy"			—	—	.3	—	1.0				
Other			—	—	.3	.7	1.0				
Subtotal			5.9	7.2	3.5	6.0	7.2				
Total number of grains counted	300	162	249	259	300	150	95				
Wt.% of total sample for each size fraction	25.84	18.79	12.08	4.01	11.02	8.37	8.55	3.67	2.76	1.01	None

[a]Sample 72441,7 was taken from station 2 at the base of the South Massif and on the "light mantle" deposit. Agglutinate versus nonagglutinate grains were identified by using a scanning electron microscope in the size ranges $< 20\ \mu m$ and 20 to 45 μm.

[b]The $< 20\ \mu m$ fraction is 79.0 percent nonagglutinate; the 20 to 45 μm fraction is 50.0 percent nonagglutinate.

[c]No visual estimate was made for the 500 to 1000 μm fraction (wt.% = 3.91).

TABLE 3-VI.—Compilation of Maturity Indices

The values of I_s/FeO are measured on the < 250 μm sieve fraction of soil. Soils are classified as immature, submature, and mature according to the following breakdown in I_s/FeO: immature, 0 to 30 units; submature, 30 to 60 units; mature, >60 units. Petrographic agglutinates were determined for the 90 to 150 μm sieve fraction.

No.	Sample	FeO, wt.%	I_s/FeO (Arb.), < 250 μm	N, μg/g	C, μg/g	^4He, 10^{-2} cm^3/g	^{36}Ar, 10^{-4} cm^3/g	Petrog. agglut-inates, percent	Mag. fraction, percent	Mean grain size (μm) for < 1 cm	< 1 mm	Fe/FeO	No.
1	10084,853	15.8	78.0	92	—	21.9	4.36	—	84	—	52	0.025	1
2	12032,24	15.1	12.0	—	60	—	—	—	—	—	—	—	2
3	12033,40	14.2	4.6	—	45	—	—	—	—	—	—	—	3
4	12037,18	17.3	21.0	—	65	—	—	—	—	—	—	—	4
5	12041,10	14.2	63.0	—	—	—	—	—	—	—	—	—	5
6	12042,27	16.8	61.0	—	130	9.76	3.01	—	—	—	—	—	6
7	12044,11	15.7	57.0	—	—	8.42	3.06	—	—	—	—	—	7
8	12057,43	16.6	40.0	—	—	—	—	—	—	—	—	—	8
9	12060,6	16.9	24.0	—	—	—	—	—	—	—	—	—	9
10	12070,29	16.5	47.0	79	—	8.60	2.94	—	—	—	—	.042	10
11	14003,71	10.4	66.0	92	140	6.26	3.54	60	76	129	99	—	11
12	14141,30	10.2	5.7	—	42	—	—	5	23	616	123	—	12
13	14148,23	10.4	74.0	—	160	5.50	2.67	50	74	77	60	—	13
14	14149,39	10.0	53.0	—	135	5.10	2.39	26	63	230	92	—	14
15	14156,23	10.4	68.0	—	110	5.20	3.21	48	68	70	64	—	15
16	14161,46	10.2	48.0	—	—	—	—	—	—	—	—	—	16
17	14163,178	10.4	57.0	—	115	6.05	3.09	—	71	76	56	.052	17
18	14230,113	10.2	59.0	—	—	—	—	53	—	109	85	—	18
19	14230,121	10.4	55.0	—	—	—	—	57	—	74	70	—	19
20	14230,130	10.2	50.0	—	—	—	—	52	—	118	103	—	20
21	14259,52	10.5	81.0	—	160	—	4.39	52	83	69	63	.066	21
21	14259,111	10.5	89.0	—	—	—	—	—	—	—	—	—	21
22	14260,4	10.0	72.0	—	—	—	—	—	83	117	86	—	22
23	15001,21	15.0	19.0	—	—	—	—	25	—	81	62	—	23
24	15001,38	15.0	17.0	—	—	—	—	20	—	73	65	—	24
25	15001,265	15.0	17.0	—	—	—	—	8	—	—	73	—	25
26	15001,266	15.0	19.0	—	—	—	—	6	—	—	52	—	26
27	15001,267	15.0	28.0	—	—	—	—	28	—	—	—	—	27
28	15001,268	15.0	33.0	—	—	—	—	24	—	—	—	—	28
29	15001,269	15.0	33.0	—	—	—	—	22	—	—	—	—	29
30	15001,270	15.0	35.0	—	—	—	—	26	—	—	55	—	30
31	15001,271	15.0	28.0	—	—	—	—	21	—	—	—	—	31
32	15002,24	15.0	34.0	—	—	—	—	41	—	73	66	—	32
33	15002,326	15.0	41.0	—	—	—	—	23	—	—	—	—	33
34	15002,327	15.0	40.0	—	—	—	—	22	—	—	74	—	34
35	15002,328	15.0	39.0	—	—	—	—	30	—	—	—	—	35
36	15002,329	15.0	40.0	—	—	—	—	23	—	—	78	—	36
37	15002,330	15.0	46.0	—	—	—	—	35	—	—	—	—	37
38	15002,331	15.0	42.0	—	—	—	—	25	—	—	238	—	38
39	15002,332	15.0	36.0	—	—	—	—	24	—	—	—	—	39
40	15002,333	15.0	46.0	—	—	—	—	28	—	—	50	—	40
41	15002,334	15.0	42.0	—	—	—	—	30	—	—	—	—	41
42	15003,19	15.0	30.0	—	—	—	—	27	—	60	55	—	42
43	15503,26	15.0	30.0	—	—	—	—	25	—	51	44	—	43
44	15003,321	15.0	25.0	—	—	—	—	12	—	—	57	—	44
45	15003,322	15.0	18.0	—	—	—	—	11	—	—	105	—	45
46	15003,323	15.0	34.0	—	—	—	—	23	—	—	—	—	46
47	15003,324	15.0	46.0	—	—	—	—	34	—	—	48	—	47
48	15004,17	15.0	37.0	—	—	—	—	47	—	63	59	—	48

TABLE 3-VI.—Continued

No.	Sample	FeO, wt.%	I_s/FeO (Arb.), < 250 μm	N, μg/g	C, μg/g	^{4}He, 10^{-2} cm^3/g	^{36}Ar, 10^{-4} cm^3/g	Petrog. agglut-inates, percent	Mag. fraction, percent	Mean grain size (μm) for < 1 cm	< 1 mm	Fe/FeO	No.
49	15004,24	15.0	38.0	—	—	—	—	34	—	—	70	—	49
50	15004,131	15.0	40.0	—	—	—	—	36	—	—	53	—	50
51	15004,132	15.0	38.0	—	—	—	—	43	—	—	54	—	51
52	15004,133	15.0	26.0	—	—	—	—	22	—	—	52	—	52
53	15005,16	15.0	22.0	—	—	—	—	24	—	97	86	—	53
54	15005,23	15.0	26.0	—	—	—	—	33	—	73	65	—	54
55	15005,390	15.0	36.0	—	—	—	—	30	—	—	—	—	55
56	15005,391	15.0	39.0	—	—	—	—	34	—	—	46	—	56
57	15005,392	15.0	32.0	—	—	—	—	23	—	—	—	—	57
58	15005,393	15.0	36.0	—	—	—	—	30	—	—	49	—	58
59	15005,394	15.0	39.0	—	—	—	—	34	—	—	—	—	59
60	15005,395	15.0	39.0	—	—	—	—	33	—	—	46	—	60
61	15006,17	15.0	52.0	—	—	—	—	51	—	63	58	—	61
62	15006,24	15.0	54.0	—	—	—	—	41	—	—	65	—	62
63	15006,176	15.0	73.0	—	—	—	—	—	—	—	—	—	63
64	15006,200	15.0	65.0	—	—	—	—	57	—	—	50	—	64
65	15006,201	15.0	57.0	—	—	—	—	58	—	—	51	—	65
66	15006,202	15.0	78.0	—	—	—	—	58	—	—	47	—	66
67	15006,203	15.0	77.0	—	—	—	—	60	—	—	61	—	67
68	15006,204	15.0	82.0	—	—	—	—	65	—	—	50	—	68
69	15021,21	15.0	70.0	—	175	—	2.29	—	81	—	—	0.051	69
70	15031,70	15.0	68.0	—	135	—	2.37	—	—	—	—	—	70
71	15041,51	14.3	94.0	—	160	—	3.57	—	—	—	—	—	71
72	15210,2	13.0	54.0	—	155	—	—	—	—	—	—	—	72
73	15251,49	12.0	75.0	—	175	6.78	2.98	—	66	—	—	—	73
74	15261,26	12.1	77.0	106	120	—	—	—	—	—	—	—	74
75	15271,64	12.2	63.0	91	140	7.07	3.15	—	68	—	—	.044	75
76	15291,34	11.6	63.0	—	110	5.94	3.08	—	—	—	—	—	76
77	15301,88	15.5	48.0	—	130	—	2.33	—	63	—	—	.031	77
78	15401,61	18.3	5.6	—	29	—	—	—	—	133	61	—	78
79	15426,97	19.7	3	—	21	—	—	0	—	—	—	.001	79
80	15471,50	16.4	34.0	—	76	2.55	1.70	—	58	—	—	.0140	80
81	15601,101	19.2	29.0	60	98	—	.95	—	67	—	—	.025	81
82	60009,454	5.3	37.0	—	—	—	—	15	—	77	67	—	82
83	60009,455	3.6	32.0	—	—	—	—	13	—	101	80	—	83
84	60009,456	5.2	53.0	—	—	—	—	22	—	102	53	—	84
85	60009,457	2.0	27.0	—	—	—	—	3	—	139	74	—	85
86	60009,458	5.2	52.0	—	—	—	—	29	—	86	51	—	86
87	60051,15	4.5	57.0	52	105	2.71	1.81	—	—	—	—	—	87
88	60601,9	5.5	85.0	—	—	4.50	4.64	—	65	—	—	.091	88
89	61161,2	5.4	82.0	72	—	—	—	36	—	90	66	—	89
90	61181,2	5.5	82.0	—	—	3.78	4.08	38	—	94	64	—	90
91	61221,12	4.9	9.2	15	100	.63	1.20	6	12	216	68	—	91
92	61241,14	5.4	47.0	—	110	5.09	5.29	27	57	120	72	.076	92
93	62281,9	5.5	76.0	—	—	4.04	4.87	40	—	134	70	—	93
94	63321,14	4.7	47.0	60	140	3.03	2.80	33	36	153	87	—	94
95	63341,9	4.5	54.0	59	160	2.80	2.75	40	34	144	80	—	95
96	63501,51	4.7	46.0	70	135	2.96	2.60	10	40	110	71	—	96
97	64421,16	5.0	83.0	118	—	4.58	4.90	54	56	—	—	—	97
98	64501,11	5.2	61.0	82	—	3.07	3.51	52	42	104	65	—	98
99	64801,35	5.2	71.0	86	172	4.32	4.68	—	63	—	—	.094	99
100	65501,4	6.0	38.0	60	90	2.96	2.71	—	—	—	—	—	100
101	65511,1	6.0	55.0	—	—	3.37	3.41	—	—	—	—	—	101

TABLE 3-VI.—Concluded

No	Sample	FeO wt. %	I_s/FeO (Arb.), < 250 μm	N, μg/g	C, μg/g	^{4}He, 10^{-8} cm^3/g	^{36}Ar, 10^{-8} cm^3/g	Petrog agglut-inates, percent	Max fraction, percent	Mean grain size (μm) for < 1 cm	< 1 mm	Fe/FeO	No
102	65701,8	5.7	106.0	118	190	4.90	5.90	—	61	—	—	.137	102
103	66041,12	6.0	90.0	105	175	4.21	4.31	39	—	—	—	.092	103
104	66081,28	6.2	80.0	110	170	3.36	4.02	53	76	—	—	—	104
105	67010,4	4.2	26.0	—	—	—	—	—	—	—	—	—	105
106	67481,23	4.2	31.0	30	65	1.72	1.66	23	15	178	110	—	106
107	67601,15	4.0	45.0	39	—	2.29	2.14	36	29	116	82	.068	107
108	67701,17	4.2	39.0	47	75	2.06	1.86	16	19	140	92	—	108
109	67711,16	3.0	2.8	4	31	—	—	2	2	166	71	—	109
110	67941,13	4.2	29.0	27	59	—	—	12	—	202	97	—	110
111	68501,36	5.3	85.0	83	130	3.43	3.53	39	—	106	68	—	111
112	68841,29	5.6	70.0	97	140	3.78	3.78	—	68	—	—	—	112
113	69941,25	5.7	85.0	118	170	4.24	4.64	—	64	—	—	—	113
114	69961,33	5.7	92.0	125	140	—	—	—	—	—	—	—	114
115	70011,19	16.0	54.0	77	120	22.0	3.36	—	—	—	—	—	115
116	70161,1	17.1	46.0	—	150	—	—	34	—	68	59	—	116
117	70181,10	16.4	47.0	—	165	—	—	56	78	67	58	—	117
118	71041,	17.7	29.0	—	90	—	—	27	—	114	56	—	118
119	71061,1	17.8	14.0	—	40	—	—	9	—	170	58	—	119
120	71501,18	18.3	35.0	60	75	23.2	2.86	35	73	83	65	.030	120
121	72141,15	13.5	81.0	—	155	14.8	4.01	51	—	57	50	—	121
122	72150,2	14.5	82.0	—	—	—	—	53	—	—	—	—	122
123	72321,7	8.7	73.0	—	—	—	3.28	45	—	53	47	.072	123
124	72441,7	8.7	68.0	—	135	6.79	3.60	42	—	65	53	.054	124
125	72461,5	8.6	71.0	—	—	7.40	3.27	43	—	80	61	—	125
126	72501,1	8.7	81.0	70	125	8.60	3.40	48	—	67	57	.062	126
127	72701,24	8.8	61.0	81	130	7.60	3.65	43	63	62	54	—	127
128	73121,10	8.5	78.0	—	120	7.34	3.67	42	62	64	58	—	128
129	73141,8	8.1	48.0	—	120	5.94	2.53	32	—	—	—	—	129
130	73221,1	8.9	43.0	44	155	—	—	26	38	95	64	—	130
131	73241,9	8.8	18.0	22	—	—	—	8	—	127	51	—	131
132	73261,1	8.9	45.0	51	170	—	—	34	—	87	56	—	132
133	73281,1	8.8	34.0	40	—	—	—	25	—	90	49	—	133
134	74121,12	10.0	88.0	—	140	—	—	52	—	54	49	—	134
135	74220,6	22.0	1.0	7	5	1.43	.17	2	—	—	41	.003	135
136	74241,61	14.9	5.1	19	55	15.9	1.58	8	—	130	56	.132	136
137	74261,9	15.3	5.0	13	45	14.2	1.71	8	—	127	56	—	137
138	75061,2	18.0	33.0	44	—	13.0	2.00	24	—	128	81	—	138
139	75081,36	17.1	40.0	—	115	16.0	3.10	35	—	87	67	.033	139
140	75111,5	16.0	58.0	—	—	—	—	52	—	—	—	—	140
140	75111,6	16.0	50.0	—	—	—	—	—	—	—	—	—	140
141	75121,6	16.0	66.0	—	45	14.4	4.39	63	87	—	—	—	141
141	75121,7	16.0	68.0	—	—	—	—	—	—	—	—	—	141
142	76240,9	10.9	56.0	—	125	—	—	48	—	100	53	—	142
143	76261,26	10.9	58.0	—	100	8.99	3.07	45	—	87	58	—	143
144	76281,6	11.3	45.0	—	—	9.87	2.86	45	—	86	53	—	144
145	76321,10	9.8	93.0	—	140	12.5	3.51	39	—	69	53	—	145
146	76501,19	10.3	58.0	68	120	11.6	3.60	47	—	67	51	.050	146
147	77531,1	11.7	79.0	—	180	—	—	54	—	63	49	—	147
148	78221,7	11.7	93.0	—	190	—	—	57	—	50	45	—	148
149	78421,1	12.0	92.0	101	165	—	—	63	—	46	41	.057	149
150	78501,55	13.2	36.0	73	170	9.69	2.77	35	—	42	34	.035	150
151	79221,1	15.4	81.0	—	160	29.2	6.10	44	—	90	53	—	151
152	79261,1	15.0	43.0	—	145	12.3	2.72	22	—	125	70	—	152

IGNEOUS ROCKS

1. Mare Basalts:

The mare basalts are igneous rocks derived from the interior of the Moon as liquids by well-known igneous processes. The mare basalts can be divided into two major chemical groups based on titanium dioxide (TiO_2) content: those that have $TiO_2 > \approx 9.0$ weight percent (primarily reported from the Apollo 11 and 17 sites) and those that have $TiO_2 < 5.0$ weight percent. The range of composition for the major oxides in each group is shown in table 3-VII. In addition to TiO_2, there are significant differences in SiO_2 with the high-titanium basalts (HTB) being 4 to 10 weight percent lower than the low-titanium basalts (LTB). All the other oxides show significant overlap. The LTB's do generally have more MgO and FeO. Analyses of representative lunar samples are shown in table 3-VIII.

One advantage of this chemical grouping, in addition to the obvious differences, is that these basalt types can be differentiated at a 1-kilometer scale on the Moon from Earth-based spectral studies. Much of the near side of the Moon has already been mapped with respect to distinguishing these two basalt units.

Differences in the chemistry are quite logically reflected in significant differences in the modal mineralogy (based on volume percent of the minerals present) as shown in table 3-IX. The differences in titanium content are reflected in the much higher content of opaque minerals (ilmenite and armalcolite) in the HTB's. The differences in silica are evident in a corresponding decrease in the relative plagioclase and pyroxene content of the HTB's.

TABLE 3-VII.—Range of Major Element Chemistry

Chemical	*High-Ti basalts (HTB), wt.%*	*Low-Ti basalts (LTB), wt.%*
SiO_2	37.8 to 40.7	43.9 to 48.4
TiO_2	9.6 to 13.4	1.8 to 4.8
Al_2O_3	8.0 to 10.9	7.3 to 10.8
FeO	16.5 to 19.8	19.3 to 22.5
MnO	0.2 to 0.3	0.2 to 0.3
MgO	6.7 to 10.3	6.5 to 16.5
CaO	10.1 to 12.7	8.0 to 11.8
Na_2O	0.3 to 0.5	0.2 to 0.4
K_2O	0.1 to 0.3	0.5 to 0.7
Cr_2O_3	0.3 to 0.6	0.3 to 0.6
P_2O_5	0.1 to 0.2	0.4 to 0.11
S	0.1 to 0.2	0.4 to 0.8

In texture, the two groups are not mutually exclusive. They both show variants from the vitrophyric basalts to coarse-grain ophitic basalts or fine- to medium-grain gabbros. In general, the coarser grain the rock the more friable it is. Some of the most easily disaggregated rocks are the fine- to medium-grain gabbros. Residual glass and crystal shape appear to be the agents primarily responsible for the toughness of the rocks and, where the glass is lacking and the crystals are equant to subequant, the rocks are more friable. Some specimens have micrometer to centimeter scale cavities (vugs and vesicles).

TABLE 3-VIII.—Chemistry of Mare Basalts

Chemical	*High-Ti basalts*			*Low-Ti basalts*				
	10003	*10017*	*70215*	*12064*	*12021*	*12009*	*15555*	*15076*
				Weight percent				
SiO_2	39.8	40.6	37.8	46.3	46.7	45.0	44.6	48.4
TiO_2	11.3	11.8	13.0	4.0	3.5	2.9	2.1	1.9
Al_2O_3	10.7	8.0	8.9	10.7	10.8	8.6	8.7	9.0
Cr_2O_3	.3	.4	.4	.4	.4	.6	.6	.3
FeO	19.8	19.7	19.7	19.9	19.3	21.0	22.5	20.3
MnO	.3	.2	.3	.3	.3	.3	.3	.3
MgO	6.9	7.7	8.4	6.5	7.4	11.6	11.4	8.6
CaO	11.1	10.7	10.7	11.8	11.4	9.4	9.4	10.5
Na_2O	.6	.5	.4	.3	.3	.2	.3	.3
K_2O	.06	.3	.05	.07	.07	.06	.04	.07
P_2O_5	.1	.2	.09	.04	.09	.07	.06	.07
S	.18	.22	.18	.07	—	.06	.06	.08
Total	101.14	100.32	99.92	100.38	100.26	99.79	100.06	99.82
				Trace chemicals				
Li ppm	9	18.1	7.1	—	8.37	—	6.36	—
Rb ppm	.49	5.63	.356	—	1.14	—	.445	0.917
Sr ppm	152.7	175	121	—	128	—	84.4	12
Ba ppm	108	309	56.9	—	71.1	—	32.2	62.7
La ppm	14.7	26.6	5.22	6.76	—	6.1	8.06	7.38
Ce ppm	45.5	77.3	16.5	17.5	19.8	16.8	6.26	15.1
Nd ppm	38.3	59.5	16.7	16	14.4	16	2.09	10.6
Sm ppm	14.4	20.9	6.69	5.51	4.84	4.53	.688	3.52
Eu ppm	1.36	2.14	1.37	1.16	1.12	.94	2.9	.978
V ppm	63	46	50	119	—	153	—	135
Sc ppm	74	86	86	63	50	46	—	47
Co ppm	14	31	23	27	28	49	—	41

TABLE 3-VIII.—Concluded

Chemical	*High-Ti basalts*			*Low-Ti basalts*				
	10003	*10017*	*70215*	*12064*	*12021*	*12009*	*15555*	*15076*
				Trace chemicals - concluded				
Gd ppm	19.5	27.4	10.4	7.2	6.59	5.2	2.9	4.95
Dy ppm	21.9	31.7	12.2	9.03	7.86	7.13	3.27	5.60
Er ppm	13.6	20.0	7.4	6	4.53	3.6	1.7	3.40
Yb ppm	13	14.2	7.04	4.59	4.12	3.74	1.45	2.77
Lu ppm	1	2.66	1.03	.67	.64	.55	—	36
Zr ppm	309	476	—	114	—	107	76	—
Hf ppm	11.6	17.9	6.33	3.9	4.1	4	—	2.1
Th ppm	.97	2.97	.34	.84	.93	.88	.46	.59
U ppm	.254	.784	.13	.22	.26	.24	.13	.15
Ir ppb	—	.02	.003	—	—	.08	.006	—
Re ppb	—	—	.0015	—	—	—	.0013	—
Au ppb	—	.72	.026	—	—	—	.139	—
Ni ppm	2.6	60	13	—	—	52	42	11
Sb ppb	—	—	.18	—	—	—	.67	—
Ge ppb	—	—	1.66	—	—	<41	8.5	—
Se ppb	—	215	176	—	—	—	156	—
Te ppb	—	—	2.1	—	—	—	3.4	—
Ag ppb	—	16	1.1	—	—	—	1.0	—
Bi ppb	—	1.15	.099	—	—	—	.089	—
Zn ppm	—	18	2.1	—	—	1.8	.78	—
Cd ppb	—	68	1.8	—	—	2.2	2.1	—
Tl ppb	—	6.16	.16	—	—	—	.20	—

The ranges of mineral compositions are shown in tables 3-IX and 3-X for both the HTB's and LTB's. The differences in mineral compositions between the two basalt types are most significant for the TiO_2 content of the opaques. The higher TiO_2 content in the HTB opaques reflects the presence of armalcolite which is not found in the LTB's.

2. Plutonic Rocks:

Occasional coarse-grain rocks have been returned from the Moon, and their modal data and mineral chemistries are summarized in tables 3-XI and 3-XII. The plagioclase in these rocks is very rich in anorthite (90 to 97 vol.%), the olivine is very rich in forsterite (Fo_{90}), and the pyroxenes are very magnesium-rich (En/Fs > 9). Their chemistries are reported in table 3-XIII. The very plagioclase-rich specimens (15415 and 60025) are discussed as cataclastic anorthosites in the section on breccias.

TABLE 3-IX.—Range of Modal Mineralogy (vol.%)

Composition	*High-Ti basalts*	*Low-Ti basalts*
Pyroxene	42 to 60	42 to 70
Olivine	0 to 10	0 to 36
Plagioclase	15 to 33	17 to 33
Opaques	10 to 34	1 to 11
Silica	0 to 6	0 to 5
Mesostasis	0 to 9	0 to 3
Vesicles and holes	0 to 10	0 to 2
Others	0 to 4	0 to 2

TABLE 3-X.—Ranges of Chemical Compositions for Major Minerals (wt.%)

(a) High-titanium basalts

Chemical	*Pyroxene*	*Olivine*	*Plagioclase*	*Opaques*
SiO_2	44.1 to 53.8	29.2 to 38.6	46.9 to 53.3	<1.0
Al_2O_3	0.6 to 7.7	—	28.9 to 34.5	0 to 2.0
TiO_2	0.7 to 6.0	—	—	52.1 to 74.0
Cr_2O_3	0 to 1.0	0.1 to 0.2	—	0.4 to 2.2
FeO	8.1 to 45.8	25.4 to 28.8	0.3 to 1.4	14.9 to 45.7
MnO	0 to 0.7	0.2 to 0.3	—	<1.0
MgO	1.7 to 22.8	33.5 to 36.5	0 to 0.3	0.7 to 8.6
CaO	3.7 to 20.7	0.2 to 0.3	14.3 to 18.6	<1.0
Na_2O	0 to 0.2	—	0.7 to 2.7	—
K_2O	—	—	0 to 0.4	—

(b) Low-titanium basalts

Chemical	*Pyroxene*	*Olivine*	*Plagioclase*	*Opaques*
SiO_2	41.2 to 54.0	33.5 to 38.1	44.4 to 48.2	<1.0
Al_2O_3	0.6 to 11.9	—	32.0 to 35.2	0.1 to 1.2
TiO_2	0.2 to 3.0	—	—	50.7 to 53.9
Cr_2O_3	0 to 1.5	0.3 to 0.7	—	0.2 to 0.8
FeO	13.1 to 45.5	21.1 to 47.2	0.4 to 2.6	44.1 to 46.8
MnO	0 to 0.6	0.1 to 0.4	—	0.3 to 0.5
MgO	0.3 to 26.3	18.5 to 39.2	0.1 to 1.2	0.1 to 2.3
CaO	2.0 to 16.9	0 to 0.3	16.9 to 19.2	<1.0
Na_2O	0 to 0.1	—	0.4 to 1.3	—
K_2O	—	—	0 to 0.3	—

3. Pyroclastic Materials:

Glass spheres are common in the lunar soils. Two peculiar concentrations of these have been found: the green glass (sample 15426) and the orange glass (sample 74220). Their analyses are recorded in table 3-XIII.

4. Granite Glasses:

Glass fragments have been reported that are very high in SiO_2. Chemistries range up to extremes like the composition shown in the following table.

"Granite" Glass (ref. 3-8)

Chemical	*Weight percent*
SiO_2	73.12
TiO_2	.50
Al_2O_3	12.37
Cr_2O_3	.35
FeO	3.49
MgO	.13
CaO	1.27
Na_2O	.61
K_2O	5.91

It must be emphasized that these glass fragments are rare (<1 percent by weight of material), but are ubiquitous in that some examples are found in almost every soil sample.

TABLE 3-XI.—Modal Mineralogy of Plutonic Rocks (vol.%)

Lunar mineral	*Sample number—*			
	15415	*60025*	*72415*	*76535*
Pyroxene	3	1	3	4 to 5
Plagioclase	97	98 to 99	4	37 to 60
Olivine	—	—	93	35 to 58

TABLE 3-XII.—Mineral Chemistries of Plutonic Rocks (wt.%)

(a) Sample 72415

Chemical	*Plagioclase*	*Low-Ca pyroxene*	*High-Ca pyroxene*	*Olivine*	*Cr-spinel*	*Metal*
SiO_2	44.79	56.05	54.13	40.24	0.04	0.05
TiO_2	<.01	.28	.11	.02	1.05	<.01
Al_2O_3	35.00	.96	1.22	<.01	16.71	—
Cr_2O_3	—	.26	1.11	.04	51.81	.54
MgO	.23	32.29	18.40	47.65	10.60	.01
FeO	.14	6.94	2.71	12.29	19.27	67.65
MnO	—	.15	.11	.13	.58	.02
CaO	19.25	2.24	22.50	.13	—	.01
Na_2O	.62	.01	.05	—	—	—
K_2O	.09	—	—	—	—	—
BaO	.04	—	—	—	—	—
ZrO_2	—	—	—	—	<.01	—
V_2O_3	—	—	—	—	.37	—
Nb_2O_3	—	—	—	—	.05	—
NiO	—	—	—	<.01	—	30.42
Co	—	—	—	—	—	1.42
Total	110.17	99.18	100.34	100.50	100.48	100.13

(b) Sample 76535

Chemical	*Plagioclase*	*Olivine*	*Low-Ca pyroxene*	*Low-Ca pyroxene*	*High-Ca pyroxene*	*Cr-spinel*
SiO_2	44.21	40.30	55.89	56.43	53.48	.14
TiO_2	.03	.01	.42	.27	.53	.78
Cr_2O_3	—	.02	.80	.72	.72	50.72
Al_2O_3	35.89	<.01	1.26	1.07	1.00	16.02
MgO	.07	47.96	32.23	33.47	18.11	9.24
CaO	19.60	.03	1.44	.66	23.44	—
FeO	.10	12.30	7.55	8.14	2.87	20.84
MnO	—	.16	.17	.16	.06	.76
BaO	<.01	—	—	—	—	—
Na_2O	.29	—	.02	.03	.02	—
K_2O	.05	—	—	—	—	—
ZrO_2	—	—	—	—	—	.06
V_2O_3	—	—	—	—	—	.72
Nb_2O_3	—	—	—	—	—	<.01
NiO	—	<.01	—	—	—	—
Total	100.25	100.78	99.78	100.95	100.23	99.29

5. Synthetic Lunar Sample:

The most systematic study of the physical properties of melts having the composition of lunar materials was conducted by Murase and McBirney (ref. 3-9). The data presented here were extracted from their study of a synthetic lunar sample (SLS). (The information in this subsection is reported in the units of measurement used by the authors in their original data.) The artificial sample was prepared according to the analysis of specimen 22 of the Apollo 11 collection (Lunar Sample Preliminary Examination Team, 1969). The composition is given in table 3-XIV.

TABLE 3-XIII.—Chemistry of Plutonic and Pyroclastic Samples

Chemical	*Plutonic rocks*			*Pyroclastics*		
	15415	*60025*	*72415*	*76535*	*15426*	*74220*
			Weight percent			
SiO_2	44.1	44.3	39.9	42.9	45.2	38.8
TiO_2	.02	.02	.03	.05	1.1	8.8
Al_2O_3	35.5	35.2	1.5	20.7	15.1	6.4
Cr_2O_3	.003	.03	.3	.1	.4	.7
FeO	.2	.5	11.3	5.0	13.7	22.2
MnO	0	.02	.1	.07	.2	.3
MgO	.1	.2	43.6	19.1	12.14	17.4
CaO	19.7	19.2	1.1	11.4	11.11	7.7
Na_2O	.3	.5	<.02	.2	.4	.4
K_2O	<.01	.03	0	.03	.1	.08
P_2O_5	.01	.003	.04	.03	.09	.04
S	0	—	.01	0	.06	.07
Total	99.94	100.00	97.90	99.58	99.60	102.89
			Trace chemicals			
Li ppm	1.0	—	4.9	3.0	—	10.7
Rb ppm	.17	<.1	.066	.24	—	1.11
Sr ppm	178	—	2.24	114	—	2.09
Ba ppm	6.2	—	3.27	32.7	—	76.4
La ppm	—	.28	.05	1.51	—	6.25
Ce ppm	.32	.65	.07	3.81	—	19.0
Nd ppm	.20	.42	.07	2.30	—	17.8
Sm ppm	.49	.092	.022	.61	—	6.53
Eu ppm	.807	1.04	.016	.73	—	1.80

TABLE 3-XIII.—Concluded

Chemical	Plutonic rocks			Pyroclastics		
	15415	60025	72415	76535	15426	74220
			Trace chemicals - concluded			
Gd ppm	0.062	—	0.030	0.73	—	8.52
Dy ppm	.063	0.19	.035	.80	—	9.40
Er ppm	—	.05	.04	.53	—	5.10
Yb ppm	.045	.048	.045	.56	—	4.43
Lu ppm	—	.006	.008	.079	—	.611
Zr ppm	—	—	3.0	24	—	—
Hf ppm	—	.02	.015	.52	—	—
Th ppm	.027	—	—	.16	—	—
U ppm	.0098	—	< .005	.056	—	—
Ir ppb	< .01	.0057	.0052	—	0.22	.214
Re ppb	.00084	.0016	.0048	—	.020	.0553
Au ppb	.117	.0074	.255	—	.188	1.07
Ni ppm	—	.3	149	—	—	70
Sb ppb	.067	.035	.47	—	.12	25.3
Ge ppb	1.2	2.30	29.8	—	37	191
Se ppb	.23	21.7	4.9	—	69	460
Te ppb	2.1	65	< .36	—	3.3	49
Ag ppb	1.73	.22	.25	—	8.9	75
Bi ppb	.097	3.58	.41	—	.38	1.53
Zn ppm	.26	.17	2.1	—	19	200
Cd ppb	.57	7.25	.37	—	46	260
Tl ppb	.09	26	.049	—	1.13	9.9

TABLE 3-XIV.—Chemical Composition of SLS

Chemical	Weight percent
SiO_2	43.0
TiO_2	11.0
Al_2O_3	7.7
Fe_2O_3	—
FeO	21.0
MnO	.26
MgO	6.5
CaO	9.0
Na_2O	.40
K_2O	.21
Total	99.1

a. Crystallization of SLS:

Crystallization of the SLS was examined under conditions approximating those of the iron-wusite buffer used in experiments with the rock. On cooling, there appeared to be a change in the properties of the liquid SLS at approximately 1643 K (1370° C), but the first minerals to crystallize (opaque oxides) did not appear until a somewhat lower temperature was reached (approximately 1623 K (1350° C)). Plagioclase and clinopyroxene began to appear at approximately 1473 K (1200° C).

The SLS was heated in an iron crucible in an argon atmosphere, approximating the conditions under which such rocks would be extruded as lavas on the lunar surface. No attempt was made to evaluate the effects of pressure or water content on the crystallization or physical properties of the SLS.

b. Viscosity:

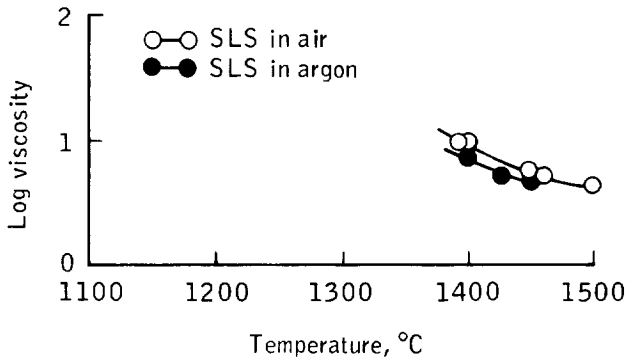

c. Density:

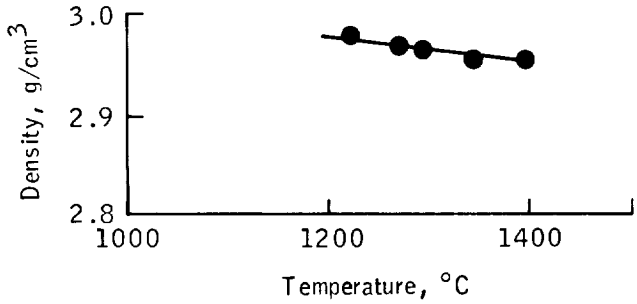

Room temperature density of SLS quenched from liquids at 1673 K (1400° C) is 3.05 g/cm^3.

d. Thermal Expansion:

The coefficient of thermal expansion calculated from the slope of the density-temperature curve is 2.5×10^{-5} deg^{-1}.

e. Ultrasonic Velocities:

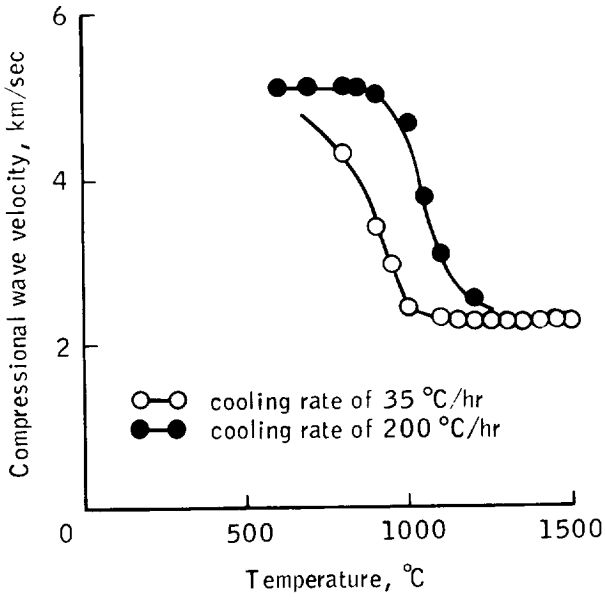

f. Isothermal Compressibility:

Temperature, °C	*Compressibility,* 10^{-12} cm^2/dyne
800	3.0
900	5.0
1000	5.8
1100	6.1
1200	6.5
1300	7.0
1400	7.8

g. Attenuation:

Temperature, °C	*Log* Q^{-1}
1400	−0.44
1450	−.37
1500	−.27

h. Electrical Conductivity:

The variation of conductivity with temperature above the solidus temperature may be expressed as

$$K = A_K \exp(-E_K/RT)$$

where A_K is a constant, E_K is the activation energy for electrical conductivity, R is the gas constant, and T is the absolute temperature.

The conductivity of the liquid SLS is illustrated in the following figure:

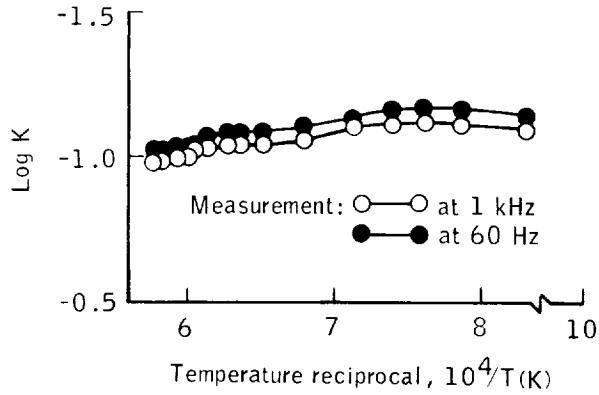

The following are the values for A_K and E_K for the SLS. Both values will vary with silica content.

$$\ln A_K = -1 \qquad E_K = 5 \text{ kcal/mole}$$

i. Thermal Conductivity:

Thermal conductivity may be determined from radial heat flow according to the following relation:

$$K = \frac{1}{2\pi LJ} \ln \frac{R_2}{R_1} \frac{IV}{T_1 - T_2}$$

where L is the length of the cylindrical heat source, J is the mechanical equivalent of heat, R_1 and R_2 are distances from the central axis to inner and outer thermocouples, V is the potential, I is the current through the electric heater, and T_1 and T_2 are the temperatures at the inner and outer thermocouples.

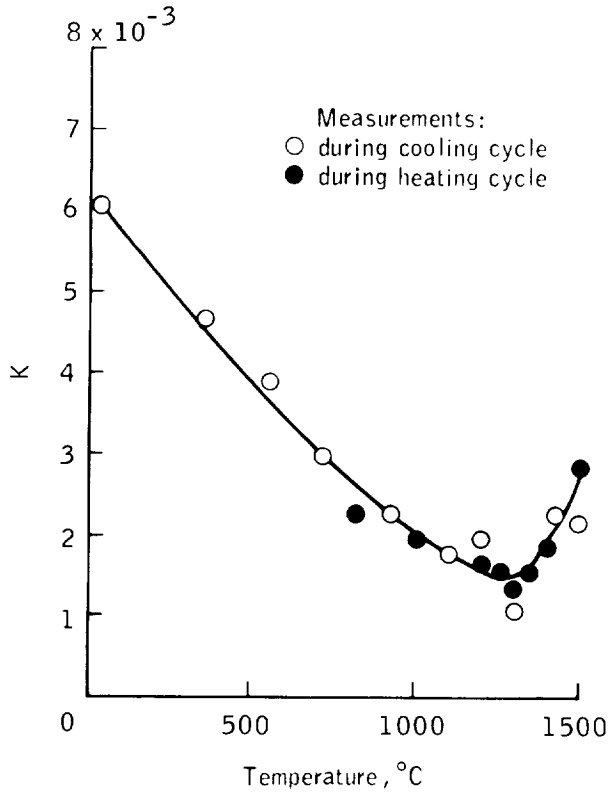

j. Surface Tension:

Temperature, °C	*Surface tension, dyne/cm*
1375	344
1400	350
1450	355
1500	368

BRECCIAS

Meteorite impact is the dominant process affecting the physical nature of the lunar surface. The loose deposits produced by impacts constitute the regolith. Those deposits that have been lithified (turned into rock) by impact are called breccias.

Breccias display various physical and chemical properties. Physical properties are dependent upon the environment of the deposition, whereas chemical properties reflect the average composition of the surface struck by the meteorite.

Physical properties range from friable rocks with approximately one-third pore space to tough rocks with almost no pore space. Grain sizes may be "well sorted" or "poorly sorted." Pore space may consist of micrometer-size cracks and gashes to millimeter- or centimeter-size holes. Breccias may contain from 0 to 50 percent glass.

Impacts are effective mixers of target materials, and all deposits from a single impact have approximately the same composition. It is also true that all impacts in a given region have approximately the same target composition. Therefore, the breccias in the lunar highlands have compositions similar to the lunar crust, whereas the breccias in the mare plains have compositions similar to mare basalts.

Essentially, every sample returned from the lunar highlands during the Apollo and Luna missions is a breccia. Approximately one-third of the samples returned from the mare plains are breccias, the remainder being basalts.

For this handbook, the following classification is used to distinguish rocks with different physical and chemical properties:

Physical properties	*Chemical subgroup*
Vitric-matrix	Mare — High Ti
	Mare — Low Ti
	KREEP
	Anorthositic gabbro
Light matrix	
Cataclastic anorthosite	
Crystalline matrix	KREEP
	Anorthositic gabbro
Granulitic matrix	

Typical members of each group are described in this section. Major, minor, and trace elements for a representative member of each subgroup are given in table 3-XV.

Before beginning the systematic descriptions, it is well to note that all lunar samples, especially the breccias, are more-or-less fractured. Each sample has through-going fractures that are commonly branched. In some cases (e.g., the Apollo 14 breccias), these fractures are so abundant that the samples are dominated by the fractures and the debris of the fracture zones.

1. Vitric-Matrix Breccias:

Vitric-matrix breccias consist of an assemblage of mineral, glass, and rock fragments bound together by grain-to-grain sintering and by smaller glass fragments that act as cement. Samples range from very friable to tough. These rocks are very porous; they commonly have bulk densities between 2.0 and 3.0. Polished surfaces display a network of micrometer-size fractures and irregular cavities whose abundance is an inverse function of the sample's density. The shapes of fragments vary from angular to subrounded. Size distribution of the fragments is such that as the size decreases, the abundance increases. Detailed study of size distribution for lunar materials has not been accomplished. Similar suites of terrestrial materials, however, follow a log-log

TABLE 3-XV.—Chemistry of Breccias

Chemical	Mare			Highland						
	Vitric matrix						Crystalline matrix			
	Low Ti	High Ti	KREEP	Anor. gabbro	Light matrix	Cata. Anor.	KREEP		Anor. gabbro	Gran. matrix
	For sample number —									
	12034	10060	14047	60255	14063	60025	14305	76015	68415	79215
	Weight percent									
SiO_2	47.8	40.0	47.2	45.2	45.5	45.3	48.3	46.2	45.3	43.8
TiO_2	2.3	8.5	1.7	.69	1.3	.02	1.5	1.5	.3	.3
Al_2O_3	15.5	11.3	18.2	26.1	23.0	34.2	16.2	17.2	28.7	27.7
Cr_2O_3	—	.3	.1	.1	.16	.003	.2	.2	.1	.2
FeO	12.4	17.7	10.5	5.9	5.8	.5	10.4	9.8	4.1	4.6
MnO	.2	.2	.1	.06	.1	.008	.1	.1	.05	.06
MgO	8.3	7.7	8.9	6.4	9.6	.2	10.3	13.0	4.3	6.3
CaO	10.8	14.5	11.5	15.1	13.0	19.8	9.9	10.8	16.2	15.9
Na_2O	.7	.5	.7	.5	.7	.5	.8	.7	.5	.5
K_2O	.5	.2	.5	.1	.1	.1	.6	.3	.09	.1
P_2O_5	.5	.1	.5	.1	—	—	.6	.3	.06	.4
S	.09	.15	.08	.04	—	—	—	.09	—	—
Total	99.1	101.15	99.98	100.29	99.26	100.63	98.90	100.19	99.70	99.86
	Trace chemicals									
Li ppm	18	7	—	—	—	—	38.4	21.6	5.1	—
Rb ppm	—	4	16	—	3.5	.1	25	6.57	1.9	—
Sr ppm	—	180	180	—	235	213.6	190	177	140	—
Ba ppm	720	250	730	140	460	10	830	358	70	—
La ppm	—	24	80	12.6	19.4	.28	109	33.4	6.81	2.65
Ce ppm	176.7	62	235	35	47	.65	200	84.9	16.3	6.8
Nd ppm	92	82	102	—	36	.42	140	54	9.92	—
Sm ppm	28.3	24	28	—	9.17	.092	23	15.2	2.88	1.19
Eu ppm	2.69	2	2.6	1.3	2.55	1.04	2.6	1.99	1.13	.84
Gd ppm	—	28	31	—	11.6	.0895	38	18.9	3.27	—
Dy ppm	—	41	33	—	12	.19	43	19.9	3.62	—
Er ppm	—	30	19	—	7	.05	32	11.7	2.18	—
Yb ppm	21.7	22	17	—	6.8	.048	—	10.8	2	1.37
Lu ppm	3.14	2	3	0.7	.99	.0056	3.5	1.3	.33	.24
Zr ppm	630	580	780	—	325	.48	—	507	72	—
Hf ppm	20.4	13	17	5.2	11	.02	26	12.9	—	—
Th ppm	13	3	12	5.2	3.2	—	17.4	5.56	—	—
U ppm	3	.6	3.2	—	.82	.135	5.15	1.96	445	—
Ir ppb	—	—	11.2	12.2	1.37	.0057	10	3.41	4.58	21.3
Re ppb	—	—	1.06	—	.064	.0016	—	.315	.434	1.90
Au ppb	—	—	5.4	5.6	.28	.0074	6.7	1.89	2.65	8.27
Ni ppm	—	70	—	391	—	1.1	200	135	184	255
Sb ppb	—	5	2.1	—	1.3	.035	—	1.02	.53	2.79
Ge ppb	—	1400	—	912	36	2.3	440	164	73	33
Se ppb	—	90	.320	—	8	21.7	—	76	98	176
Te ppb	—	—	85	—	3	6.75	—	—	13.5	17
Ag ppb	—	10	11	—	.87	3.4	—	1.02	4.8	1.16
Bi ppb	—	—	1.1	—	.28	.36	—	.22	.45	.16
Zn ppb	—	25	20	21	5.3	3.25	2.1	2.8	4.8	2.3
Cd ppb	—	300	102	60.8	18	5	—	3.2	2.75	.98
Tl ppb	—	—	17	—	5.6	1.76	—	.67	.49	.41

law with a −2 to −3 slope (i.e., a decrease in size by a factor of 10 would be accompanied by an increase in abundance by a factor of between 100 and 1000).

Composition of the included mineral and rock fragments is similar to the composition of analogous material in the surrounding regolith.

Vitric-matrix breccias may be considered as compacted and lithified regolith, and there are no major chemical differences between local regolith and local vitric-matrix breccias. Vitric-matrix breccias have been referred to as soil breccias, regolith breccias, and glassy breccias. Vitric-matrix breccias even contain enriched abundances of solar-wind-derived components such as the noble gases, carbon, nitrogen, and hydrogen.

Vitric-matrix breccias are abundant on the lunar surface. All breccias returned from the maria and approximately one-third of the breccias returned from the highlands are vitric-matrix breccias.

2. Light-Matrix Breccias:

Light-matrix breccias are similar in texture and friability to the vitric-matrix breccias except they lack glass fragments. They are but poorly bonded aggregates of mineral and rock fragments that are cemented together by grain-to-grain sintering. The light-matrix breccias may be thought of as "glass-free" vitric-matrix breccias.

Light-matrix breccias occur in the lunar samples returned from the Apollo 14 and 16 sites only. From various indirect data, one may hypothesize that light-matrix breccias make up approximately 10 or 15 percent of the lunar highlands.

3. Cataclastic Anorthosites:

Cataclastic anorthosites are crushed rocks consisting of 50 to 99 percent plagioclase feldspar. These samples are very friable. They consist of angular fragments of plagioclase, pyroxene, and olivine, bound together by tiny amounts of glass or by grain-to-grain sintering. Fragment sizes vary from approximately a micrometer to several centimeters, and pore space ranges from 20 percent to essentially nil.

Mineral compositions for cataclastic anorthosite are given in table 3-XVI. For the most part, minerals in these rocks are "pure," in that plagioclase feldspar contains low amounts of iron and pyroxenes and olivines are Mg-rich and Fe-poor. Many of the plagioclase feldspars contain submicron rods and blebs of an opaque phase, probably Fe-metal of FeS.

Approximately two-thirds of the cataclastic anorthosites returned during the Apollo Program contain more than 80 percent plagioclase. However, the proportion of samples with this abundance of plagioclase varies from site to site.

TABLE 3-XVI.— Chemical Composition of Minerals From Cataclastic Anorthosites (wt.%)

Chemical	*Plagioclase*	*Olivine*	*Low-Ca pyroxene*	*Low-Ca pyroxene*	*High-Ca pyroxene*	*Cr-spinel*	*Ilmenite*	*Troilite*
SiO_2	43.56	35.59	53.20	51.25	50.88	0.03	0.01	0.01
TiO_2	.01	.01	.35	.28	.61	2.82	53.24	<.01
Al_2O_3	35.94	<.01	.72	.72	1.50	13.14	<.01	—
Cr_2O_3	—	.05	.33	.27	.37	48.66	.33	<.01
MgO	.03	30.11	24.37	19.89	13.04	3.08	3.27	<.01
FeO	.17	34.58	19.72	24.49	11.98	31.77	42.24	63.84
MnO	—	.42	.35	.41	.37	.74	.50	<.01
CaO	20.00	.03	1.10	1.69	21.22	—	—	.03
BaO	<.01	—	—	—	—	—	—	—
Na_2O	.26	—	.01	<.01	.01	—	—	—
K_2O	.01	—	—	—	—	—	—	—
ZrO_2	—	—	—	—	—	.08	<.01	—
V_2O_3	—	—	—	—	—	.55	<.01	—
Nb_2O_3	—	—	—	—	—	<.01	<.01	—
NiO	—	.03	—	—	—	—	—	<.01
Co	—	—	—	—	—	—	—	<.01
S	—	—	—	—	—	—	—	37.76
Total	99.98	100.82	100.15	99.00	99.98	100.87	99.59	101.64

NOTE: Modal mineralogy, vol.% — plagioclase, 83 percent; olivine, 16 percent; pyroxene, 1 percent; and opaques, less than 1 percent.

Cataclastic anorthosites are rare at all landing sites. Approximately 5 percent of the material returned from the highlands is in this category of material.

4. Crystalline-Matrix Breccias:

Crystalline-matrix breccias consist of a fine-grain, uniform matrix with embedded mineral and rock clasts. The matrix consists of interlocking crystals of plagioclase feldspar, pyroxene, olivine, and ilmenite with sizes ranging from 1 to 100 micrometers. The interlocking of crystals in the matrix bonds the total rock together. Most samples are tough with a low porosity (0.5 to 4 percent). Pore spaces vary from 0.1 millimeter to 10 centimeters; they may be spherical or irregular cavities. Additional cavities, which are 5 to 50 micrometers in size and polygonal in shape, occur interstitial to the crystals in some regions of the

matrix. Clasts range in size from 50 micrometers to tens of meters; they consist of abundant plagioclase with less abundant olivine and even less abundant pyroxene plus rocks.

Crystalline-matrix breccias are chemically equilibrated in that all crystals and grains of a given mineral in each sample have approximately the same composition. Thus, both matrix plagioclase and plagioclase clasts share the same composition in each sample, and that composition is different for different samples. Typical mineral compositions are given in table 3-XVII.

Crystalline-matrix breccias occur only in the highlands, where they comprise approximately 50 percent of the samples returned.

TABLE 3-XVII.— Chemical Composition and Modal Mineralogy for Minerals From Crystalline-Matrix Breccias (wt.%)

(a) Sample 14310; coarser-grain matrix with few clasts

Chemical	*Plagioclase*	*Low-Ca pyroxene*	*High-Ca pyroxene*	*Olivine*	*Ilmenite*	*Troilite*	*Metal*	*Calcium phosphide*	*Mesostasis*	*Bulk composition*
P_2O_5	—	—	—	—	—	—	—	43.15	0.08	0.44
SiO_2	46.67	53.53	50.81	37.66	0.21	—	—	—	57.98	46.47
TiO_2	.02	.90	1.87	.09	54.16	.01	<.01	—	1.82	1.50
Al_2O_3	33.51	.99	1.95	.02	<.01	—	—	—	23.14	17.52
Cr_2O_3	—	.50	.64	.15	.44	—	—	—	.03	.20
CaO	17.78	2.43	18.74	.16	—	.08	.01	54.54	5.29	11.50
MgO	.09	26.36	17.08	35.76	6.56	.03	<.01	—	.76	12.46
FeO	.25	15.42	8.65	26.24	37.38	63.17	92.58	—	1.40	8.96
MnO	—	.19	.21	.32	.46	—	—	—	<.01	.11
BaO	<.01	—	—	—	—	—	—	—	.90	.01
Na_2O	1.51	.06	.17	—	—	—	—	—	.53	.79
K_2O	.13	—	—	—	—	—	—	—	7.21	.13
ZrO_2	—	—	—	—	.01	—	—	—	.07	<.01
V_2O_3	—	—	—	—	<.01	—	—	—	—	<.01
Nb_2O_3	—	—	—	—	.13	—	—	—	—	<.01
NiO	—	—	—	<.01	—	.04	6.99	—	—	.02
Co	—	—	—	—	—	<.01	.37	—	—	<.01
S	—	—	—	—	—	38.52	<.01	—	<.01	.09
F	—	—	—	—	—	—	—	2.31	—	.02
Total	99.96	100.38	100.12	100.40	99.35	101.85	99.96	100.00	99.22	100.22
Vol.%	56.2	25.4	5.9	8.8	1.3	0.1	0.0	0.9	1.0	Calculated
$\pm 1\sigma$	2.0	1.4	.6	.8	.3	.1	.0	.2	.2	(1307
Wt.%	50.4	28.4	6.5	10.2	2.0	.2	.2	1.0	.8	points)

TABLE 3-XVII.— Concluded

(b) Sample 72395; finer-grain matrix with abundant clasts

Chemical	*Orthopyroxene*		*Pigeonite and ferropigeonite*		*Augite*		*Plagioclase*		*K-feldspar*	*Glass*	
SiO_2	52.2	51.8	50.8	47.1	49.6	48.4	44.0	50.9	62.0	76.8	30.5
Al_2O_3	3.44	1.58	1.35	.95	2.81	1.91	34.8	30.0	18.9	11.1	3.08
TiO_2	.69	.65	.89	.74	1.53	1.85	—	—	—	.89	14.6
Cr_2O_3	.61	.48	.39	.08	.72	.04	—	—	—	—	—
FeO	11.2	16.1	19.8	34.1	13.5	18.3	.08	.39	.25	.86	35.7
MnO	.21	.28	.33	.47	.26	.29	—	—	—	.04	.36
MgO	28.4	24.8	20.3	9.17	16.4	11.4	—	—	—	.02	3.16
CaO	2.50	3.11	5.07	5.74	14.0	16.4	19.1	14.5	.37	.73	7.09
Na_2O	.02	.03	.02	.04	.09	.11	.64	2.86	.90	.94	.40
K_2O	—	—	—	—	—	—	.05	.73	14.2	7.39	.52
Total	99.3	98.8	99.0	98.4	98.9	98.7	98.6	99.4	96.7	98.8	95.4

5. Granulitic-Matrix Breccias:

Granulitic breccias are metamorphosed rocks that consist of a crystalline matrix and sparse mineral and rock clasts. These materials are tough, having virtually no porosity. The rocks are bound by the interlocking minerals of the matrix. The matrix consists of plagioclase feldspar and olivine and/or pyroxene in crystals on the order of 50 micrometers in some samples and 200 micrometers in others.

Mineral compositions are the same for the matrix minerals as for the minerals that appear as clasts. Table 3-XVIII gives the mineral chemistry for some typical granulitic breccias.

Granulitic breccias are rare on the lunar surface. Only five large rocks returned during the Apollo Program are granulitic breccias (four during Apollo 17 and one during Apollo 16). However, rock clasts in other breccias and fragments in the regolith that are granulitic breccias have been found at all the landing sites. This suggests that granulitic breccias may be common at depths of a few kilometers throughout the highlands.

TABLE 3-XVIII.— Chemical Composition of Minerals From Granulitic-Matrix Breccias (wt.%)

(a) Sample 77017; coarser-grain matrix

Chemical	Pyroxene				Olivine	Plagioclase	Spinel	Chromite	Ilmenite	Glass
SiO_2	52.32	53.78	52.31	53.62	36.49	44.81	—	—	—	43.76
TiO_2	1.11	.69	.80	.71	.05	.04	0.23	14.72	53.82	.44
Al_2O_3	2.06	.70	1.95	.84	.00	35.50	62.93	8.27	.04	25.21
Cr_2O_3	.81	.36	.77	.43	.04	—	4.02	33.00	.31	—
FeO	9.25	20.17	10.54	18.25	33.73	.12	16.27	39.63	41.25	6.40
MnO	.20	.35	.20	.31	.32	—	.10	.35	.42	—
MgO	14.96	22.96	15.74	21.60	29.06	.05	16.57	4.25	4.38	6.37
CaO	19.19	1.64	17.44	4.09	.18	19.46	—	—	—	14.87
Na_2O	—	—	—	—	—	.42	—	—	—	.35
K_2O	—	—	—	—	—	.14	—	—	—	.05
Total	99.90	100.65	99.75	99.85	99.87	100.54	100.12	100.22	100.22	97.45

(b) Sample 79215; finer-grain matrix

Chemical	Plagioclase	Olivine	Low-Ca pyroxene	High-Ca pyroxene	Whole rock
SiO_2	44.4	37.8	54.9	51.3	43.8
TiO_2	—	.06	.6	1.7	.3
Al_2O_3	35.4	.03	1.0	2.4	27.7
Cr_2O_3	—	.03	.3	.6	.2
FeO	.5	25.0	14.9	7.2	4.6
MnO	—	.3	.2	.2	.06
MgO	—	37.4	27.5	16.4	6.3
CaO	18.5	.1	1.7	20.4	15.9
Na_2O	.6	.0	.0	.1	.5
K_2O	.2	—	—	—	.1
Total	99.6	100.7	101.1	100.3	99.5

REFERENCES

3-1. Oberbeck, V. R.; and Quaide, W. L.: Genetic Implications of Lunar Regolith Thickness Variations. Icarus, vol. 9, 1968, pp. 446-465.

3-2. Watkins, J. S.; and Kovach, R. L.: Seismic Investigation of the Lunar Regolith. Proceedings of the Fourth Lunar Science Conference (Houston, Texas), vol. 3, Pergamon Press, Inc. (New York), 1973, pp. 2561-2574.

3-3. Houston, W. N.; Mitchell, J. K.; and Carrier, W. D., III: Lunar Soil Density and Porosity. Proceedings of the Fifth Lunar Science Conference (Houston, Texas), vol. 3, Pergamon Press, Inc. (New York), 1974, pp. 2361-2364.

3-4. Mitchell, J. K.; Carrier, W. D., III: et al.: Soil Mechanics. Sec. 8 of the Apollo 17 Preliminary Science Report. NASA SP-330, 1973.

3-5. Carrier, W. D., III; and Mitchell, J. K.: Geotechnical Engineering on the Moon. Lunar Utilization (abstracts of papers presented at a special session of the Seventh Annual Lunar Science Conference, March 16, 1976), David Criswell, ed., Lunar Science Institute, Houston, Texas, 1976, pp. 92-95.

3-6. Heiken, G.: Petrology of Lunar Soils. Rev. Geophys. Space Phys., vol. 13, no. 4, 1975, pp. 567-587.

3-7. Morris, R. V.: Surface Exposure Indices of Lunar Soils: A Comparative FMR Study. Proceedings of the Seventh Lunar Science Conference (Houston, Texas), vol. 1, Pergamon Press, Inc. (New York), 1976, pp. 315-335.

3-8. Reid, A. M.; Warner, J.; Ridley, W. I.; and Brown, R. W.: Major Element Composition of Glasses in Three Apollo 15 Soils. Meteoritics, vol. 7, no. 3, 1972, pp. 395-415.

3-9. Murase, T.; and McBirney, A. R.: Properties of Some Common Igneous Rocks and Their Melts at High Temperatures. Geol. Soc. of America Bull., vol. 84, 1973, pp. 3563-3592.

4. Elements

This section discusses the major lunar elements in terms of the mineralogy of lunar materials that was outlined in section 2. Elements discussed include hydrogen, silicon and silica, aluminum, titanium, iron, calcium, magnesium, oxygen, and the volatile elements.

HYDROGEN

The atmophile elements (hydrogen (H), carbon (C), nitrogen (N), oxygen (O), and the noble gases) occur in extremely low concentrations in lunar basalts and highland breccias (table 4-I), and their abundance in the lunar atmosphere (pressure = 10^{-9} N/m^2 (10^{-14} atm)) is vanishingly small. Lunar soils and soil breccias, however, may contain appreciable concentrations of these elements (table 4-II), which have been implanted by the solar wind. The flux of solar ions at the lunar surface is approximately 3×10^8 cm^{-2} sec^{-1}, most of which are hydrogen and helium. Most exposed mineral surfaces appear to saturate at approximately 10^{17} ions cm^{-2}, resulting in strong fractionations among concentrations of the gases relative to solar wind abundances. Mixing of regolith materials by meteorite impacts over approximately 3×10^9 years has mixed the solar-derived gases down to depths of several meters.

Solar ions are implanted into exposed surfaces to depths of less than 0.2 micrometer. Consequently, the largest concentrations of these elements are found in the finest grain sizes of lunar soils, which have the largest surface area to mass ratios. These same surface layers experience considerable solid state damage, due to the amount of energy deposited by the $\approx$1 keV/amu ions and occasional solar flare ions with megaelectronvolt energies. Amorphous layers are commonly formed on grain surfaces that are ion-sputtered away at a rate of 10^{-10} to 10^{-9} m/yr (1 to 10 Å/yr). A large portion of the implanted gases are incorporated into the interiors of constructional particles, such as soil breccias and glass-welded agglutinates. This effect, and other factors, cause gas concentrations to correlate less than exactly with inverse grain diameter, and to depend upon the retention probability of the element. Figure 4-1 gives the approximate relationship between concentration and grain diameter for mature lunar soils that have mean grain diameters of $\approx$60 micrometers.

Mature soils, because of their smaller mean grain diameters and greater fraction of constructional particles, contain several times the concentrations of solar-derived gases as do immature soils. This is the primary cause of the rather large range of concentrations of a given element in different soils (table 4-II). Concentrations of solar-wind-derived elements among the most mature

TABLE 4-I.—Abundance Ranges Indigenous of Lunar Materials[a]

Landing site	*Carbon, ppm*	*Sulfur, ppm*	*Sodium, wt.%*	*Potassium, wt.%*
Apollo 11	62 to 110 (6)	1500 to 2400 (9)	0.28 to 0.52	0.04 to 0.35
Apollo 12	16 to 45 (7)	350 to 1520 (31)	0.14 to 0.37	0.04 to 0.07
Apollo 14	21 to 150 (6)	200 to 1400 (9)	0.22 to 0.30	0.05 to 0.09
Apollo 15	3 to 115 (16)	30 to 1000 (21)	0.22 to 0.30	0.01 to 0.06
Apollo 16	2 to 40 (10)	20 to 1050 (10)	0.20 to 0.50	0.02 to 0.04
Apollo 17	16 to 85 (10)	1230 to 2800 (22)	0.15 to 0.38	0.02 to 0.07
Luna 16	—	1700	0.171	0.133
Luna 20	—	300	0.356	0.390
Luna 24	—	—	—	0.03 to 0.06

[a]Numbers in parentheses are the "number of analyses."

TABLE 4-II.— Typical Solar-Wind Gas Concentrations of Lunar Fines

Landing site	*Concentration, cm^3 (STP[a])/g, for —*					*Concentration, ppm, for —*		
	Helium, 10^{-2}	*Neon, 10^{-4}*	*Argon,[b] 10^{-6}*	*Krypton, 10^{-8}*	*Xenon, 10^{-8}*	*Hydrogen*	*Carbon*	*Nitrogen*
Apollo 11	11 to 25	22 to 33	4 to 5	28 to 66	8 to 37	50	142 to 226	102 to 153
Apollo 12	4 to 38	8 to 68	1.4 to 3.7	7 to 35	4 to 10	80	23 to 180	40 to 130
Apollo 14	5 to 9	10 to 18	2.9 to 5.3	16 to 42	5 to 17	70	42 to 186	80 to 164
Apollo 15	4 to 10	8 to 23	1.1 to 4.9	8 to 42	2 to 12	13 to 120	21 to 186	25 to 113
Apollo 16	0.6 to 5	2.6 to 15	1.5 to 7.2	8 to 60	4 to 24	10 to 79	31 to 280	30 to 155
Apollo 17	6 to 29	13 to 50	1.9 to 7.5	6 to 32	5 to 11	41 to 211	4 to 200	7 to 130
Luna 16	18	38	6.4	38	32	—	—	134 to 2100
Luna 20	4	11	3.5	19	8	—	—	80 to 800
Luna 24	—	—	—	—	—	—	—	—

[a]STP = standard temperature and pressure.
[b]Excludes ^{40}Ar which is formed by radioactive decay of potassium.

soils tend to be the same to within a factor of two. Differences in soil chemistry and mineralogy are less important than soil maturity in determining gas concentrations, with the exception that helium and neon are more readily retained in ilmenite (mare soils) and lost from plagioclase (highland soils).

Helium is most concentrated in the <2-micrometer-size fraction of lunar soil ilmenite. By analogy, solar-wind-derived hydrogen may also be concentrated in the fine-grain lunar ilmenite. The most optimistic estimate, however, of hydrogen concentration in the <20-micrometer fraction of lunar ilmenite is 2000 ppm. The most ilmenite-rich regions of the Moon contain approximately 5 percent ilmenite, and the <20-micrometer fraction makes up approximately 10 percent of the ilmenite. Therefore, the most optimistic estimate for availability of hydrogen from the lunar soil is

$$2000 \text{ ppm} \times 5\% \times 10\% = 10 \text{ ppm}$$

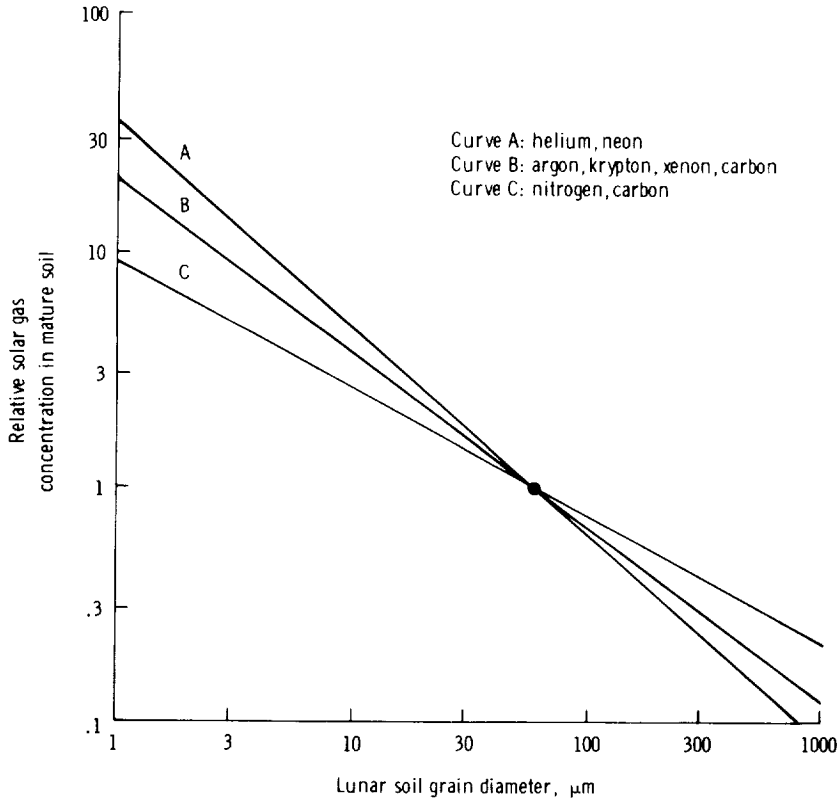

FIGURE 4-1.—Correlation between relative solar gas concentrations in mature lunar soil and lunar soil grain diameter. The mean grain size for a typical mature lunar soil is approximately 60 micrometers.

SILICON AND SILICA

As discussed in section 2 of this handbook, the dominant minerals on the lunar surface are pyroxenes, olivines, plagioclase feldspars, ilmenite, and spinels. Of these, the pyroxenes, olivines, and plagioclase are silicates. Chemical analyses of typical lunar materials (presented in section 2) list SiO_2 contents of approximately 50 percent, 37 percent, and 46 percent for pyroxene, olivine, and plagioclase, respectively. Pyroxenes are being considered as possible sources of magnesium, calcium, iron, and possibly aluminum; olivines are a potential source of magnesium and iron; and plagioclase is a potential source of aluminum. Each of these minerals may also be considered sources of silicon and silica as well. Their relative abundances on the lunar surface are presented in section 2.

Physical Properties of Silicon and SiO_2

1. Density and Molar Volume:

Density of silicon, g/cm^3 ..... 2.33
(at 293 K (20° C))

Density of SiO_2		*Molar Volume of SiO_2*	
Form	*Density, g/cm^3*	*Temperature, °C (a)*	*Molar volume, cm^3*
α-quartz	2.648	25	22.690 ± 0.005
α-cristobalite	2.334	25	25.74 ± 0.02
β-cristobalite	2.194	405	27.38 ± 0.02
α-tridymite	2.265	r	26.53 ± 0.20
β-tridymite	2.192	405	27.42 ± 0.03
Coesite	2.911	25	20.64 ± 0.05
Stishovite	4.287	r	14.016 ± 0.01
β-quartz	2.533	575	27.72 ± 0.01
Keatite	2.503	r	24.01 ± 0.30
Melanophlogite	1.989	r	30.21 ± 0.10

[a]Original data in Celsius ($T_K = T_C + 273.15$).
r = room temperature

Formula weight of SiO_2, g 60.09

2. X-Ray Crystallographic Data:

Silicon (Si)

Crystal system ..... cubic
Space group *Fd3m*
Structure type ..... diamond
Z (gram formula weights per unit cell) 8
Unit cell base vector magnitudes (at 298 K (25° C))
$a_o = 5.4305 \pm 0.0003$ Å (1 Å = 10^{-10} meter)
$\alpha_o = \beta_o = \gamma_o = 90°$
Note: α_o = angle subtended by **b** and **c**
β_o = angle subtended by **a** and **c**
γ_o = angle subtended by **a** and **b**

Silicon dioxide (SiO_2)

X-ray crystallographic data are given in table 4-III.

TABLE 4-III.—X-Ray Crystallographic Data for SiO_2

Form	*Crystal system*	*Space group*	*Structure type*	*Z*	a_o	b_o	c_o	α_o	β_o	γ_o	*Temp., °C (a)*
α-quartz	Hex	$P3_121$	—	3	4.91355	—	5.40512	—	—	—	25
		$P3_221$			±0.0001		±0.0001				
β-quartz	Hex	$P6_422$	—	3	4.9990	—	5.4592	—	—	—	575
		$P6_222$			±0.0005		±0.0005				
α-cristobalite	Tet	$P4_12_12$	—	4	4.971	—	6.918	—	—	—	25
		$P4_32_12$			±0.003		±0.003				
β-cristobalite	Cubic	$Fd3m$	—	8	7.1382	—	—	—	—	—	405
					±0.0010						
Keatite	Tet	$P4_12_12$	—	12	7.456	—	8.604	—	—	—	r
		$P4_32_12$			±0.003		±0.005				
β-tridymite	Hex	$P\bar{6}2c$	—	4	5.0463	—	8.2563	—	—	—	405
		$P6_3/mmc$			±0.0020		±0.0030				
Coesite	Mono	$B2/b$	—	16	7.152	12.379	7.152	—	120°00	—	25
					±0.001	±0.002	±0.001		±10		
Stishovite	Tet	$P4/mnm$	Rutile	2	4.1790	—	2.6649	—	—	—	r
					±0.001		±0.001				
Melanophlogite	Cubic	$P4_232$	—	48	13.402	—	—	—	—	—	r
					±0.004						

[a]Original data in Celsius ($T_K = T_C + 273.15$); r = room temperature.

3. Thermal Expansion:

Composition	*Symmetry and orientation*	*Expansion,[a] in percent, from 20° C to —*						
		100° C	*200° C*	*400° C*	*600° C*	*800° C*	*1000° C*	*1200° C*
Silicon	Cubic, vol[b]	0.066	0.171	0.398	0.631	0.875	1.109	—
Quartz (inversion	Hex, $\perp c$	.14	.30	.73	1.75	1.72	1.70	—
at 573° C)	$\parallel c$	.08	.18	.43	1.02	.98	.89	—
	vol	.36	.78	1.89	4.52	4.42	4.29	—
Tridymite (inversions	Ortho, vol	.63	2.40	3.33	3.48	3.66	3.75	3.60
at 117°, 163°, 210°,								
300°, and 475° C)								
Keatite	Tet, vol	−.06	−.11	−.11	—	—	—	—
Cristobalite (inversion	Tet, $\perp c$	.221	.503	—	—	—	—	—
at 218° C)	$\parallel c$	.346	.779	—	—	—	—	—
	vol	.791	1.795	6.271	6.414	6.499	6.575	6.651
Coesite	Mono, $\parallel a, \parallel c$	.020	.048	.116	.194	.284	.383	—
	$\parallel b$	.022	.050	.114	.193	.283	.381	—
	vol	.059	.145	.345	.580	.849	1.150	—

[a]Original data reported in Celsius ($T_K = T_C + 273.15$).
[b]vol = volumetric expansion.

Thermal Expansion of Cristobalite

Temperature, °C (a)	*Change in length, percent, for —*		*Change in volume, percent*
	$\parallel$a	$\parallel$c	
100	0.221	0.346	0.791
200	.503	.779	1.795
218 (below)	.563	.851	1.990
At 218° C the tetragonal form inverts to a cubic modification			
218 (above)	—	—	5.772
300	—	—	6.039
400	—	—	6.271
500	—	—	6.360
600	—	—	6.414
700	—	—	6.459
800	—	—	6.499
900	—	—	6.539
1000	—	—	6.575
1100	—	—	6.615
1200	—	—	6.651

[a]Original data reported in Celsius ($T_K = T_C + 273.15$).

Thermal Expansion of Quartz

Temperature, °C (a)	*Change in length, percent, for —*		*Change in volume, percent*
	⊥ c	‖c	
50	0.07	0.03	0.17
100	.14	.08	.36
150	.22	.12	.56
200	.30	.18	.78
250	.40	.23	1.03
300	.49	.29	1.27
350	.60	.36	1.56
400	.72	.43	1.87
450	.87	.51	2.25
500	1.04	.62	2.70
525	1.15	.67	2.97
550	1.29	.75	3.33
560	1.36	.80	3.52
570	1.46	.84	3.76
	Transition: α to β quartz at 573° C		
580	1.76	1.03	4.55
590	1.76	1.03	4.55
600	1.76	1.02	4.54
650	1.76	1.02	4.54
700	1.75	1.01	4.51
750	1.74	1.00	4.48
800	1.73	.97	4.43
850	1.72	.94	4.38
900	1.71	.92	4.34
950	1.70	.89	4.29
1000	1.69	.88	4.26

[a]Original data reported in Celsius ($T_K = T_C + 273.15$).

4. Compressibility and Elastic Constants:

$$\frac{V_o - V}{V_o} = aP - bP^2$$

where: V = volume
V_o = initial volume
P = pressure in megabars (Mb)
a = proportional limit
b = elastic limit

Silicon at 25° C: $a = 1.012\ \text{Mb}^{-1}$; $b = 2.5\ \text{Mb}^{-2}$ (for P less than 30 kb)

Pressure, kg/cm^2	$(V_o - V)/V_o$
5 000	0.00491
10 000	.00965
15 000	.01433
20 000	.01888
25 000	.02332
30 000	.02755
40 000	.032
50 000	.038
60 000	.043
70 000	.048
80 000	.052
90 000	.056
100 000	.060

Elastic constants may be obtained from the following relationships for the Voigt and Reuss schemes.

	Voigt	*Reuss*
Bulk modulus	$K = (A + 2B)/3$	$K = 1/(3a + 6b)$
Modulus of rigidity	$G = (A - B + 3C)/5$	$G = 5/(4a - 4b + 3c)$

with
$3A = C_{11} + C_{22} + C_{33}$ $\quad 3a = S_{11} + S_{22} + S_{33}$
$3B = C_{23} + C_{31} + C_{12}$ $\quad 3b = S_{23} + S_{31} + S_{12}$
$3C = C_{44} + C_{55} + C_{66}$ $\quad 3c = S_{44} + S_{55} + S_{66}$

where C_{pq} and S_{pq} refer to the individual crystal.

Values of C_{pq} and S_{pq} for silicon at 25° C are as follows:

$$C_{11} = 1.65773 \qquad S_{11} = 0.76809$$
$$C_{12} = 0.63924 \qquad -S_{12} = 0.21376$$
$$C_{44} = 0.79619 \qquad S_{44} = 1.2560$$

$S_{11} = S_{22} = S_{33}$; $S_{23} = S_{31} = S_{12}$; $S_{44} = S_{55} = S_{66}$;
(all others are zero)

The values of a and b are as follows for α and β quartz.

Form	a, Mb^{-1}	b, Mb^{-2}
Quartz α	2.707	24.0
linear, $\|c$	.718	6.2
linear, $\perp c$	.995	7.6
	2.697	20.4
	2.77	—
Quartz β	1.776	—

The following table lists values of $(V_o - V)/V_o$ at pressures above 12 kilobars for quartz.

Measurement	*Values of* $(V_o - V)/V_o$ *for pressures, in kg/cm², of—*					
	5000	*10 000*	*15 000*	*20 000*	*25 000*	*30 000*
Linear, $\|c$	0.00334	0.00642	0.00920	0.01170	0.01406	0.01622
Linear, $\perp c$	.00480	.00909	.01308	.01688	.02056	.02411
Volume	.01289	.02440	.03495	.04478	.05418	.06308

5. Strength and Ductility:

Stress-Strain Relationship

Temp.,[a] *°C*	*Confining pressure, bars*[a]	*Differential stress in bars for strain percent of —*				*Ultimate strength, bars*	*Total strain, percent*	*Fault angle, deg*
		1	*2*	*5*	*10*			
				Quartz (load ‖ c)				
24	0	7 000	14 000	—	—	25 000	4.8	—
24	2580	12 500	24 000	—	—	51 000	4.8	—
24	5070	14 500	28 000	—	—	52 000	4.3	—
500	5070	8 200	16 500	—	—	30 000	4.8	—
600	5070	—	—	—	—	19 000	4	—
800	5070	7 000	12 600	14 000	11 000	20 000	12.4	—
				Quartz (load ⊥ c)				
24	5070	10 000	20 000	—	—	35 000	4.5	—
500	5070	9 000	17 000	—	—	31 000	4.8	—
600	5070	7 000	13 000	—	—	25 000	4.0	—
800	5070	5 000	9 500	12 000	—	25 000	6.8	—
800	5070	4 000	—	—	—	4 000	—	—

[a]Original data reported in Celsius and bars; $T_K = T_C + 273.15$ and 1 bar = 10^5 N/m^2.

Shearing Strength Under High Confining Pressure

Normal pressure of — in kilobars	*Shear strength, kilobars*
Silicon (Si)	
10	1.0
20	2.4
30	4.6
40	6.8
50	8.6
Silicon dioxide (SiO_2)[a]	
10	—
20	—
30	—
40	—
50	14.2
Cristobalite (SiO_2)[b]	
10	—
20	—
30	—
40	—
50	14.2
Opal (SiO_2)[c]	
10	3.5
20	7.0
30	9.8
40	12
50	18

[a]Rotates with snapping, optic axis tangential.
[b]Rotates smoothly, some snaps, inverts to an unknown form of SiO_2.
[c]Rotates with much snapping, partly inverts to quartz.

6. Melting and Transformation Points:

Silicon (Si)

Melting point, K (°C)	1687 (1414)
Boiling point, K (°C)	3104 (2831)

Silicon dioxide (SiO_2)

Quartz melting point, K (°C)	1743 (1470)
Transition from trigonal to hexagonal, K (°C)	846 ± 3 (573 ± 3)
Transition from quartz to tridymite, K (°C)	1140 ± 3 (867 ± 3)
Tridymite melting point, K (°C)	1943 ± 10 (1670 ± 10)
Transition from orthorhombic to low hexagonal, K (°C)	378 ± 15 (105 ± 15)
Transition from low hexagonal to high hexagonal, K (°C)	433 ± 15 (160 ± 15)
Transition from tridymite to cristobalite, K (°C)	1743 ± 10 (1470 ± 10)
Cristobalite melting point, K (°C)	2001 ± 10 (1728 ± 10)
Transition from orthorhombic to cubic, K (°C)	473 to 543 (200 to 270)

7. Thermodynamic Properties:

Silicon (Si)

Formula weight, g	28.086
Molar volume, cm^3 (J/bar)	11.74 (1.174)
Heat of fusion, kJ	50.575
Heat of vaporization, kJ	393.027

$H^o_{298} - H^o_o = 3.219$ kJ

$S^o_T = 18.81 \pm 0.08$ J mol^{-1} K^{-1} (at 298.15 K)

where H^o_{298} = enthalpy, H^o_o = enthalpy at absolute zero, and S^o_T = entropy.

Quartz (SiO_2)

α quartz, K	298.15 to 844
β quartz, K	844 to 1800

7. Thermodynamic Properties (continued):

$C_p^o = 44.603 + 3.7754 \times 10^{-2} T - 1.0018 \times 10^6 T^{-2}$
(equation valid from 298 to 844 K)
$C_p^o = 58.928 + 1.0031 \times 10^{-2} T$
(equation valid from 844 to 1800 K)
$H_{298}^o - H_o^o = 6.916$ kJ
$S_T^o = 41.46 \pm 0.20$ J mol^{-1} K^{-1} (at 298.15 K)
Melting point = not available Enthalpy of melting = not available
Boiling point = not available Enthalpy of vaporization = not available
Molar volume, cm^3 (J/bar) 22.688 (2.2688)

Cristobalite (SiO_2)

α cristobalite, K ..... 298.15 to 523
β cristobalite, K ..... 523 to 1800

$C_p^o = -4.1596 \times 10^3 + 2.5480 T + 7.1680 \times 10^4 T^{-0.5} - 6.2859 \times 10^7 T^{-2}$ (equation valid from 298 to 523 K)
$C_p^o = 72.753 + 1.3004 \times 10^{-3} T - 4.1320 \times 10^6 T^{-2}$
(equation valid from 523 to 1800 K)
$H_{298}^o - H_o^o = 7.040$ kJ
$S_T^o = 43.40 \pm 0.13$ J mol^{-1} K^{-1} (at 298.15 K)
Melting point, K 1996
Enthalpy of melting, kJ 8.159
Boiling point ..... not available
Enthalpy of vaporization ..... not available
Molar volume, cm^3 (J/bar) 25.739 (2.5739)

Tridymite (SiO_2)

α tridymite, K ..... 298.15 to 390
β tridymite, K ..... 390 to 1800

$C_p^o = 74.904 + 3.0999 \times 10^{-3} T - 2.3669 \times 10^2 T^{-0.5} - 1.1740 \times 10^6 T^{-2}$ (equation valid from 390 to 1800 K)
$H_{298}^o - H_o^o =$ not available
$S_T^o = 43.93 \pm 0.42$ J mol^{-1} K^{-1} (at 298.15 K)
Melting point = 1943 K Enthalpy of melting = not available
Boiling point = not available Enthalpy of vaporization = not available
Molar volume, cm^3 (J/bar) 26.530 (2.6530)

7. Thermodynamic Properties (continued):

Coesite (SiO_2)

$C_p^o = 2.3306 \times 10^2 - 7.7765 \times 10^{-2}\,T + 1.9237 \times 10^{-5}\,T^2 - 3.3753 \times 10^3\,T^{-0.5} + 2.6036 \times 10^6\,T^{-2}$

(equation valid from 298 to 1800 K)

$H_{298}^o - H_o^o$ = not available

$S_T^o = 40.38 \pm 0.42$ J mol^{-1} K^{-1} (at 298.15 K)

Melting point = not available Enthalpy of melting = not available

Boiling point = not available Enthalpy of vaporization = not available

Molar volume, cm^3 (J/bar) 20.641 (2.0641)

Stishovite (SiO_2)

$C_p^o = 1.4740 \times 10^2 - 4.0271 \times 10^{-2}\,T + 1.2026 \times 10^{-5}\,T^2 - 1.5594 \times 10^3\,T^{-0.5} - 2.8339 \times 10^5\,T^{-2}$

(equation valid from 298 to 1800 K)

$H_{298}^o - H_o^o$ = not available

$S_T^o = 27.78 \pm 0.42$ J mol^{-1} K^{-1} (at 298.15 K)

Melting point = not available Enthalpy of melting = not available

Boiling point = not available Enthalpy of vaporization = not available

Molar volume, cm^3 (J/bar) 14.014 (1.4014)

Silica glass (SiO_2)

$C_p^o = 74.639 - 7.2594 \times 10^{-3}\,T + 5.5704 \times 10^{-6}\,T^2 - 3.1140 \times 10^6\,T^{-2}$

(equation valid from 298 to 1500 K)

$H_{298}^o - H_o^o$ = not available

$S_T^o = 47.40 \pm 0.21$ J mol^{-1} K^{-1} (at 298.15 K)

Melting point = not available Enthalpy of melting = not available

Boiling point = not available Enthalpy of vaporization = not available

Molar volume, cm^3 (J/bar) 27.270 (2.7270)

8. Electrical Properties:

Silicon is an intrinsic semiconductor whose conductivity varies with temperature as illustrated in figure 4-2.

The dielectric constants of quartz are as follows:

Wavelength, cm	*Dielectric constant for —*	
	⊥ to optic axis	*∥ to optic axis*
∞	4.69	5.06
10^3	4.27	4.34

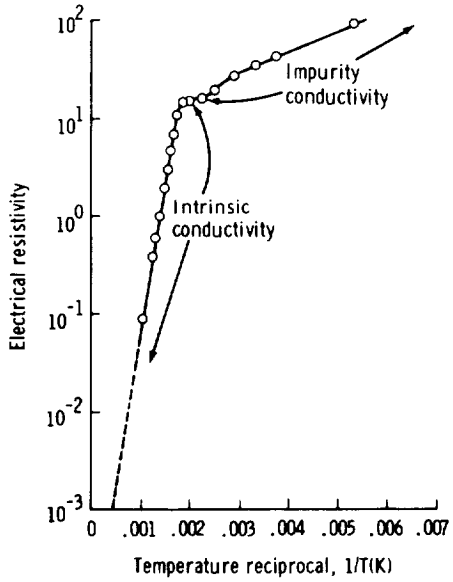

FIGURE 4-2.—Electrical resistivity of pure silicon as a function of temperature.

9. Thermal Conductivity:

α quartz (SiO_2)

$$K\Phi = K_{\perp} \sin^2 \Phi + K_{\parallel} \cos^2 \Phi$$

where $K_{\perp}$ = conductivity $\perp$ to optic axis
$K_{\parallel}$ = conductivity $\parallel$ to optic axis
Φ = angle between direction and optic axis

Temp., °C	*Thermal conductivity,[a] in watts cm^{-1} K^{-1}, for —*	
	$\parallel$ *to optic axis*	$\perp$ *to optic axis*
≈8	110	67
−190	491	246
−78	196	101
0	136	72.5
100	90	55.6
40	102×10^{-3}	—
68.1	93	—
104.3	77.8	—
25	—	61.5×10^{-3}
70.4	—	54.0
105.5	—	48.5
≈30	125	66.1
0	114.3	68.2
100	79.5	49.5
200	63.2	40.6
300	51.5	35.2
400	43.1	31.0

[a]Conversion: cal sec^{-1} cm^{-1} K^{-1} = 0.239 × watt cm^{-1} K^{-1}

10. Magnetic Properties:

Not available for lunar materials.

ALUMINUM

Data for the pyroxenes and plagioclase feldspars (section 2 of this handbook) indicate that these minerals—particularly the mineral anorthite, found in lunar plagioclase—may be potential sources of aluminum. Chemical analyses of typical samples of these lunar minerals and their relative abundance on the lunar surface are presented in section 2.

Aluminum is widely used on Earth, both as a structural material and as an electrical conductor. Its potential use in the assembly of large structures in space needs no discussion here.

Table 4-IV provides a synopsis of the physical properties of aluminum. More detailed discussions of aluminum and its alloys are presented in references 4-1 and 4-2.

TABLE 4-IV.—Condensed Table of Physical Properties of Aluminum[a]

Property	*Value*
Thermal neutron cross section	0.21 barn (10^{-24} cm^2)
Lattice constant	4.04958 ± 0.000025 Å at 25° C (77° F)
Density (solid)	2.698 g/cm^3 at 25° C
	0.0975 lb/cm^3 at 77° F
Density (liquid)	2.368 g/cm^3 at 660° C
	0.0856 lb/in.^{3} at 1220° F
Linear coefficient of thermal expansion	22.5×10^{-6} cm cm^{-1} C^{-1}
	12.5×10^{-6} in. in.$^{-1}$ °F^{-1}
Average coefficient of linear expansion	23.6×10^{-6} cm cm^{-1} C^{-1} from 20° to 100° C
	13.1×10^{-6} in. in.$^{-1}$ °F^{-1} from 68° to 212° F
Thermal conductivity	0.59 cal cm^{-1} sec^{-1} C^{-1} at 25° C
	142.7 Btu ft^{-1} hr^{-1} °F^{-1} at 77° F
Volume resistivity	2.6548 microhm cm at 20° C (68° F)
Volume conductivity	64.94 percent IACS[b]
Mass temperature coefficient of resistance	0.00429 at 20° C (68° F)
Magnetic susceptibility	0.6276×10^{-6} per g
Reflectance (electrolytically brightened), visible light	85 to 90 percent
Emissivity at 9.3 microns	3 percent
Surface tension	900 dynes/cm at 700° C (1292° F)
Viscosity	0.01275 poise at 700° C (1292° F)
Melting point	660 ± 1° C (1220 ± 1.8° F)
Heat capacity	5.82 cal mol^{-1} C^{-1} at 25° C
Boiling point	2452° C ± 15° C
	4445° F ± 27° F
Solution potential, standard hydrogen scale	−1.66 V

[a]Data are given here in the units of measurement of the original report.
[b]International analysis code system.

TITANIUM

Ilmenite ($FeTiO_3$) is identified in section 2 as one of the dominant lunar minerals, with localized abundances greater than 10 percent. Ilmenite is the principal ore of titanium on Earth and, therefore, may be considered as a source of titanium on the lunar surface. The occurrence of ilmenite on the Moon and analyses of typical samples are presented in section 2. Lunar pyroxenes also accept up to 5 percent TiO_2 into solid solutions.

The physical properties of commercially pure titanium are summarized in the following table. (Additional data for titanium and titanium alloys are available in reference 4-2.)

Physical Properties of Titanium (Commercially Pure)

Melting point, K	1943.2
Boiling point, K	3533.2
Density, g/cm^3 at 293.2 K	4.5
Thermal conductivity, cal cm^{-1} sec^{-1} K^{-1} between 273.2 and 373.2 K	0.041
Mean specific heat, cal g^{-1} K^{-1} between 273.2 and 373.2 K	0.126
Resistivity, microhm cm at 293.2 K	55
Temperature coefficient of resistivity between 273.2 and 373.2 K	4.1×10^3
Coefficient of expansion between 273.2 and 373.2 K	8.9×10^6

IRON

Iron is present on the Moon in pyroxenes (ferrosilite ($FeSiO_3$)), olivine (fayalite (Fe_2SiO_4)), ilmenite ($FeTiO_3$)), and spinels (Fe_2TiO_4, $FeCr_2O_4$, and $FeAl_2O_4$); also, iron may be found in the native form. Section 2 presents the analyses and abundances of pyroxenes, olivines, and ilmenite.

The following table presents some of the physical properties of iron. (Additional data concerning the properties of iron and steel are available in reference 4-2.)

Physical Properties of Iron

Melting point, K	1810.2
Boiling point, K	3343.2

Density, g/cm^3 at 293.2 K	7.87
Thermal conductivity, cal cm^{-1} sec^{-1} K^{-1} between 273.2 and 373.2 K	0.17
Mean specific heat, cal g^{-1} K^{-1} between 273.2 and 373.2 K	0.109
Resistivity, microhm cm at 293.2 K	9.71
Temperature coefficient of resistivity between 273.2 and 373.2 K	6.51×10^3
Coefficient of expansion between 273.2 and 373.2 K	29.0×10^6

CALCIUM

Calcium is present on the Moon in pyroxenes (wollastonite ($CaSiO_3$)), and plagioclase (anorthite ($CaAl_2Si_2O_8$)). Section 2 presents the analyses and abundances of these minerals.

The following table presents some of the physical properties of calcium. (Additional data are available in reference 4-2.)

Physical Properties of Calcium

Melting point, K	1123.2
Boiling point, K	1713.2
Density, g/cm^3 at 293.2 K	1.54
Thermal conductivity, cal cm^{-1} sec^{-1} K^{-1} between 273.2 and 373.2 K	0.3
Mean specific heat, cal g^{-1} K^{-1} between 273.2 and 373.2 K	0.149
Resistivity:	
Soft calcium, microhm cm	4.1
Hard calcium, microhm cm	4.37
Temperature coefficient of resistivity between 273.2 and 373.2 K	4.6×10^3
Coefficient of expansion between 273.2 and 373.2 K	22×10^6

MAGNESIUM

Magnesium is present on the Moon in pyroxenes (enstatite ($MgSiO_3$)), olivine (forsterite (Mg_2SiO_4)), spinels (picrochromite ($MgCr_2O_4$), $MgAl_2O_4$, and Mg_2TiO_4), and in small amounts of geikielite ($MgTiO_3$)) in mixtures with ilmenite. Section 2 presents the analyses and abundances of these minerals.

The following table presents some of the physical properties of magnesium. (Additional data are available in reference 4-2.)

Physical Properties of Magnesium

Melting point, K	923.2
Boiling point, K	1376.2
Density, g/cm^3 at 293.2 K	1.74
Thermal conductivity, cal cm^{-1} sec^{-1} K^{-1} between 273.2 and 373.2 K	0.4
Mean specific heat, cal g^{-1} K^{-1} between 273.2 and 373.2 K	0.248
Resistivity, microhm cm at 293.2 K	3.9
Temperature coefficient of resistivity between 273.2 and 373.2 K	4.2×10^3
Coefficient of expansion between 273.2 and 373.2 K	26.0×10^6

OXYGEN

Oxygen is present in all the major minerals available on the Moon (oxides and silicates). Each of these minerals may be considered as a source of oxygen since they contain 30 to 45 percent oxygen (by weight).

The following table presents some of the physical properties of oxygen.

Physical Properties of Oxygen

Melting point, K	54.8
Boiling point, K	90.2
Density, g/cm^3 at 293.2 K	1.429×10^{-3}

VOLATILE ELEMENTS

This subsection presents information on the elements which commonly exist as gases on Earth (e.g., H_2O, CO_2, N_2, Ar, etc.); also a few select elements that are readily volatilized from lunar material (e.g., Na, K, S). These elements and their compounds have in common the fact that they may be partially or entirely driven from lunar material by heating.

The occurrence of the atmophile elements (H, C, N, and the noble gases) and the location of solar-wind-derived elements on the Moon are discussed in the subsection entitled "Hydrogen."

Most of the geochemical information on the easily volatilized elements in the lunar regolith was obtained by analyses of lunar soils.

Carbon abundances in lunar soils are greater than those found in lunar crystalline rocks. It has been shown that most of the carbon found in lunar soils derives from the solar wind, whereas the carbon in the rocks is indigenous to the Moon. Carbon abundances for lunar basalts range from 20 to 100 μg/g and, for lunar anorthosites, between 2 and 40 μg/g (table 4-I). Lunar breccias typically contain carbon abundances intermediate to the soils and rocks.

Lunar crystalline rocks range in sulfur from 20 μg/g for anorthosites to 2800 μg/g for some lunar basalts. Lunar basalts are typically 5 to 10 times more enriched in sulfur than terrestrial basalts. In general, sulfur content of soils is similar to the rock types which constitute the soil; this indicates that the solar wind and meteoritic components of sulfur in soils is minor.

Lunar materials are depleted in the volatile elements potassium and sodium as compared to terrestrial rocks. The lunar basalts range in sodium concentrations from 0.14 to 0.52 wt.%. No major differences in sodium abundances exist between mare materials and highland materials (table 4-I). Lunar basalts range from 0.01 to 0.35 wt.% potassium with most crystalline materials containing 0.05 $\pm$ 0.03 wt.% potassium. In contrast to most terrestrial surface rocks, potassium is so low in concentration in lunar rocks as to constitute a minor or trace element and resembles the concentration levels in low-potassium oceanic tholeiites or in chondritic meteorites. Sodium is depleted in lunar materials relative to terrestrial basalts by a factor of approximately five.

The easily volatilized elements are lost from lunar samples over a wide temperature range, which leads to insight as to the origin of these species. Lightly adsorbed species and contamination products (e.g., spacecraft exhausts) are generally removed from lunar soils at temperatures below 423 K (150° C). Solar-wind-derived gases may be released from fines from approximately 873 K ($\approx$600° C) to sample melting, with lighter gases being released at lower temperatures. Solar-wind-derived species (such as H_2O, H_2, CH_4, and a portion of the N_2 and CO) are removed from lunar fines at temperatures between 473

and 1173 K (200° and 900°C). At temperatures near 1173 K (900° C), chemical reactions and decompositions of mineral phases begin with the loss of S, CO, N_2, Na, Rb, and K. Near the melting temperature of soils (1373 to 1532 K (1100° to 1259° C)), chemical reactions occur between various phases present, with the evolution of reaction products CO, H_2S, SO_2, H_2, and CO_2. A summary of the gas evolution regions for various lunar materials is given in figure 4-3.

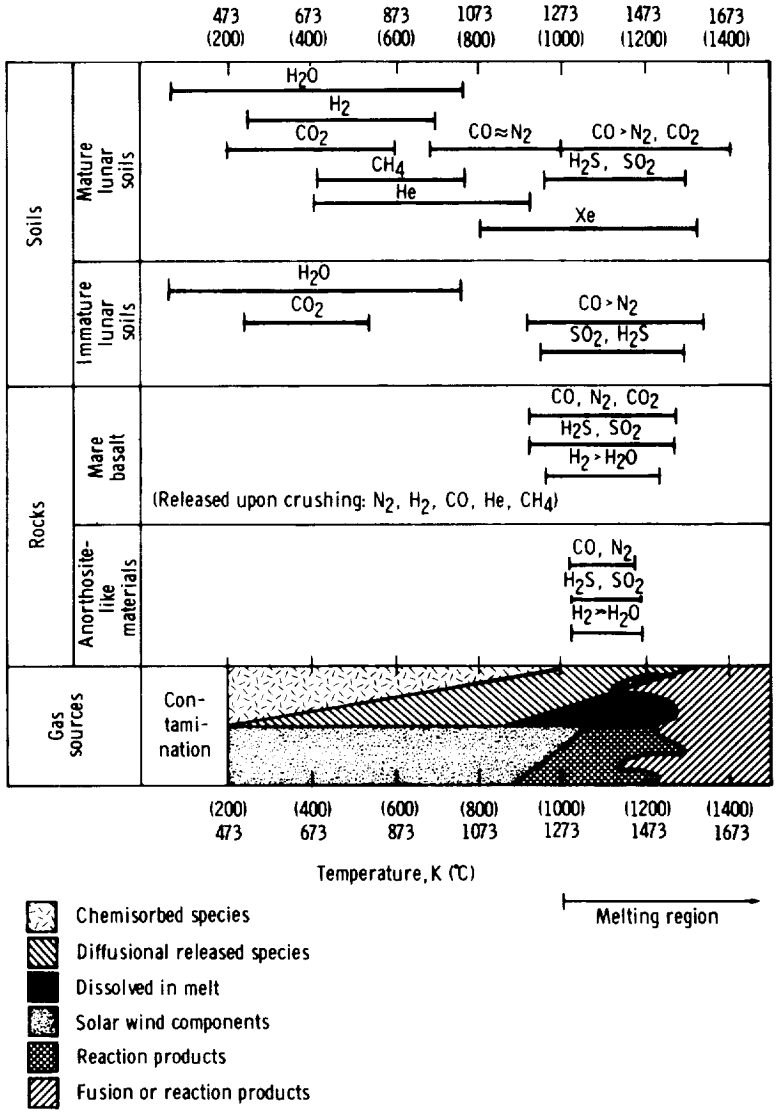

FIGURE 4-3.—Summary of gas evolution regions for lunar materials.

Volatilization studies of lunar fines has shown that substantial quantities of carbon and sulfur are evolved in vacuum at temperatures as low as 1023 K (750° C). Figure 4-4 presents data from step-wise volatilization studies of lunar mare and highland soils. The alkali elements are lost from lunar fines at temperatures beginning near 1273 K (1000° C). The relative volatility of the alkali elements is Rb > K > Na for lunar materials. Loss of sodium does not occur readily until temperatures of 1223 K (950° C). Sulfur loss from lunar fines is substantial during vacuum pyrolysis. At temperatures of 1373 K (1100° C) (below the melting temperature of most soil components), between 85 and 95 percent of the sulfur has been lost from lunar soils.

Several trace elements (such as Zn, Cd, In, Hg, Pb, Ge, and the halogens), which generally occur in surface materials in concentrations of 10 to 0.001 ppm, also readily undergo volatilization and migration on the lunar surface because of heating and melting of soils by solar radiation and meteorite impact. As a result, these elements are often found in considerably higher concentrations in areas shadowed by large rocks and on grain surfaces of the finest grain sizes of soils.

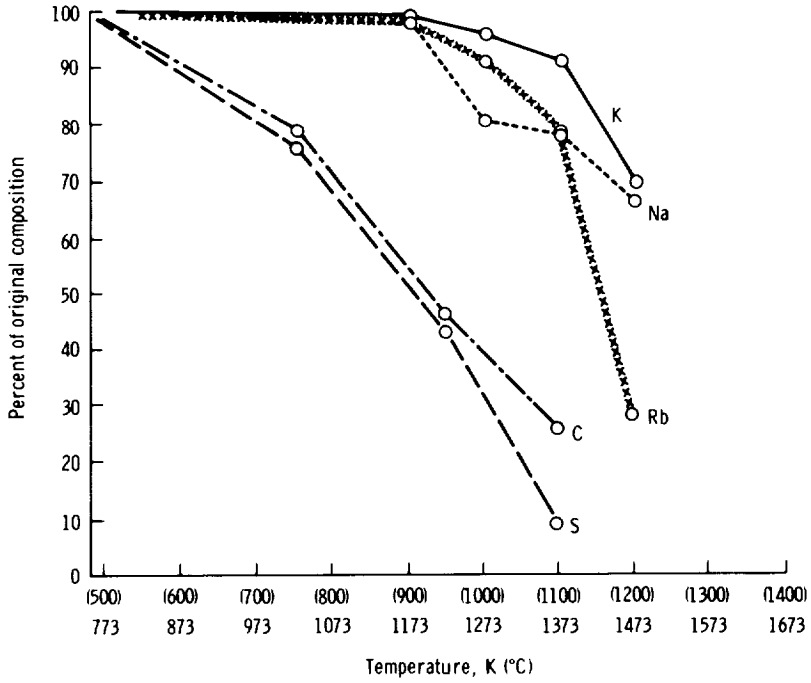

FIGURE 4-4.—Volatile element loss from lunar soils that were heated under vacuum. The data presented are an average of four mare and highland soils.

The concentration of indigenous water in lunar basalts is vanishingly small (< 10 ppm) compared to terrestrial rocks and is difficult to distinguish from terrestrial contamination. Essentially, all H_2O found in lunar soils has been formed by interaction of solar wind hydrogen with oxygen-bearing silicates.

Pyrolysis of lunar materials has failed to release any organic compounds that could not be explained by contamination or as simple compounds formed from the solar wind. The upper limit of indigenous organics in lunar samples is approximately one part per billion.

REFERENCES

4-1. Van Horn, Kent R., ed.: Aluminum. The American Society for Metals, 1967.

4-2. Smithells, Colin J., ed.: Metals Reference Book. Fourth ed. Plenum Press, 1967.

Appendix A—Glossary

Definitions of specialized terms used in the geological sciences are best obtained from the *Glossary of Geology and Related Sciences*, published by the American Geological Institute, Washington, D.C. An abridged version is available as the *Dictionary of Geological Terms*, Dolphin Books, Doubleday and Company, Inc., Garden City, N. Y.

In the study of lunar materials, some terms have taken on slightly different or derivative definitions. The glossary in this handbook presents definitions that are peculiar to lunar studies; it also includes many definitions of common geologic terms that are used frequently in this work.

acid — A general term for rocks or minerals rich in SiO_2; loosely applied to rocks containing light colored minerals (cf., silicic and basic).

anorthite — Calcium aluminum silicate ($CaAl_2Si_2O_8$), a mineral of the plagioclase feldspar group. The term is applied to minerals that contain more than 90 percent $CaAl_2Si_2O_8$, but lunar use has generalized the term to include all calcium-rich feldspars. The terms feldspar, anorthite, and plagioclase are sometimes used interchangeably.

anorthosite — A plutonic rock composed almost wholly of plagioclase, sometimes generalized to a rock of any origin which is composed of more than 85 percent anorthite.

basalt — An extrusive rock, composed primarily of calcic plagioclase, pyroxene, with or without olivine; more generally, any fine-grained, dark-colored igneous rock.

basic — A general term for rocks and minerals which are low in SiO_2; usually applied to rocks with less than 50 percent SiO_2; loosely applied to rocks containing dark-colored minerals (cf., mafic and acid).

breccia	(1) A fragmental rock, whose components are angular and, therefore, as distinguished from conglomerates, are not waterworn. (2) A rock made up of highly angular, coarse fragments; may be sedimentary or formed by crushing and grinding along fault lines. Lunar breccias are, in part, the result of crushing and grinding associated with meteorite impact.
dunite	A rock consisting almost wholly of olivine and containing accessory pyroxene and chromite.
feldspar	See anorthite.
gabbro	A plutonic rock consisting of calcic plagioclase (commonly labradorite) and clinopyroxene, with or without orthopyroxene and olivine. In terrestrial gabbros, apatite and magnetite or ilmenite are common accessories. Lunar gabbros do not contain magnetite. The term is often used loosely to refer to coarse-grained varieties of basalts.
ilmenite	A mineral, $FeTiO_3$; the principal ore of titanium.
KREEP	A composition of lunar material known by this acronym derived from the elements potassium (K), rare earth elements (REE) and phosphorus (P) which are present in unusually high abundances in the material; thus, KREEP basalts, KREEP breccias, etc.
lithic	Of, or pertaining to, rocks; as in "a lithic fragment"—i.e., "a rock fragment."
mafic	In petrology, subsilicic or basic, pertaining to or composed dominantly of the magnesian rock-forming silicates; generally synonymous with "dark minerals."
matrix	Usually the finest grained portion of a rock.
mineral	A naturally occurring substance, sometimes restricted to inorganic, crystalline substance.
olivine	Chrysolite or peridot; a mineral series, solid solutions of forsterite (Mg_2SiO_4), with fayalite (Fe_2SiO_4), the composition often expressed as mole percent of the constituents (abbreviated Fo, Fa).

ore — A naturally occurring material from which useful products can be extracted for economic advantage.

plagioclase — A mineral group, formula $(Na,Ca)Al(Si,Al)Si_2O_8$. A solid solution series from $NaAlSi_3O_8$ (albite) to $CaAl_2Si_2O_8$ (anorthite). Commonly, the series is designated in terms of the mole-fraction of the albite component (abbr. Ab) and the anorthite component (abbr. An) as follows (Ab + An = 100): albite (Ab100 to 90), oligoclase (Ab90 to 70), andesine (Ab70 to 50), labradorite (Ab50 to 30), bytownite (Ab30 to 10), and anorthite (Ab10 to 0). See anorthite.

plutonic — A general term denoting one of three great subdivisions of rocks under a classification proposed by Reed, including the granitic, megmatitic and metamorphic rocks, the great granitic complexes, the gneisses and schists; generally applied to the class of igneous rocks which have crystallized at great depth and have, therefore, as a rule, assumed the granitoid texture.

polymict — An adjective indicating multiple rock types combined in a single sample. In lunar petrology, the term is usually applied to breccias that contain fragments of other breccias; thus the term, polymict breccia.

porphyritic — A textural term for those igneous rocks in which larger crystals (phenocrysts or insets) are set in a finer groundmass that may be crystalline or glassy or both.

pyroclastic rocks — A general term for indurated deposits of volcanic ejecta, including volcanic agglomerates, breccias, tuff breccias, tuffs, conglomerates, and sandstones.

pyroxene — A mineral group, general formula $ABSi_2O_6$, where A is chiefly Mg, Fe", Ca, and Na; B is chiefly Mg, Fe", and Al; and Si may be replaced in part by Al.

regolith — Mantle rock, saprolith; the layer or mantle of loose, incoherent rock material, of whatever origin, that nearly everywhere forms the surface of the Moon and rests on the hard "bed" rock. The terms regolith and soil are often used interchangeably.

resource	A potential ore.
rock	A naturally formed aggregate or mass of mineral matter; usually restricted to coherent or cohesive aggregations.
sinter	To bring about agglomeration by heating.
soil	See regolith.
spinel	A mineral, $(Mg,Fe)Al_2O_4$; a mineral group of general formula AB_2O_4 where A = Mg, Fe″, Zn, Mn″, Ni, and B = Al, Fe‴, Cr.
vitric	Referring to glass, as in "vitric clast"—i.e., a fragment that is mostly glass.
vitrophyre	Porphyritic volcanic glass.

1. Report No. RP-1057	2. Government Accession No.	3. Recipient's Catalog No.
4. Title and Subtitle HANDBOOK OF LUNAR MATERIALS		5. Report Date February 1980 6. Performing Organization Code
7. Author(s) Richard J. Williams, JSC, and James J. Jadwick, Lockheed Electronics Co., Inc., editors		8. Performing Organization Report No. S-494 10. Work Unit No. 790-40-37-00-72
9. Performing Organization Name and Address Lyndon B. Johnson Space Center Houston, Texas 77058		11. Contract or Grant No. 13. Type of Report and Period Covered Reference Publication
12. Sponsoring Agency Name and Address National Aeronautics and Space Administration Washington, D. C. 20546		14. Sponsoring Agency Code
15. Supplementary Notes		

16. Abstract

The physical, chemical, thermodynamic, and geologic data on lunar rocks, minerals, and processes are summarized, and a set of data metals that might be extracted from lunar materials is presented.

17. Key Words (Suggested by Author(s))

Moon
Physical properties
Chemistry
Thermodynamic data
Minerals
Rocks
Metals

18. Distribution Statement

STAR Subject Category:
91 (Lunar and Planetary Exploration)

19. Security Classif. (of this report)	20. Security Classif. (of this page)	21. No. of Pages	22. Price*
Unclassified	Unclassified	132	$6.00

*For sale by the National Technical Information Service, Springfield, Virginia 22161

NASA-Langley, 1980